



DOCTORAL THESIS

3rd Cycle Doctoral (D-LMD)

Presented by

Mohamed Seghir JABALLAH

With a view to obtain the doctoral diploma in 3rd Cycle Doctoral (D-LMD)

Branch: Civil Engineering

Specialty: Geotechnics

Topic

Development of intelligent systems for active and hybrid control of structures under earthquake excitation considering soil-structure interaction

Supported, on **30/11/2022**, before the jury composed of:

First and Last name	Grade	Institution of affiliation	Designation
Mr Slami SAADI	Professor	Université de Djelfa	President
Mr Salaheddine HARZALLAH	MCA	Université de Djelfa	Supervisor
Mr Fouad BOURADA	MCA	Université de Tissemsilt	Examiner
Mr Salim GUETTALA	Professor	Université de Djelfa	Examiner
Mr Mohamed BADAOU	MCA	Université de Djelfa	Examiner
Mr Bachir NAIL	MCB	Université de Tissemsilt	Invited Guest



Dedication

I dedicate this work to my dear mom, to the soul of my father, to my sisters
Eva, khadra and Ahlem and to my big brother Hamza.

Thanks to everyone who helped me and supported me during those years of
hard work and pain.

I really couldn't have done this without anyone of you.

Love you all !.....

Mohamed Seghir Jaballah



Acknowledgements

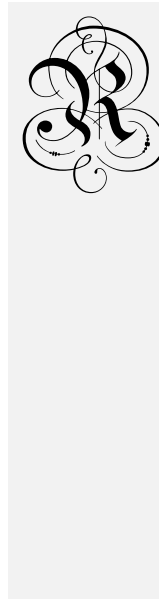
Acknowledgements

First of all, I would like to give big thanks to my supervisor **Dr. Salaheddine HARZALLAH**, I couldn't have done this or reach this stage without you. I can remember your encouragements and your help every single time. Sometimes when I'm with you I really felt like you are a father or a big brother to me, you given me motivation, words of encouragement, ideas, experiences, suggestions, and help whenever I needed them the most. For this thank you infinitely.

Dr. Bachir NAIL, my gratitude to you for all you have done, which I will never forget. I truly appreciate you and your time you spent helping me on many occasions. Thank you very much for everything.

My thanks also go to the members of the jury for agreeing to judge this work.

Finally, I would like to extend my most sincere thanks to all the teachers in the department of Civil Engineering from the University of Djelfa who have always supported and encouraged me throughout my journey.



Resume

ملخص

يمكن للكوارث الطبيعية مثل الزلازل أو الرياح ان تدمر الهياكل المدنية وتعرض سلامة الناس للخطر. في السنوات الأخيرة ، أصبحت حماية هذه الهياكل من هاته الظواهر موضوع بحث مكثف لضمان السلامة الهيكلية باستخدام تقنيات مختلفة للتحكم في الاهتزازات الهيكلية للحد من خطورتها هاته الظواهر. حيث يكون الهدف الرئيسي هو حماية هذه الهياكل وتوفير السلامة لشاغلها.

في هذه الدراسة ، قمنا بإجراء تحقيقات لهذا النوع من التحكم على العديد من الهياكل لإثبات فعاليتها في الحد من الآثار الزلزالية ، باستخدام ثلاثة قوانين تحكم مثل: PID و LQR و Fractional Order PID. أظهرت هذه الدراسة أن هذا النوع من التحكم هو حل موثوق به لحماية الهياكل من الزلازل. في جزء آخر من هذه الدراسة ، قدمنا تأثير تفاعل بنية التربة (SSI) في استجابة الهياكل الخاضعة للرقابة. وقد أظهر هذا أنه إذا كانت التربة الموجودة أسفل قاعدة الهياكل ذات قابلية عالية للتشوه ، فمن المهم جدًا إدخال تأثير التفاعل من أجل العثور على السلوك الحقيقي للهياكل.

Résumé

Les catastrophes naturelles telles que les tremblements de terre ou les vents peuvent endommager les structures civiles et mettre en danger la sécurité des personnes. Ces dernières années, la protection de ces structures contre les risques naturels est devenue un sujet de recherche intensive pour assurer la sécurité structurelle en utilisant différentes techniques de contrôle des vibrations structurelles pour réduire les vibrations structurelles. Où l'objectif principal est de protéger ces structures et d'assurer la sécurité des occupants humains.

Dans cette étude, nous avons investigué ce type de contrôle sur plusieurs structures afin de démontrer son efficacité à réduire les effets sismiques, en utilisant trois lois de contrôle telles que : les contrôleurs LQR, PID et PID d'ordre fractionnel. Cette étude a montré que ce type de contrôle est une solution fiable pour protéger les ouvrages contre les séismes.

Dans une autre partie de cette étude, nous avons introduit l'effet de l'interaction sol-structure (SSI) dans la réponse des structures contrôlées. Ceci a montré que si le sol sous la base des structures a une grande déformabilité, il est très important d'introduire l'effet d'interaction afin de trouver le comportement réel des structures.

Mots-clés : Contrôle hybride, LQR, Contrôleur PID, Contrôleur PID d'ordre fractionnaire, Interaction sol-structure (ISS).

Abstract

Natural hazards like earthquakes or winds can damage civil structures and risk people's safety. In recent years, protecting these structures against natural hazards has become a subject of intensive research to ensure structural safety by using different structural vibration control techniques to reduce structural vibrations. Where the main goal is to protect these structures and provide safety to human occupants.

In this study, we made investigations of this type of control on several structures to demonstrate its effectiveness in reducing seismic effects, by using three control laws such as : LQR, PID and Fractional Order PID controllers. This study has shown that this type of control is a reliable solution for protecting structures to earthquakes.

In another part of this study, we introduced the effect of soil-structure interaction (SSI) in the response of controlled structures. This has shown that if the soil beneath the base of structures have a high deformability, it is very important to introduce the effect of interaction in order to find the real behavior of structures.

Key-words : Hybrid control, LQR, PID Controller, Fractional Order PID Controller, Soil-structure interaction (SSI).

List of scientific productions

Journal articles:

1. **Mohamed Seghir Jaballah**, Salaheddine Harzallah, and Bachir Nail. "A Comparative Study on Hybrid Vibration Control of Base-isolated Buildings Equipped with ATMD." *Engineering, Technology & Applied Science Research* 12.3 (2022): 8652-8657. [Link](#).
2. **Mohamed Seghir Jaballah**, Salaheddine Harzallah, and Bachir Nail. "Vibration control and seismic damages reduction for structural buildings based on optimal fractional-order controller and a graphical user interface development". *Under Review on second stage, after a minor revision is required*.
3. **Mohamed Seghir Jaballah**, Salaheddine Harzallah, and Bachir Nail. "Hybrid vibration control for seismically excited building structures using PID controller optimized by Artificial Hummingbird algorithm". *Under Review on second stage, after a major revision is required*.

Book Chapters:

1. **Seghir, Jaballah Mohamed**, Nail Bachir, Harzallah Salaheddine, and Guettala Salim. " Hybrid vibration control of structures using fractional order $PI^{\lambda}D^{\mu}$ controller." In *International Conference on Artificial Intelligence in Renewable Energetic Systems*, pp. 569-577. Springer, Cham, 2021. [Link](#).

Conference-paper:

1. **2021** | Simulating two structures using Hybrid systems, one with LQR controller and the other with PID controller. And after validating the results with previous works and using a metallic structure as a study item. I have published my work into the *3rd International Conference on Metallic and Mixed Construction CICCOM 2021 – ORAN*
2. **2021** | Linking the civil engineering field with the electrical engineering field by developing a two new algorithms called Digital PID and Digital LQR, which allow us to transform the structural response DATA into a digital signal that later on will allow us to directly drives the actuators (ATMD for example). This work also has been accepted in *The 2nd International Conference on Artificial Intelligence and its Applications (aiap2021) – OuedSouf*
3. **2022** | Simulating a multi-story building that uses a Hybrid system for vibration control and turning another type of PID controller, called the fractional-order PID , that has proven to give better results. This work also has been accepted in the *5th International Conference on Artificial Intelligence in Renewable Energetic System*
4. **2022** | *Contrôle des vibrations des structures isolées à la base équipée d'un amortisseur actif à masse accordée Proceedings of 1st National Conference of Materials sciences And Engineering, (MSE'22)*
5. **2022** | *Soil-structure interaction effects on the vibration control of building structures 6th International Conference on Artificial Intelligence in Renewable Energetic Systems IC-AIRES2022*

Workshop:

- **2021** | Workshop, Structural Vibration Control Simulator software. German Academic Exchange Service, Germany from 8th and 15th December.

My accounts in scientific organizations:

- Personal Website : <https://jaballahms.blogspot.com/>
- Google scholar : <https://scholar.google.com/citations?user=Ih3Tf1wAAAAJ&hl=fr>
- Researchgate : <https://www.researchgate.net/profile/Mohamed-Seghir-Jaballah>
- Scopus : <https://www.scopus.com/authid/detail.uri?authorId=57384825300>
- ORCID : <https://orcid.org/0000-0002-3130-0650>
- Web of science : <https://www.webofscience.com/wos/author/record/AHC-0548-2022>

Table of Contents

Table of Contents

Contents

- Acknowledgements IV
- Abstract VI
- List of scientific productions..... VIII
- Table of Contents..... XI
- List of Tables.....XIII
- List of FiguresXIV
- Nomenclature.....XVIII
- GlossaryXX
- General Introduction 1
- CHAPTER 1 PRINCIPLES OF VIBRATION CONTROL SYSTEMS5**
 - 1.1 Introduction5
 - 1.2 History 6
 - 1.3 Different control systems 8
 - 1.3.1 Passive control 8
 - 1.3.2 Base-isolation systems 8
 - 1.3.3 Passive Energy Dissipation Systems..... 14
 - 1.4 Active control 26
 - 1.4.1 Active Tendon Systems 28
 - 1.4.2 Active Brace Damper..... 29
 - 1.4.3 Active Tuned Mass Damper (ATMD)..... 30
 - 1.5 Hybrid control..... 31
 - 1.5.1 Hybrid Base Isolation32
 - 1.5.2 Hybrid Mass Damper32
 - 1.6 Semi-Active control.....33
 - 1.6.1 Magnetorheological and Electrorheological Dampers..... 34
 - 1.7 Conclusion.....35
- CHAPTER 2 MATHEMATICAL FORMULATION AND CONTROLLING ALGORITHMS..... 38**
 - 2.1 Introduction..... 38
 - 2.2 Equation of motion and mathematical representation..... 38
 - 2.2.1 Structure without control 38
 - 2.2.2 Structure with control 40
 - 2.3 State-space representation..... 48
 - 2.3.1 Introduction..... 48
 - 2.3.2 Why use state-space representations..... 49

2.4 Classic Feedback control	50
2.5 Linear Quadratic Regulator (LQR)	50
2.6 PID controller.....	52
2.7 Fractional Order PID controller	54
2.8 Optimization Algorithms.....	55
2.8.1 Introduction.....	55
2.8.2 Artificial Hummingbird Algorithm.....	55
2.8.3 Genetic Algorithms	60
2.8.4 Grey Wolf Algorithm.....	63
2.9 Conclusion.....	63
CHAPTER 3 HYBRID VIBRATION CONTROL FOR STRUCTURES: SIMULATION AND NUMERICAL RESULTS	66
3.1 Introduction.....	66
3.2 Comparative study on hybrid vibration control of base-isolated buildings equipped with ATMD..	66
3.3 Hybrid vibration control for seismically excited building structures using optimized PID controller	71
3.3.1 Numerical Results.....	73
3.4 Hybrid vibration control for seismically excited building structures using optimized Fractional Order PID controller	88
3.4.1 Numerical results	88
CHAPTER 4 HYBRID VIBRATION CONTROL FOR STRUCTURES WITH SOIL-STRUCTURE INTERACTION: SIMULATION AND NUMERICAL RESULTS	108
4.1 Introduction	108
4.2 Results and discussion.....	111
4.3 Conclusion.....	115
General Conclusion	117
SVCS Software.....	129

List of Tables

TABLE 3.1 : BUILDING PARAMETERS	67
TABLE 3.2 : EARTHQUAKES CONSIDERED IN THE NUMERICAL STUDY	71
TABLE 3.3 : PARAMETERS OF THE AHA.	72
TABLE 3.4 : THE OPTIMUM VALUES OF THE OBJECTIVE FUNCTION FOUND BY DIFFERENT USED ALGORITHMS.....	73
TABLE 3.6 : MAXIMUM RESPONSES UNDER DIFFERENT EARTHQUAKE EXCITATIONS.	82
TABLE 3.7 : AVERAGE ACCELERATIONS UNDER DIFFERENT EARTHQUAKE EXCITATIONS.	87
TABLE 3.8 : PARAMETERS OF THE AHA.	88
TABLE 3.9 : THE OPTIMUM VALUES OF THE OBJECTIVE FUNCTION FOUND BY DIFFERENT USED EARTHQUAKES	88
TABLE 3.10 : THE OPTIMUM PARAMETERS OF THE PID AND FO-PID CONTROLLERS OBTAINED BY DIFFERENT USED EARTHQUAKES.	95
TABLE 3.11 : MAXIMUM RESPONSES UNDER DIFFERENT EARTHQUAKE EXCITATION.....	100
TABLE 3.12 : AVERAGE ACCELERATIONS UNDER DIFFERENT EARTHQUAKE EXCITATION.....	105
TABLE 4.1 : PARAMETERS OF THE FOUNDATION AND SOIL TYPES.....	110
TABLE 4.2 : EARTHQUAKES ARE CONSIDERED IN THE NUMERICAL STUDY.	111

List of Figures

FIGURE 1.1 : DIFFERENT VIBRATION CONTROL TYPES	6
FIGURE 1.2 : WATER TOWER WITH DAMPING DEVICES	7
FIGURE 1.3 : BASE ISOLATION SYSTEM	8
FIGURE 1.4 : PRINCIPLE OF OPERATION OF PARA-SEISMIC BEARINGS	9
FIGURE 1.5 : ELASTOMERIC BEARING WITH STEEL SHIMS	9
FIGURE 1.6 : LEAD RUBBER BEARING	11
FIGURE 1.7 : (A) HIGH-DAMPING NATURAL RUBBER BEARING (B) A SECTION CUT	12
FIGURE 1.8 : FRICTION PENDULUM ISOLATOR	13
FIGURE 1.9 : FRICTION PENDULUM BEARING WITH DOUBLE CONCAVE SURFACE	13
FIGURE 1.10 : TYPICAL TYPES OF METALLIC YIELD DAMPERS: (A) TYLER’S YIELDING STEEL BRACING SYSTEM AND (B) ADDED DAMPING AND STIFFNESS (ADAS) DEVICE.	15
FIGURE 1.11 : FRICTION DAMPER, (A) SUMITOMO-TYPE FRICTION DAMPER AND (B) ITS INSTALLATION	16
FIGURE 1.12 : VISCOELASTIC (VE) DAMPER: (A) DAMPER DETAIL, (B) INSTALLATION AS CHORD, AND (C) INSTALLATION AS DIAGONAL BRACING.	17
FIGURE 1.13 : TWIN TOWERS OF THE WORLD TRADE CENTER IN NEW YORK	18
FIGURE 1.14 : MAXWELL MODEL	19
FIGURE 1.15 : EXAMPLE OF VISCOUS FLUID DAMPER	19
FIGURE 1.16 : A) CYLINDRICAL CONTAINER FLUID DAMPER, B) THE VISCOUS DAMPING WALL	20
FIGURE 1.17 : VERTICAL TMDs INSTALLED UNDER THE DECK OF THE MILLENNIUM FOOTBRIDGE IN LONDON	21
FIGURE 1.18 : THE TAIPEI 101 SKYSCRAPER WITH THE TUNED MASS DAMPER	22
FIGURE 1.19 : THE MECHANISM OF A TMD	22
FIGURE 1.20 : SYDNEY TOWER (CENTER POINT) FIGURE 1.21 : CITICORP CENTER NEW YORK	23
FIGURE 1.22 : CONTROL TOWER (WASHINGTON AIRPORT) FIGURE 1.23 : JOHN HANCOCK TOWER (BOSTON)	23
FIGURE 1.24 : CHIBA PORT TOWER (JAPAN)	23
FIGURE 1.25 : TUNED LIQUID DAMPER WORKING PRINCIPLE	24
FIGURE 1.26 : TLDs TYPES	25
FIGURE 1.27 : TUNED LIQUID-COLUMN DAMPER (COMCAST BUILDING IN PHILADELPHIA).	25
FIGURE 1.28 : SCHEMATIC DIAGRAM OF AN ACTIVE CONTROL SYSTEM.	27
FIGURE 1.29 : ACTIVE TENDON SYSTEM.	28
FIGURE 1.30 : ACTIVE BRACING SYSTEM WITH HYDRAULIC ACTUATOR	29
FIGURE 1.31 : AN ACTIVE TUNED MASS DAMPER SYSTEM	30
FIGURE 1.32 : SCHEMATIC OF HYBRID MASS DAMPER	33
FIGURE 1.33 : SENDAGAYA INTES BUILDING (TOKYO, JAPAN)	33
FIGURE 1.34 : SCHEMATIC OF ER DAMPER	35
FIGURE 1.35 : SCHEMATIC OF MR DAMPER	35
FIGURE 2.1 : MULTI-STORY SHEAR BUILDING STRUCTURE.	39

FIGURE 2.2 : MATHEMATICAL MODEL FOR BASE ISOLATION SYSTEM	41
FIGURE 2.3 : BUILDING STRUCTURE WITH BASE ISOLATION SYSTEM.....	41
FIGURE 2.4 : 1DOF BUILDING STRUCTURE WITH FIXED AND ISOLATED BASE.	42
FIGURE 2.5 : A SHEAR BUILDING STRUCTURE EQUIPPED WITH AN ATMD AT THE TOP FLOOR.....	44
FIGURE 2.7 : BLOCK DIAGRAM REPRESENTATION OF THE STATE-SPACE EQUATIONS [130].	49
FIG.2.8 : LQR CONTROLLER	51
FIGURE 2.9 : BLOCK DIAGRAM OF THE PID CONTROLLER.	53
FIGURE 2.10 : BLOCK DIAGRAM OF AN FO-PID CONTROLLER.	55
FIGURE 2.11 : VISIT TABLE OF A HUMMINGBIRD’S POPULATION.....	56
FIGURE 2.13 : FORAGING BEHAVIORS OF AHA.....	57
FIGURE 2.14 : THREE FLIGHT BEHAVIORS OF HUMMINGBIRDS.	58
FIGURE 2.15 : PSEUDOCODE OF THE AHA	60
FIGURE 2.16 : GENETIC ALGORITHM FLOW CHART	60
FIGURE 2.17 : ONE POINT Crossover	61
FIGURE 2.18 : MULTIPPOINT Crossover.....	62
FIGURE 2.19 : UNIFORM Crossover	62
FIGURE 2.20 HIERARCHY OF GREY WOLF.	63
FIGURE 3.1 : BASE ISOLATED BUILDING EQUIPPED WITH ATMD ON THE TOP FLOOR	67
FIGURE 3.2 : TOP FLOOR RESPONSE UNDER EL CENTRO SEISMIC EXCITATION	68
FIGURE 3.3 : TOP FLOOR RESPONSE UNDER KOBE SEISMIC EXCITATION.....	68
FIGURE 3.4 : TOP FLOOR RESPONSE UNDER NORTHRIDGE SEISMIC EXCITATION.	69
FIGURE 3.5 : MAXIMUM STORY DRIFT FOR THE STRUCTURE UNDER THE DIFFERENT EARTHQUAKE EXCITATIONS. (A) EL CENTRO, (B) KOBE, AND (C) NORTHRIDGE.....	70
FIGURE 3.6 : TIME HISTORIES FOR THE CONSIDERED EARTHQUAKE GROUND MOTION RECORDS.	72
FIGURE 3.7 : THE CONVERGENCE HISTORY OF THE OBJECTIVE FUNCTION FOR THE AHA, GWO, DA, WOA, AND ALO ALGORITHMS UNDER THE DIFFERENT EARTHQUAKE EXCITATIONS. (A) NORTHRIDGE, (B) EL CENTRO, (C) CHI-CHI, (D) KOBE AND (E) LOMA PRIETA.	75
FIGURE 3.8 : PID CONTROLLER PARAMETERS EVOLUTION FOR ALL ALGORITHMS.	76
TABLE 3.5 : THE OPTIMUM PARAMETERS OF THE PID CONTROLLER OBTAINED BY DIFFERENT USED ALGORITHMS.....	77
FIGURE 3.9 : MAXIMUM STORY DRIFT FOR THE STRUCTURE UNDER DIFFERENT EARTHQUAKE EXCITATIONS.	78
FIGURE 3.10 : TIME HISTORY DISPLACEMENT OF THE TOP STORY OF THE STRUCTURE DURING NORTHRIDGE EARTHQUAKE EXCITATION USING THE DIFFERENT OPTIMIZATION ALGORITHMS.	79
FIGURE 3.11 : TIME HISTORY DISPLACEMENT OF THE TOP STORY OF THE STRUCTURE DURING EL CENTRO EARTHQUAKE EXCITATION USING THE DIFFERENT OPTIMIZATION ALGORITHMS.	79
FIGURE 3.12 : TIME HISTORY DISPLACEMENT OF THE TOP STORY OF THE STRUCTURE DURING CHI-CHI EARTHQUAKE EXCITATION USING THE DIFFERENT OPTIMIZATION ALGORITHMS.	80
FIGURE 3.13 : TIME HISTORY DISPLACEMENT OF THE TOP STORY OF THE STRUCTURE DURING KOBE EARTHQUAKE EXCITATION USING THE DIFFERENT OPTIMIZATION ALGORITHMS.	80
FIGURE 3.14 : TIME HISTORY DISPLACEMENT OF THE TOP STORY OF THE STRUCTURE DURING LOMA PRIETA EARTHQUAKE EXCITATION USING THE DIFFERENT OPTIMIZATION ALGORITHMS.	81

FIGURE 3.15 : THE REDUCTION OF MAXIMUM RESPONSE FOR THE TOP STORY.	83
FIGURE 3.16 : TOP STORY ACCELERATION DURING NORTHRIDGE EARTHQUAKE EXCITATION USING THE DIFFERENT OPTIMIZATION ALGORITHMS.	84
FIGURE 3.17 : TOP STORY ACCELERATION DURING EL CENTRO EARTHQUAKE EXCITATION USING THE DIFFERENT OPTIMIZATION ALGORITHMS.	85
FIGURE 3.18 : TOP STORY ACCELERATION DURING CHI-CHI EARTHQUAKE EXCITATION USING THE DIFFERENT OPTIMIZATION ALGORITHMS. ...	85
FIGURE 3.19 : TOP STORY ACCELERATION DURING KOBE EARTHQUAKE EXCITATION USING THE DIFFERENT OPTIMIZATION ALGORITHMS.	86
FIGURE 3.20 : TOP STORY ACCELERATION DURING LOMA PRIETA EARTHQUAKE EXCITATION USING THE DIFFERENT OPTIMIZATION ALGORITHMS.	86
FIGURE 3.21 : THE CONVERGENCE HISTORY OF THE OBJECTIVE FUNCTION FOR THE AHA, GWO, DA, WOA, AND ALO ALGORITHMS UNDER THE DIFFERENT EARTHQUAKE EXCITATIONS. (A) NORTHRIDGE, (B) EL CENTRO, (C) CHI-CHI, (D) KOBE AND (E) LOMA PRIETA.....	90
FIGURE 3.22 : PID GAINS EVOLUTION (Kp, Ki, Kd) UNDER NORTHRIDGE EARTHQUAKE.	90
FIGURE 3.23 : PID GAINS EVOLUTION (Kp, Ki, Kd) UNDER EL CENTRO EARTHQUAKE.	90
FIGURE 3.24 : PID GAINS EVOLUTION (Kp, Ki, Kd) UNDER CHI-CHI EARTHQUAKE.	91
FIGURE 3.25 : PID GAINS EVOLUTION (Kp, Ki, Kd) UNDER KOBE EARTHQUAKE.	91
FIGURE 3.26 : PID GAINS EVOLUTION (Kp, Ki, Kd) UNDER LOMA PRIETA EARTHQUAKE.	91
FIGURE 3.27 : FO-PID GAINS EVOLUTION (Kp, Ki, Kd) UNDER NORTHRIDGE EARTHQUAKE.	92
FIGURE 3.28 : FO-PID GAINS EVOLUTION (λ, μ) UNDER NORTHRIDGE EARTHQUAKE.	92
FIGURE 3.29 : FO-PID GAINS EVOLUTION (Kp, Ki, Kd) UNDER EL CENTRO EARTHQUAKE.....	92
FIGURE 3.30 : FO-PID GAINS EVOLUTION (λ, μ) UNDER EL CENTRO EARTHQUAKE.	93
FIGURE 3.31 : FO-PID GAINS EVOLUTION (Kp, Ki, Kd) UNDER CHI-CHI EARTHQUAKE.....	93
FIGURE 3.32 : FO-PID GAINS EVOLUTION (λ, μ) UNDER CHI-CHI EARTHQUAKE.	93
FIGURE 3.33 : FO-PID GAINS EVOLUTION (Kp, Ki, Kd) UNDER KOBE EARTHQUAKE.	94
FIGURE 3.34 : FO-PID GAINS EVOLUTION (λ, μ) UNDER KOBE EARTHQUAKE.	94
FIGURE 3.35 : FO-PID GAINS EVOLUTION (Kp, Ki, Kd) UNDER LOMA PRIETA EARTHQUAKE.	94
FIGURE 3.36 : FO-PID GAINS EVOLUTION (λ, μ) UNDER LOMA PRIETA EARTHQUAKE.....	95
FIGURE 3.37 : MAXIMUM STORY DRIFT FOR THE STRUCTURE UNDER THE DIFFERENT SEISMIC EXCITATIONS,	96
(A) NORTHRIDGE, (B) EL CENTRO, (C) CHI-CHI, (D) KOBE AND (E) LOMA PRIETA.	96
FIGURE 3.38 : TIME HISTORY DISPLACEMENT OF THE TOP STORY OF THE STRUCTURE DURING NORTHRIDGE EARTHQUAKE EXCITATION USING THE DIFFERENT OPTIMIZATION ALGORITHMS.	97
FIGURE 3.39 : TIME HISTORY DISPLACEMENT OF THE TOP STORY OF THE STRUCTURE DURING EL CENTRO EARTHQUAKE EXCITATION USING THE DIFFERENT OPTIMIZATION ALGORITHMS.	97
FIGURE 3.40 : TIME HISTORY DISPLACEMENT OF THE TOP STORY OF THE STRUCTURE DURING CHI-CHI EARTHQUAKE EXCITATION USING THE DIFFERENT OPTIMIZATION ALGORITHMS.	98
FIGURE 3.41 : TIME HISTORY DISPLACEMENT OF THE TOP STORY OF THE STRUCTURE DURING KOBE EARTHQUAKE EXCITATION USING THE DIFFERENT OPTIMIZATION ALGORITHMS.	98
FIGURE 3.42 : TIME HISTORY DISPLACEMENT OF THE TOP STORY OF THE STRUCTURE DURING LOMA PRIETA EARTHQUAKE EXCITATION USING THE DIFFERENT OPTIMIZATION ALGORITHMS.	99
FIGURE 3.43 : THE REDUCTION OF MAXIMUM RESPONSE FOR THE TOP STORY.	101

FIGURE 3.44 : TOP STORY ACCELERATION DURING NORTHRIDGE EARTHQUAKE EXCITATION USING THE DIFFERENT OPTIMIZATION ALGORITHMS.	102
FIGURE 3.45 : TOP STORY ACCELERATION DURING EL CENTRO EARTHQUAKE EXCITATION USING THE DIFFERENT OPTIMIZATION ALGORITHMS.	102
FIGURE 3.46 : TOP STORY ACCELERATION DURING CHI-CHI EARTHQUAKE EXCITATION USING THE DIFFERENT OPTIMIZATION ALGORITHMS. .	103
FIGURE 3.47 : TOP STORY ACCELERATION DURING KOBE EARTHQUAKE EXCITATION USING THE DIFFERENT OPTIMIZATION ALGORITHMS.	103
FIGURE 3.48 : TOP STORY ACCELERATION DURING LOMA PRIETA EARTHQUAKE EXCITATION USING THE DIFFERENT OPTIMIZATION ALGORITHMS.	104
FIGURE 4.1 : BUILDING STRUCTURE EQUIPPED WITH ATMD INCLUDING SSI EFFECTS.	109
FIGURE 4.2 : TOP STORY DISPLACEMENT WITH AND WITHOUT SSI EFFECT, EL CENTRO EARTHQUAKE, DENSE SOIL.....	112
FIGURE 4.3 : TOP STORY DISPLACEMENT WITH AND WITHOUT SSI EFFECT, EL CENTRO EARTHQUAKE, MEDIUM SOIL.	112
FIGURE 4.4 : TOP STORY DISPLACEMENT WITH AND WITHOUT SSI EFFECT, EL CENTRO EARTHQUAKE, SOFT SOIL.....	113
FIGURE 4.5 : TOP STORY DISPLACEMENT WITH AND WITHOUT SSI EFFECT, NORTHRIDGE EARTHQUAKE, DENSE SOIL.....	113
FIGURE 4.6 : TOP STORY DISPLACEMENT WITH AND WITHOUT SSI EFFECT, NORTHRIDGE EARTHQUAKE, MEDIUM SOIL.	114
FIGURE 4.7 : TOP STORY DISPLACEMENT WITH AND WITHOUT SSI EFFECT, NORTHRIDGE EARTHQUAKE, SOFT SOIL.....	114

Nomenclature

$[A]$	system matrix
$[B]$	input matrix
c_{ATMD}	viscous damping of the active tuned mass damper
C_r	rocking damping
C_s	swaying damping
$[C]$	output matrix
$\{d\}$	control force vector
$[D]$	feedthrough matrix
$f(t)$	active control force
G_s	shear wave modulus
I_0	Foundation moment of inertia
$\{x\}$	state vector
$\{u\}$	input vector
$\{y\}$	output vector
$[M]$	mass matrix
n	number of structure stories
m	mass of a SDOF structure
m_{ATMD}	mass of the active tuned mass damper
m_i	mass at the i^{th} d.o.f of a structure, $i = 1, \dots, n$
m_b	mass of isolation system
M_0	Foundation mass
$[C]$	damping matrix
k_d	the derivative gain
k_i	the integrator gain
k_p	the proportional gain
K_r	spring stiffness
K_s	spring stiffness
$[K]$	stiffness matrix
$[N]$	order of state equations, or order of plant matrix

h_i	the height of the structure story at level i
J	performance index
I_0	foundation mass moment of inertia with respect to point 0
$[I]$	identity matrix
k_{ATMD}	stiffness of the active tuned mass damper
k_b	lateral stiffness of the isolation system
k_i	stiffness at the i^{th} d.o.f of a structure, $i = 1, \dots, n$
$[Q]$	structural force matrix, or weighting matrix in performance indices, or state weighting matrix
$\{r\}$	influence vector
R_0	foundation radius
$[R]$	weighting matrix in performance indices, or control weighting matrix
u_i	nodal horizontal displacement at node i
V_s	velocity
x	simplified notation of relative displacement of a SDOF system
x_{atmd}	active tuned mass damper displacement
x_b	displacement of the base
x_i	the i^{th} floor relative displacement
$\{\dot{x}\}$	velocity vector
$\{\ddot{x}\}$	acceleration vector
$\ddot{x}_g(t)$	earthquake ground acceleration
$\{\mathbf{1}\}$	$\mathbf{1} \times n$ unit vector

_____ Greek Symbols _____

α	Rayleigh damping coefficient in $[C] = \alpha[M] + \beta[K]$
β	damping ratio
ω	harmonic excitation frequency
ν_s	Poisson's ratio
ρ_s	soil density
η	ratio of the post yield stiffness to the elastic stiffness, or fluid viscosity

Glossary

ABS	Active Bracing System
AMD	Active Mass Damper
ATMD	Active Tuned Mass Damper
BI	Base Isolator
LQG	Linear Quadratic Gaussian
LQR	Linear Quadratic Gaussian
MDF	Multi Degree of Freedom
SDF	Single Degree of Freedom
N/A	Numerical / Analog
TLD	Tuned Liquid Damper
TLCD	Tuned Liquid-Column Damper
TMD	Tuned Mass Damper
PID	Proportional Integrator Derivative
FO-PID	Fractional Order - Proportional Integrator Derivative
SSI	Soil-Structure Interaction
AHA	Artificial Hummingbird Algorithm
GWO	Grey Wolf Optimization
ALA	Ant Lion Algorithm
DA	Dragonfly Algorithm
WOA	Whale Optimization Algorithm

General Introduction

Earthquakes and strong winds are a natural geological activity. They cause significant destruction and can damage civil structures and risk people's safety. In recent years, protecting these structures against natural hazards has become a subject of intensive research to ensure structural safety and to prevent the collapse of these structures. Where the main goal obviously is to protect these structures and provide safety to human occupants [1-3].

Earthquakes have always represented a significant challenge for construction engineering, which has always aimed at the implementation of safe and economic structures. The damage observed after several strong earthquakes such as El Centro 1940, Northridge 1994, Loma Prieta 1989, Kobe 1995, Athena 1999, Boumerdes 2003, and recently Mila 2020, showed the great importance of seismic design, but despite intense efforts in code design and construction resistant to winds and earthquakes, the structures are always vulnerable to the excitations of high intensity. Traditionally, structures are designed to be totally dependent on their own stiffness and their low damping rate to withstand the earthquake excitations and dissipate vibration energy. But since these structures have limited capacity of energy dissipation, they cannot adapt to every external environmental excitation, such as earthquake excitations or strong winds.

The introduction of structural vibration control devices is currently a solution of choice when it comes to protecting, improving, or reinforcing structures against the destructive effects of earthquakes [4][5][6]. Appearing at the end of the 80s and more and more widespread nowadays, these devices provide additional damping and dissipate more seismic energy by adding devices and systems to the structure in order to increase its strength to resist against natural hazard specially earthquakes. By implementing these vibration control devices our structure will be called "Smart structure". This recent technology is becoming of subject of intensive research to improve structure's safety and the lifetime [7-14].

Generally listed according to their modes of operation, these control systems can be classified as four categories: passive, active, semi-active and hybrid control systems [4].

In general, passive control systems are using the principle of distributing energy between the building and the system without the need for an external energy source, and as a result, the control system consumes a huge part of the vibration energy caused by the earthquake [5].

Passive control systems are considered to be less adaptable to frequency content excitations variable such as earthquakes. As an example of passive control, we have base isolators devices, which considered to be one of the widely used devices for structural vibration control. Those devices are placed and installed between the building and the foundation of the building, Base isolators can be implemented in many different building structures or bridges, they can be formed with the use of sliding bearings or elastomeric bearings. Under high intensity excitations, these devices can undergo a large deformation.

active for the systems of damping control controllable by an external energy source and hybrid for devices combining the two, which can be controlled but with a low input external energy.

Even if active control systems are introduced to avoid the inability of passive control systems to adapt to different operating conditions and powerful seismic excitations [9]. However, active control systems still have two main disadvantages. First, the need for an external source of power to operate, and second, active control devices (actuators) are very expensive. Therefore, Hybrid control systems are invented [10].

The hybrid vibration control system is a type of control that combines both passive control systems and active control systems, where the objective is to obtain the advantages of both the passive control system and the active control system, which is the passive system's robustness and reliability and the active system's adaptability [11][12].

This work consists of four chapters, the content of which will be briefly presented below:

The first chapter : in this chapter we will cite the different methods of structural vibration control as well as a historical overview of these methods.

The second chapter : is devoted to the mathematical development of the active and passive control of the seismic response of structures, we will present the analysis model of actively controlled structures, by control systems, using equation of motion and state-space representation as well.

The third chapter : In this chapter simulation results and numerical results are presented, In the first section a comparative study is done between a classical none tuned PID controller and an LQR controller, in the second section an optimized PID controller using grey wolf optimization is compared to a classical PID controller. In the fourth section an optimized Fractional-Order PID is compared to an optimized classical PID controller, the performance results will be evaluated using a hybrid vibration control to reduce the response of a 5-story building.

The fourth chapter : We end with a fourth chapter in which we will study the hybrid control with the effect of soil-structure interaction (SSI) in order to bring reality closer to the behavior of structures under seismic stresses.

Chapter

PRINCIPLES OF VIBRATION CONTROL SYSTEMS

1

CHAPTER 1 PRINCIPLES OF VIBRATION CONTROL SYSTEMS

1.1 Introduction

Civil engineering structures, such as skyscrapers, buildings, bridges, or towers, can be damaged severely or collapse when subjected to powerful earthquake or strong winds. For civil engineers, designing structures to withstand seismic damage is still difficult. Structures are still susceptible to severe winds or seismic excitations despite extensive efforts to create wind and earthquake-resistant designs in code development and construction. Also, due to the insufficiency of the proper damping of the structure, devices are added to the structure to increase its energy dissipation capacity. These structures are called "smart structures", which they don't rely only on its own characteristics to resist seismic excitations but also on embedded devices or systems. These smart structures technology has become an interesting alternative to increase security and functionality structures because it can greatly improve the seismic performance of structural systems [13-19].

Tuned liquid dampers (TLDs) or tuned mass dampers (TMDs) are passive control systems [20]. In general, passive control systems are using the principle of distributing energy between the building and the system without the need for an external energy source, and as a result, the control system consumes a huge part of the vibration energy caused by the earthquake [21].

Traditionally, vibrations have been passively reduced. This takes advantage of the physical properties of the structure. Vibrations can be attenuated by manipulation of mass, stiffness or geometric properties of structure, vibration isolation, Helmholtz resonators, shock absorbers, and many other techniques. Unfortunately, these methods lead to increased weight, poor response, and detection of low vibration energy. In this context, active control methods appear a priori more appropriate.

Even if active control systems are introduced to avoid the inability of passive control systems to adapt to different operating conditions and powerful seismic excitations [22]. However, active control systems still have two main disadvantages. First, the need for an external source of power to operate, and second, active control devices (actuators) are very expensive. Therefore, Hybrid control systems are invented [23].

The hybrid vibration control system is a type of control that combines both passive control systems and active control systems, where the objective is to obtain the advantages of both

the passive control system and the active control system, which is the passive system's robustness and reliability and the active system's adaptability [24-25].

In this chapter, we will present the basics of seismic response control of structures from their equations of motion then, the state of the art of various research that have been carried out in this line of research is given. Afterwards, we will explain the different control systems and methods, which are passive, active, semi-active and hybrid (as shown in figure 1.1).

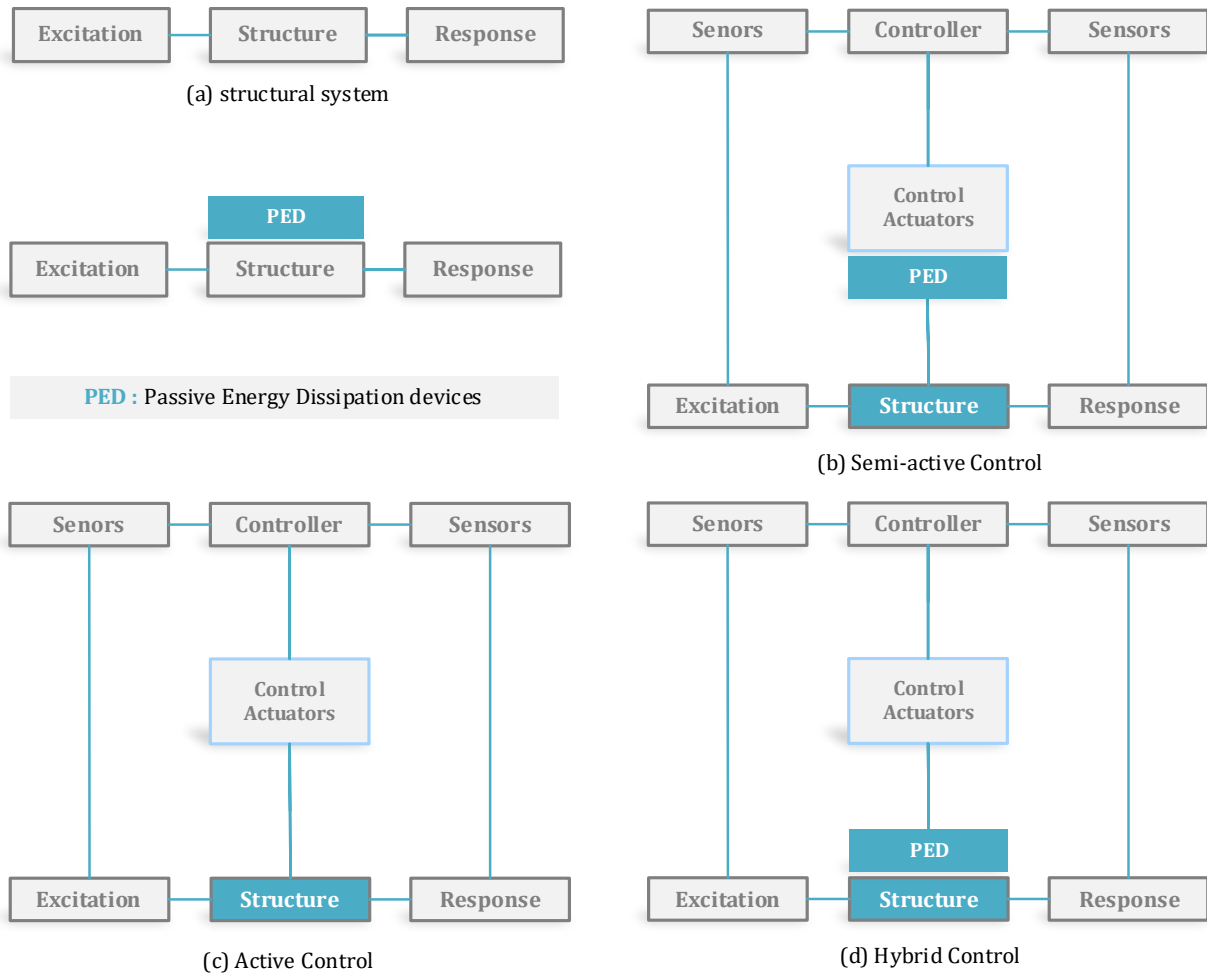


Figure 1.1 : Different vibration control types

1.2 History

The addition of systems to structures for vibration suppression has a long story. Passive dampers emerged in the 1900s. An application recent use of these shock absorbers in the field of civil engineering has been found in towers with elevated water reservoirs [26]. Passive dampers were available in the trade since the 1970s and have been widely applied for the suppression vibrations in automobiles, aircraft and civil engineering structures. The modern control technologies and adaptive systems are also mature in the mechanical and electrical

industries. However, structural technology intelligent in civil engineering, for controlling the response to the wind and earthquakes, was not done until the 1950s [27] because it is a very difficult to develop control systems for large structures importance.

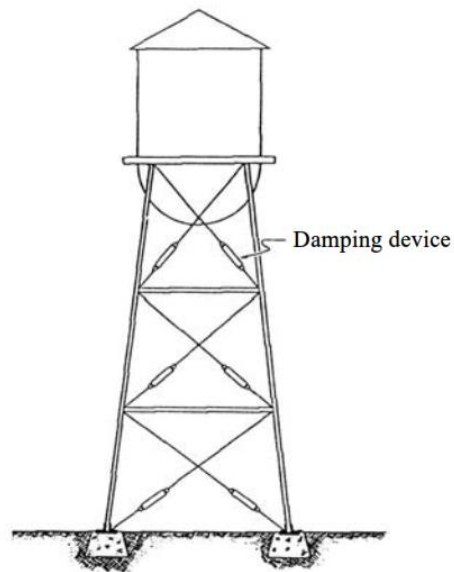


Figure 1.2 : Water tower with damping devices

The concept of controlling the seismic response of structures originated in the 1950s with the Japanese researchers Kobori and Minai [28]. They found a result important regarding the seismic response control that must be done on the extremity of the reception of the response of the structure. While Yao [29] found that in such structural system, earthquakes and winds are not only countered by structural members, but also by an external controlling force.

Remarkable progress has followed these initial concepts in controlling the seismic response of structures.

Japan has taken the lead in the practical application of control systems for structures. In 1985, tests on the control system were started to progress towards practical applications. In 1989, an active mass damper granted (Active Tuned Mass Damper, ATMD) was installed in a building to reduce its seismic response. The ATMD system has been verified by real-time observation and numerical simulation [30].

In the United States, under the direction of the NSF (National Science Foundation), following support large number of different earthquake control research projects, a group of American experts in structural control research was officially established, and a 5-year research program was launched in 1992 for the safety, performance, and risk mitigation [31].

1.3 Different control systems

1.3.1 Passive control

Passive damping techniques, structural vibrations, use the integration or addition of materials or systems, possessing properties damping, coupled to the structure in such a way that the vibrations of the structure are damped passively, i.e. without any external intervention additional and without energy input from outside [32]. Mainly, there are two categories of passive systems: the first is **base-isolation systems** (such as base-isolators) and the second is **Passive energy dissipation systems** (such as TMD, TLD, friction dampers, viscous fluid dampers...) [33].

1.3.2 Base-isolation systems

1.3.2.1 Introduction

Base-Isolation system is a well-known application of the passive control approach. These systems consist of placing, between the foundations and the superstructure, they have very high horizontal deformability and a very high vertical stiffness. These devices make it possible to decouple the movement of the ground from the superstructure whose purpose is to reduce the forces transmitted to it, as shown in Figure 1.3.

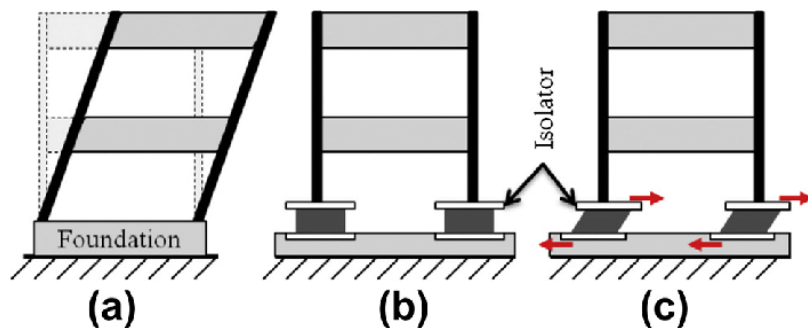


Figure 1.3 : Base isolation system

The isolators absorb inelastic deformations and filters high frequency accelerations from such that the insulated superstructure essentially moves in a rigid mode undergoing low accelerations and almost no deformations [34]. Thus, the insulation of the base is an effective tool to ensure the seismic protection of rigid structures because they are characterized by high frequencies (see figure 1.4).

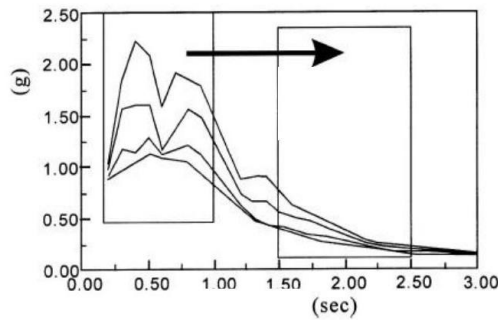


Figure 1.4 : Principle of operation of para-seismic bearings

Several types of para-seismic bearings exist. Some have already been used, while others have remained at the stage of theoretical studies. According to their mode of operation, they can be classified into several categories:

- Deformation supports.
- Sliding supports.
- Deformation and sliding supports.

1.3.2.2 Elastomeric Bearings

Elastomeric bearings are made from natural rubber, their properties and performance were improved later on with adding plates made with steel, known also as steel shims. Adding this steel shims can reduce greatly the vertical deformation of the elastomeric bearings, compared to using only pure rubber, and it can also preserve the rubber layers from being laterally bulging. Figure 1.5 represents an elastomeric bearing with steel shims. The natural rubber layer width can be between 3 to 7.5 inches, while the steel shims thickness is approximately 1 inch [16,35-37].

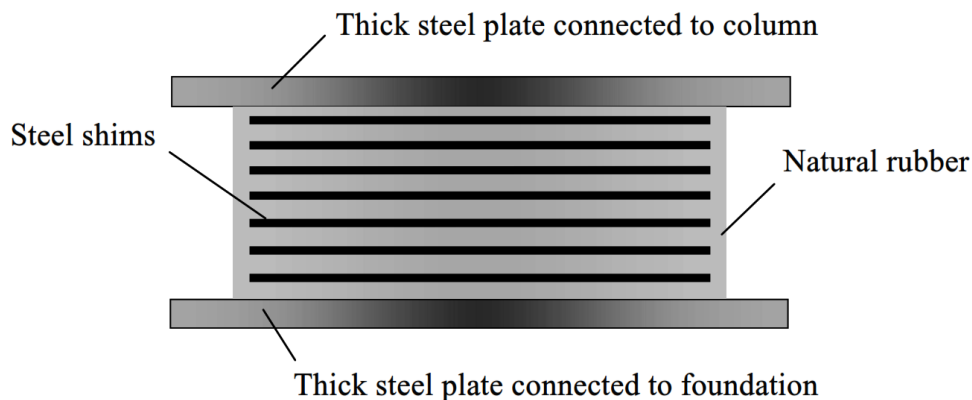


Figure 1.5 : Elastomeric bearing with steel shims

Synthetic rubbers, such as neoprene, can be used as an alternative to natural rubber during the manufacture of the bearings. The two types of rubber properties are very stable and do not show long-term creep under load. The elastomeric bearings have been used successfully in buildings and other structures such as bridges. They have worked well for over 50 years of service.

Due to the flexibility of the rubber and the long elastic deformation distance of the shear, the critical damping of elastomeric isolators only varies from 2% to 3%. By Therefore, elastomeric isolators are also called low damping isolators [16,36,38].

Elastomeric bearings are easy to manufacture, and the cost of manufacturing and maintenance is relatively low compared to other types of isolators. In addition, their mechanical properties are independent of temperature and aging. However, due to the low damping critically, elastomeric isolators have little service load resistance, and additional damping devices is needed to control large sideways movements [16,37].

1.3.2.3 Lead Rubber Bearings

The disadvantages of elastomeric bearings being weak can be solved by inserting a lead bar into the layers of the insulator.

A pre-formed hole, slightly smaller than the lead bar, is usually located in the center of the elastomeric bearing. Once the lead bar is fitted in the made hole, the two parts become a unit and form a lead bar rubber insulator (LRB-Lead Rubber Bearing) as shown in Figure 1.6.

The performance of LRB isolators depends on the imposed lateral force. If the lateral force is small, the movement of the steel plates are restrained by the lead core and the support presents high lateral stiffness. When the lateral force becomes larger, the steel plates force lead core to deform or yield, and hysteretic damping is developed with the energy absorbed by the lead core. Therefore, the lateral stiffness of the insulator is scaled down. The equivalent damping of LRB isolators ranges from 15% to 35%. A bilinear model or non-linear is generally used to describe the mechanical properties of LRB isolators [39-42].

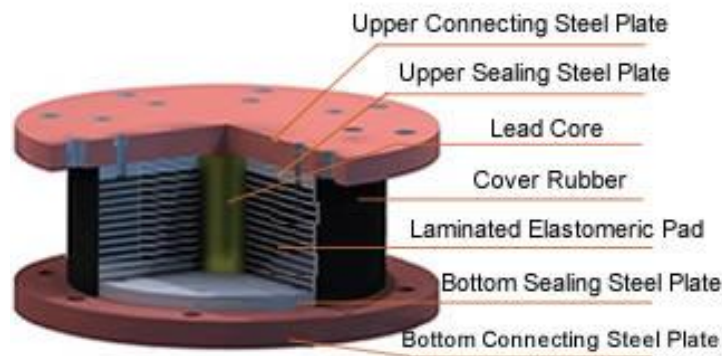
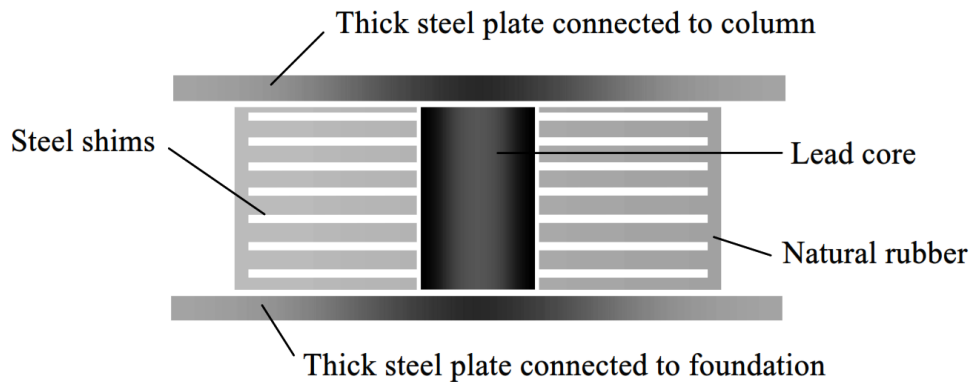


Figure 1.6 : Lead Rubber Bearing

1.3.2.4 High-Damping Rubber Bearings

Another effective method for increasing the damping of elastomeric bearings is to modify the composition of the rubber (either natural or synthetic). For example, the addition of carbon black or other types of rubber additives alter the properties of the rubber and gives higher damping results.

An elastomeric insulator with a high damping rate is composed solely of a layer of rubber and steel, but it has the flexibility and energy dissipation capacity necessary. Figure 1.7 shows an elastomeric bearing with a high damping rate [43,44].

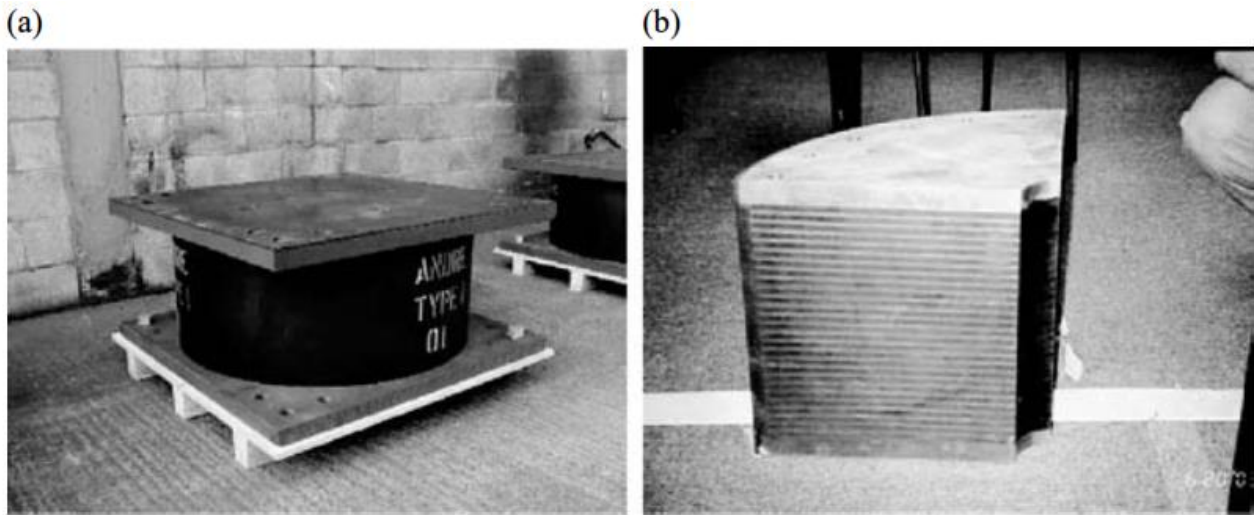


Figure 1.7 : (a) High-Damping natural rubber bearing (b) a section cut

1.3.2.5 Friction Pendulum Bearings

Friction bearings have flat sliding surfaces. The imposed lateral force is countered by the product of the coefficient of friction and the vertical load applied to the bearing surfaces [45].

The major disadvantage of the friction bearing with flat sliding surfaces is that the structure is unable to return to its original position after an earthquake. This is due to the fact that once the imposed lateral force is less than the resistance generated by friction, the movement of the structure stops and causes a certain distance of the structure from the center of the insulator [45,46].

After the initial shaking may force the building to move from the stationary position and even further from the original position. As a result, building movement can exceed the surface of the insulator and cause its failure.

To reduce the distance to the center of the isolator after an earthquake, a friction isolator with a spherical or concave sliding surface has been developed. This type of insulator is called friction pendulum bearing and is shown in Figure 1.8 [16].

The spherical sliding surface is usually coated with teflon with a coefficient of friction of about 3%. The imposed lateral force pushes the bearing in both horizontal and vertical directions and a Once the lateral force disappears, a restoring force is generated [47]. A component of the vertical load applied along the tangential direction to the surface spherical helps the bearing move towards the center. The movement stops when the friction is equal to or greater than the applied vertical load component.

A notable feature of the pendulum friction bearing, called static friction, is that the lateral force required to initiate sliding is greater than that required to maintain the slide [16,46].

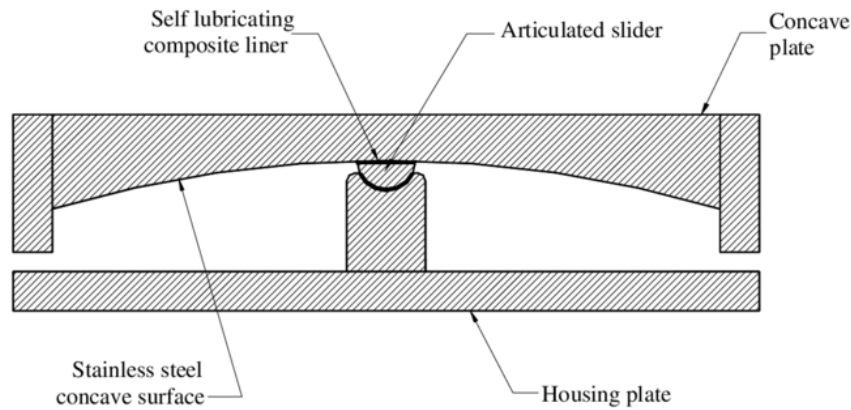


Figure 1.8 : Friction pendulum isolator

The pendulum friction bearing has the advantage of low maintenance. Teflon coated on steel stainless steel effectively protects the sliding surface against corrosion. as the insulator only slips during an earthquake, the Teflon coated can last the life of the insulator. In In addition, the effects of aging and temperature variations seriously affect the mechanical properties of the bearing [48].

A double concave surface friction bearing has recently been developed. Figure 1.9 shows schematically this type of insulator. Comparing to friction pendulum bearing with only one concave surface. The use of double concave surfaces can result in the same distance of horizontal movement with an insulator surface this is due because the horizontal movement is provided by the upper and lower sliding surfaces [49,50].

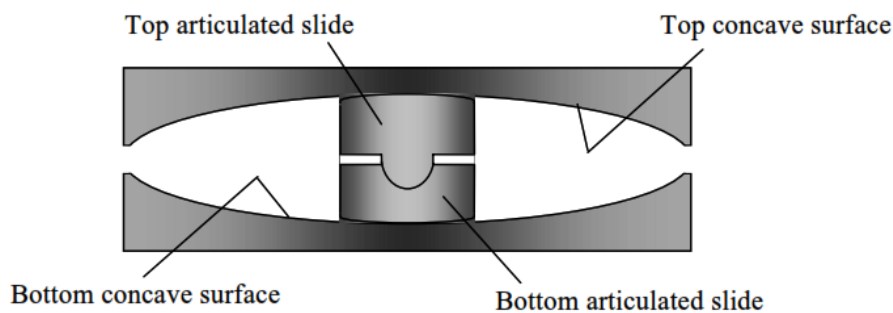


Figure 1.9 : Friction pendulum bearing with double concave surface

1.3.3 Passive Energy Dissipation Systems

1.3.3.1 Introduction

Passive energy dissipation systems have the same basic principle as that of seismic isolators when incorporated into the structure: they can absorb a portion of the external excitation energy. Additionally, they can reduce substantially the differential movement between the elements of the structure and by consequently reduce the damage of the latter [51-53]. In recent years, efforts seriously have improved the concept of energy dissipation systems, and several devices have been installed in structures all over the world. In general, they are characterized by their ability to dissipate vibrational energy from the structure or convert to another mode of vibration or another form of energy [54,55]. The main systems are:

- Metallic Yield Devices
- Friction Dampers.
- Viscoelastic Dampers.
- Viscous Fluid Dampers.
- Tuned Mass Dampers (TMD).
- Tuned Liquid Dampers (TLD).

1.3.3.2 Metallic Yield Devices

In the 1970s, researchers initiated conceptual and experimental work on metallic devices, since the inelastic deformation of metals can be a perfect mechanism for energy dissipation, this concept led to the idea of installing metallic hysteresis behavior devices separated in a structure to absorb seismic energy. Metal hysteretic damper devices generally exhibit stable hysteretic behavior, low cycle fatigue, long term reliability and relative insensitivity to ambient temperature [56, 57].

Conceptual and experimental works on metallic hysteretic devices were initiated by *Kelly et al.* [2], *Skinner et al.* [58].

A widely known model is the ADAS device (Added Damping and Stiffness) is illustrated on Figure 1.10. This system consists of several X-shaped steel plates, and the deformation occurs along the entire length of the device. Rigid boundary elements are used in such a way so that the X plates are deformed in double curvature. The implementation of shock absorbers metal hysteresis for large-scale structures started in New Zealand in the 1970s.

Since then, various metallic hysteretic damper devices have been used to improve the seismic design of new structures or to upgrade the seismic capacity existing structures *Aiken et al.* [59], *Aiken et al.* [60], *Martinez-Romero* [61]. The devices of Metallic hysteretic dampers typically exhibit hysteretic behavior stability, low cycle fatigue, long term reliability and relative insensitivity to ambient temperature. However, they cannot absorb more energy during their initial elastic behavior. Energy dissipation occurs after a large inelastic deformation. In addition, metallic yield dampers behave non-linear way; they increase structural strength, in addition to damping. This behavior complicates analysis and requires an iterative design process.

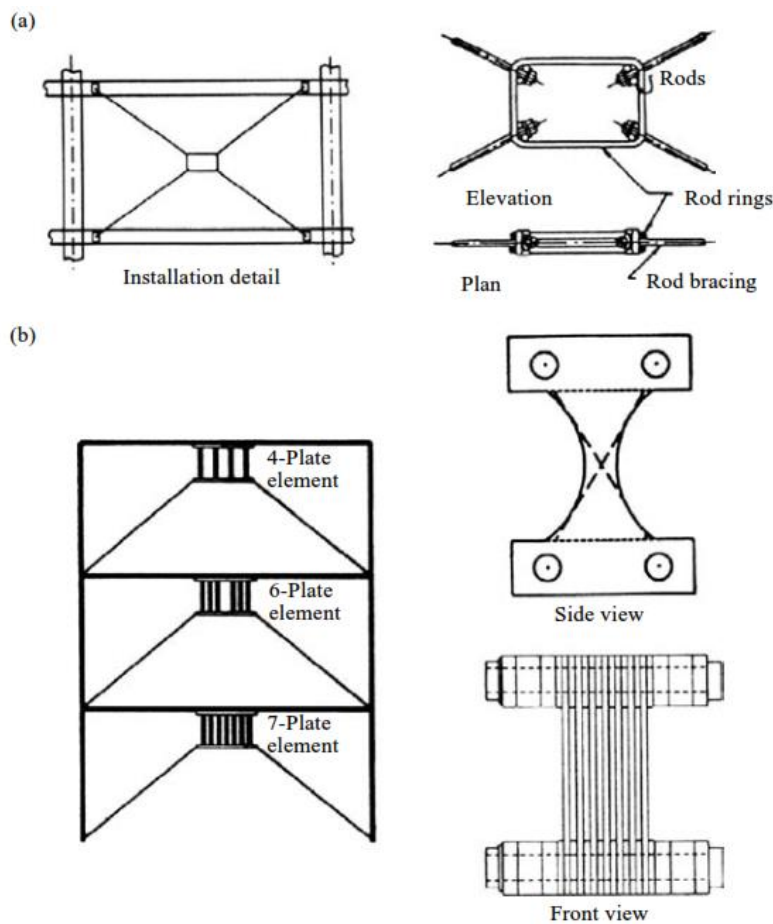


Figure 1.10 : Typical types of metallic yield dampers: (a) Tyler's yielding steel bracing system and (b) added damping and stiffness (ADAS) device.

1.3.3.3 Friction Dampers

These devices use the friction created by sliding between two surfaces to dissipate the energy of seismic vibrations. Their friction is based on a hysteresis loop. Most of these devices

produce rectangular hysteresis loops. The friction of these shock absorbers resembles that of Coulomb.

Generally, these mechanisms have a better performance, and their behavior is less sensitive to frequent loadings, to the number of loading cycles and to temperature variation [62,63]. In addition, these mechanisms have a high resistance to fatigue.

Several friction devices have been applied to many constructions to improve seismic protection.

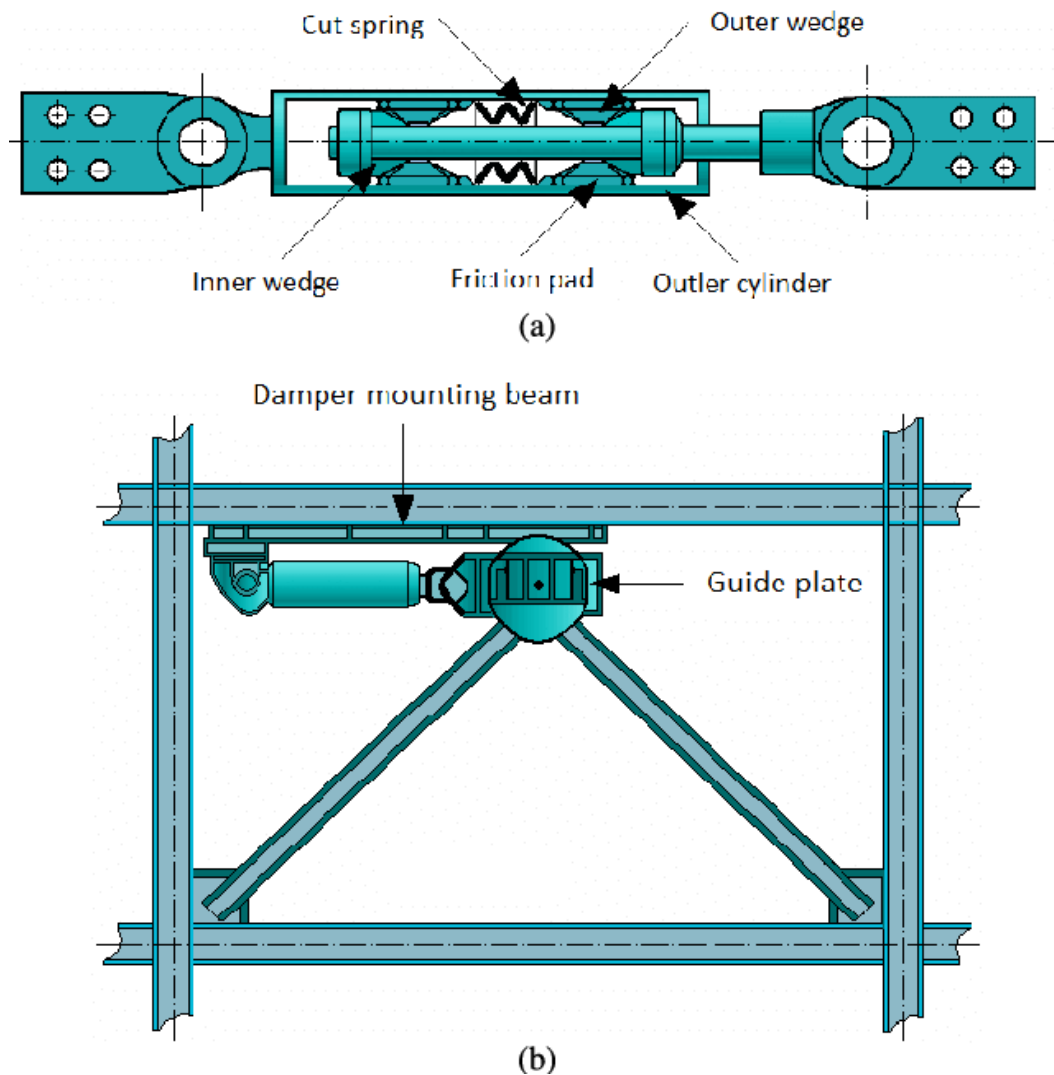


Figure 1.11 : Friction Damper, (a) Sumitomo-type friction damper [59] and (b) its installation [60].

1.3.3.4 Viscoelastic Dampers

Viscoelastic dampers commonly use polymeric or rubbery materials. Viscoelastic materials used in structural application to absorb energy when subjected to shear deformation.

Figure 1.12 shows a viscoelastic device which consists of two layers of polymer sandwiched between a central plate and two outer plates [64]. Once the device is installed in a structure, shear deformation, and therefore energy dissipation, respectively. Shear deformation occurs and energy is dissipated when the structural vibration induces relative motion between the outer steel flanges and the center plate. Applications of VE dampers can be found in References [13] and [65].

These systems are particularly effective at high and low frequencies, in particular to protect buildings subjected to strong winds or earthquakes of medium intensity.

Studies have shown that these devices not only add damping to the system but also stiffness, thereby increasing the natural frequency of the structure [66].

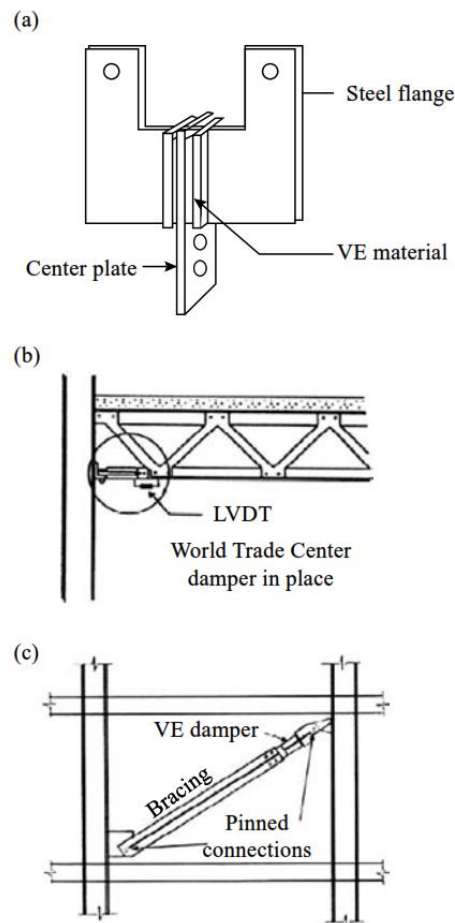


Figure 1.12 : Viscoelastic (VE) damper: (a) damper detail, (b) installation as chord, and (c) installation as diagonal bracing.

Moreover, the properties of the damper (modules of conservation and losses analogous respectively to a constant spring and damper) depend on the frequency and the temperature

of the environment. However, research shows that these properties remain fairly constant with deformations of less than 20%, for a fixed temperature and frequency [67].

Due to temperature dependence, these devices cannot be effective in structures where the climate is not continuously controlled [68].

Viscoelastic dampers were first applied in the Twin Towers of the World Trade Center in New York in 1969 in an attempt to reduce movement under wind loads.

In Japan, these dampers have also been installed in several constructions, such as the Seavans tower in Tokyo (1991) and the Goushoku Hyogo distribution center (1998), for which the viscoelastic dampers make it possible to reduce the seismic response by half [69].



Figure 1.13 : Twin Towers of the World Trade Center in New York

1.3.3.5 Viscous Fluid Dampers

These devices are widely used in the aerospace field (satellites) and for military applications. They are characterized by linear viscous damping over a wide frequency band and insensitivity to temperature [70].

Fluid viscoelastic devices, which work by shearing viscoelastic fluids, have behaviors that resemble those of solid viscoelastic devices, except that fluid viscoelastic dampers do not exhibit stiffness when static loads are applied [71; 72]. These devices can be modeled with Maxwell's model (Figure 1.14), which consists of a spring and a damper mounted in series [71-73].

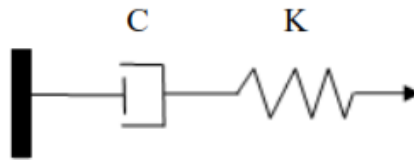


Figure 1.14 : Maxwell Model [71].

The most promising viscous fluid damper design is shown in Figure 1.15. A simple design is achieved with a conventional damper and dissipation occurs by converting kinetic energy into heat as the piston moves and deflects a highly viscous fluid. The fluid viscous damper was manufactured by Taylor Company and used as a component of *Hüffmann* seismic isolation systems [74]. Relative movement of the damper piston toward the damper housing drives viscous damper fluid rearward through the orifice. The energy is dissipated by the friction between the fluid and the orifice.

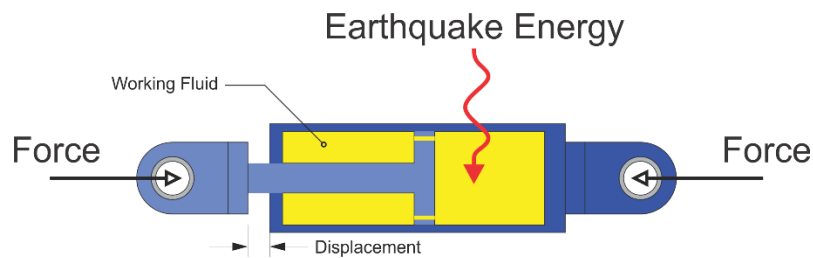


Figure 1.15 : Example of Viscous Fluid Damper

If the fluid is purely viscous (Newtonian), the force of the damper is directly proportional to the speed of the piston. However, for a wide frequency band, the damper has a viscoelastic behavior. The simplest model to represent this behavior is that of Maxwell. Other researchers like Makris and Constantinou (1991) [75] have developed another more general model than that of Maxwell which can be expressed in the following form:

$$f + \lambda^r D^r[f] = c_0 + D^q[x] \quad (1.1)$$

Where:

- f : is the external force.
- λ^r : is the relaxation time.
- c_0 : is the damping constant.
- x : is the displacement of the piston.
- q : is the material constant.

$D^r[f]$ and $D^q[x]$ are fractional derivatives and if $r = q = 1$, the model is equivalent to the Maxwell's model.

A viscous damping system has been developed by construction company Sumitomo in Japan which is called “viscous damping walls”. This device has been used in several constructions.

By using these viscous damper walls, significant reductions, between 33% and 75%, were observed in acceleration responses during earthquakes [76].

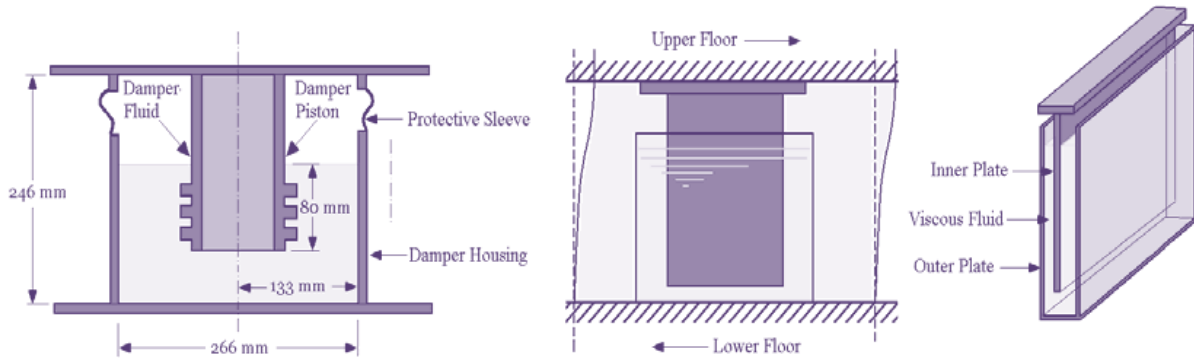


Figure 1.16 : a) Cylindrical container fluid damper, b) the viscous damping wall [77]

1.3.3.6 Tuned Mass Dampers (TMD)

In recent years, to control the vibrations of structures, several control devices have been developed. Among these devices, Tuned Mass Dampers (TMD) which are most commonly used in various fields of application in civil engineering such as buildings and structures, allowing the reduction of oscillations caused by earthquake or other causes [78]. This is attached to the structure to reduce the dynamic response of the structure. The damper is "tuned" because its frequency is tuned to a particular value such that when the frequency is excited, the damper will resonate out of phase with the movement of the structure, thereby absorbing energy on the structure [79]. The research efforts started by **Frahm (1911)**, **Ormondroyd et al. (1928)** and **Den Hartog (1947)** are among the first application studies of this device to different mechanical systems.

Tuned Mass Dampers (TMD) are widely used nowadays for passive control. They have been developed in many fields of application such as automotive, aeronautics, ships, buildings, and engineering structures [80].

TMDs are widely used in industry or generally in mechanical systems. The application of a tuned mass damper in building structures is more complex because the structures are very

heavy such as bridges and buildings. The vibrations of the main structure can cause the movement of the TMD, part of the energy transfers to the vibration energy of the TMD. The damping of the TMD dissipates its vibration energy, and vice versa, the vibrations of the structure are attenuated by TMD damping [80,81].

TMD is a simple, effective, inexpensive, and reliable device for suppressing undesirable structural vibrations caused by earthquake excitations or strong winds. Its effectiveness depends on the mass ratio, the frequency ratio, and the damping ratio of the AMA [82].

The first construction equipped with an TMD is the CN Tower in Toronto (Canada).

TMDs can be designed mainly in two forms, the best known of which is that formed by a mass attached to the main structure using a spring and a damper (mass-spring-damper). We can cite the vertical TMDs installed under the deck of the Millennium footbridge in London (Figure 1.17) in order to correct the effect of excitations induced by pedestrians.

A second type of TMD is that with a pendulum tuned mass (Figure 1.18). The best-known use of this type of shock absorber is that of the 730-ton pendulum in the Taipei Tower in Taiwan.



Figure 1.17 : Vertical TMDs installed under the deck of the Millennium footbridge in London

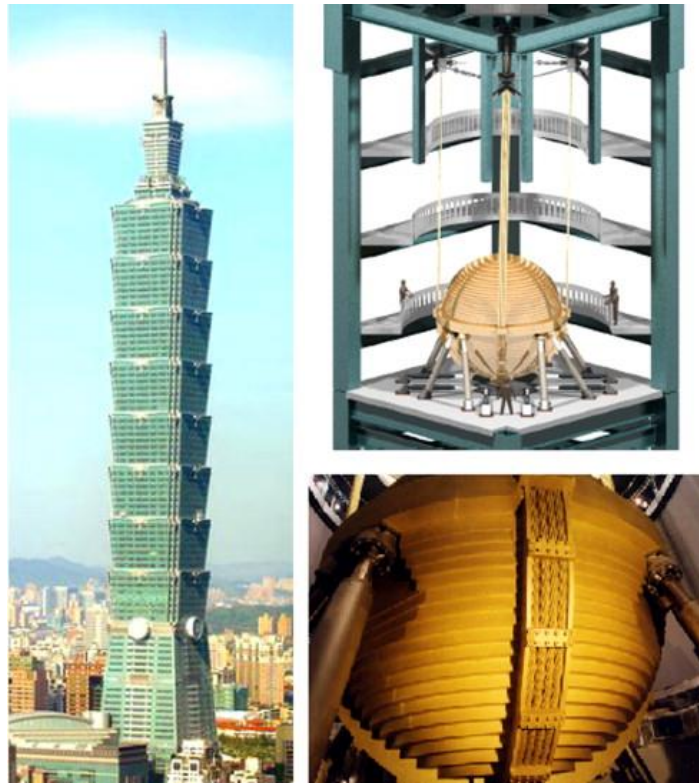


Figure 1.18 : The Taipei 101 skyscraper with the tuned mass damper

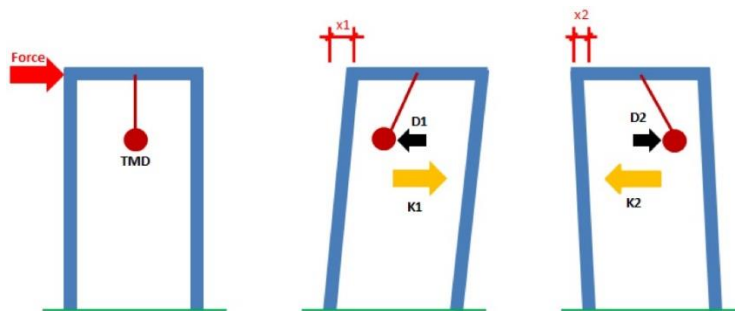


Figure 1.19 : The mechanism of a TMD

Generally, the wind excites the low frequency modes. This is how *Mansfield (2004)* [83] developed the design of an TMD reducing the motion of the structure at low frequency.

McNamara (1977) [84] studied the effectiveness of an TMD under wind excitation, placing this type of damper in the City Corp Center building at a height of 278 m.

A large number of AMAs have been installed in skyscrapers and chimneys in order to reduce the vibration responses of structures subjected to dynamic excitations.

There are also various constructions equipped by TMDs in the USA. The 67.5 m Washington airport control tower and the 241 m John Hancock airport control tower in Boston. In Japan, the first TMD was installed in the “Chiba Port” tower.



Figure 1.20 : Sydney Tower (center point)



Figure 1.21 : Citicorp Center New York



Figure 1.22 : Control Tower (Washington Airport)



Figure 1.23 : John Hancock Tower (Boston)



Figure 1.24 : Chiba Port Tower (Japan)

1.3.3.7 Tuned Liquid Dampers (TLD)

The Tuned Liquid Damper is another type of dynamic absorber for reducing structural vibration. Water or another liquid acts as the moving mass in a TLD, while gravity produces the restoring force. The TLD is shaken by the structural vibration, which also causes the liquid within the container to move. Structural vibrational energy is absorbed by the turbulence of the liquid flow and the friction between the liquid and the container, which turns fluid dynamic energy into heat. Note that neither a TLD nor a TMD have sophisticated mechanisms; rather, they all work on the same basic principle to absorb the energy of structural vibration. The distinction is that the liquid supplies all of the auxiliary system properties of a TLD, including mass, damping, and stiffness [85].

TLDs were first used on ships, and in the 1980s, they were also used to regulate vibration in civil engineering constructions [86,87]. Figure 1.25 depicts two common TLD kinds. The sloshing damper inserts meshes or rods into the liquid to offer damping capability, and the liquid's depth or container size are used to modify the damper's natural frequency. The air pressure and column shape are used to modify the natural frequency of the turbulence created by the column damper at high flow rates through the orifice. To lessen structural vibration in all directions, cross-tube containers can be fitted with the TLD column [88].

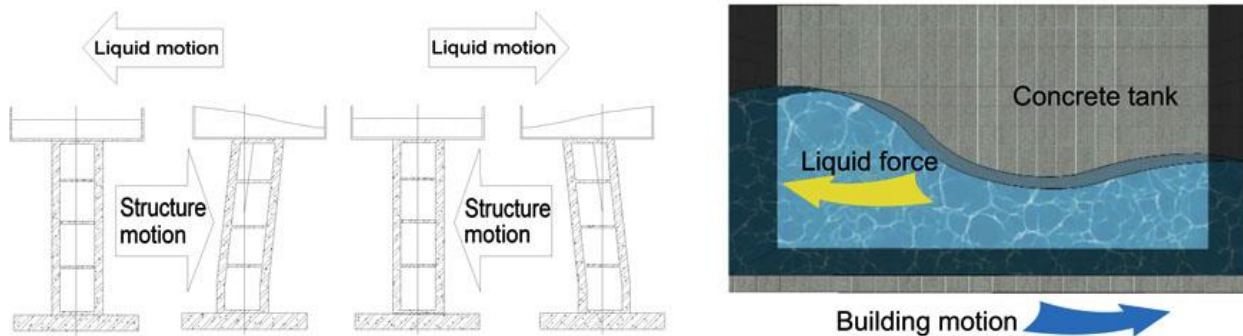


Figure 1.25 : Tuned Liquid Damper working principle

Similar to TMD, TLDs have been utilized to reduce wind-induced vibrations in thin structures like skyscrapers and airport towers [89,90]. TLDs offer two benefits. The water used for TLD can have a dual purpose by serving as part of the supply for building fire prevention in addition to being effective in any direction of lateral vibration. TLDs, however, have two disadvantages. Liquids have a lower density than TMD materials like concrete or steel, therefore they take up more room. Due to sloshing, TLDs also exhibit a strong no response

linear. The design and analysis processes for TLD systems are made more difficult by this system's innate nonlinearity.

There are two primary types of tuned liquid dampers (TLDs), known as tuned sloshing dampers (TSDs) and tuned liquid column dampers, and they can be used as active or passive devices (TLCDs).

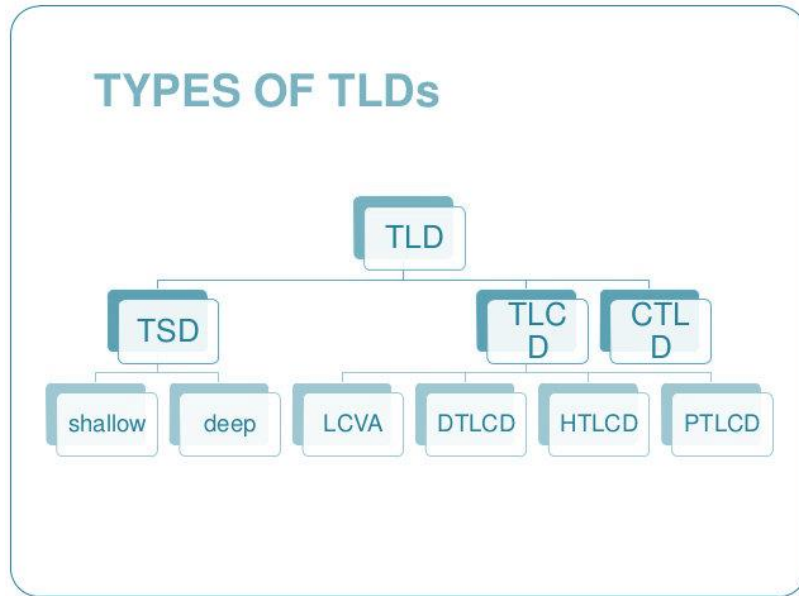
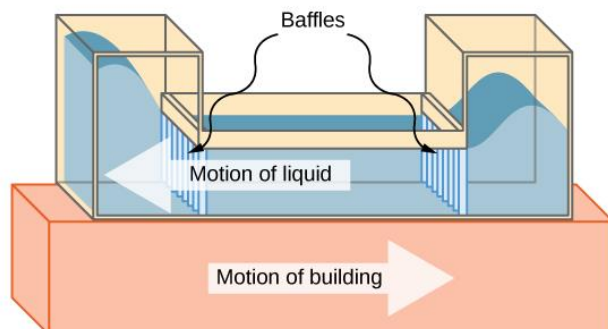


Figure 1.26 : TLDs types

TSD: Tuned Sloshing Damper, TLCD: Tuned Liquid Column Damper, LCVA: Liquid Column Vibration Absorbers, DTLCD: Double Tuned Liquid Column Damper, HTLCD: Hybrid Tuned Liquid Column Damper, PTLCD: Pressurized Tuned Liquid Column Damper.



(a)



(b)

Figure 1.27 : Tuned Liquid-Column Damper (Comcast building in Philadelphia).

Figure 1.27 (a) In Philadelphia, Pennsylvania, the Comcast Building towers over the cityscape at a height of about 305 meters (1000 ft). Due to earthquake activity and shifting winds, the top floors might sway back and forth at this altitude. Figure 1.27 (b) An illustration of a tuned liquid-column mass damper with a 300,000-gallon water reservoir built at the top of the Comcast building is shown above. Its purpose is to dampen oscillations.

1.4 Active control

Due to the limits of the passive control systems, like being insufficiently adaptive to earthquake excitations, and some of them, like tuned (mass/liquid) dampers can be only effective to reduce the structural vibrations with one dominant mode. Some systems, such as TMDs and TLDs, are only effective in a narrow band of frequency because they are designed on the frequency of the first mode of the structure. These systems can be applied to the vibration suppression of structures under the excitations whose first mode dominates the response, but they lack the ability to control the seismic response in the case where several modes are important. The intelligent structures using passive systems have limited intelligence as they are unable to adapt to the excitation and the overall structural response. From where the appearance of active control.

For all previous mentioned reasons, a more adaptive and powerful system is needed, this system is called an active vibration control system. Active control uses special devices, called actuators, to control and reduce the responses of the building. Different sensors are mounted on different floors to collect the structural responses (displacement, velocity, and acceleration), later on, this data will be sent to a computer (controller). The computer will generate a controlling signal and send it to the actuators, this last one is known as the control force. This control force is directly applied to the building. Control algorithms are very important to control structural responses, many control algorithms have been proposed by scientists and researchers, and their performance and efficiency have been proved by different studies and experiments [91,92].

Active control emerged in the 1930s and was developed with advances in microprocessors. In recent years, there has been a growing interest in active control in civil engineering, making it possible to reduce the effects of external forces on structures such as buildings, bridges and control towers, external forces such as earthquakes, strong winds or even traffic. An active control system can be defined as a system that generally requires a significant source of energy for the operation of electro-hydraulic or electro-mechanical actuators that provide

control forces to the structure [93-95]. This system has the basic configuration shown in Figure 1.28.

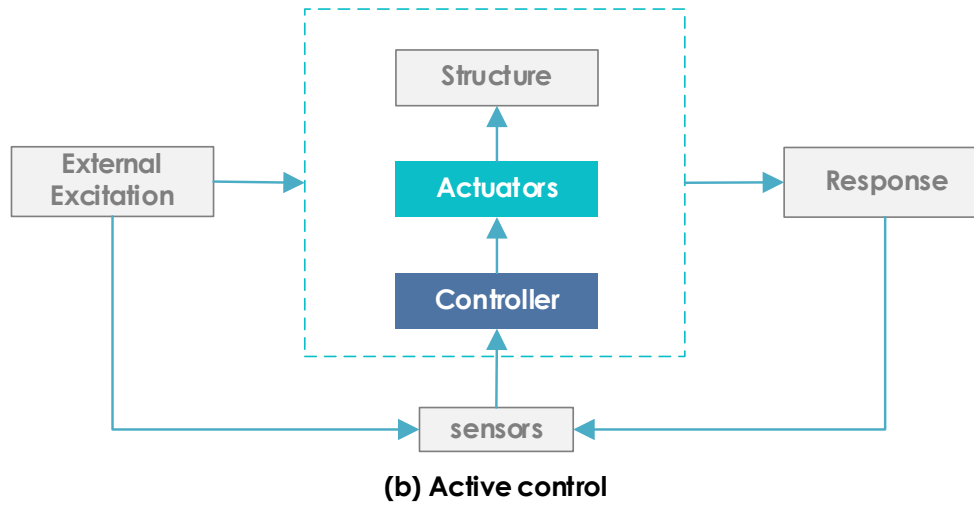


Figure 1.28 : Schematic diagram of an active control system.

Control forces are developed based on feedback from sensors that measure the excitation and/or response of the structure. Structural response feedback can be measured at locations other than the location of the active control system. The generation of control forces by electro-hydraulic actuator requires a significant source of energy, which is of the order of tens of kilowatts for small structures and can reach several megawatts for large structures [93, 94].

An active control system requires, on the one hand, a network of sensors in order to know the vibratory state, and on the other hand, a set of actuators to act on the structure to be controlled by applying forces on it. according to a control law. To ensure proper operation, these actuators use a significant source of external energy.

Active control systems include active mass dampers (AMD), active tuned mass systems (ATMD), active tendon systems, active bracing systems, and active variable stiffness systems; some of which we will present in what comes. These systems have been successfully used for aircraft, spacecraft, mechanical devices and various structures over the past two decades.

Active systems are more complex than passive systems [95-96], since they rely on computer control, motion sensors, feedback mechanisms, and moving parts that may require service or maintenance [94]. The general idea of active control is revolutionary. It has the ability to elevate structural concepts from a static and passive level to a dynamic and adaptable level [97]. Studies carried out on the application of active control systems in civil engineering have shown their effectiveness in reducing structural responses. The advantage of an active control

system is that it achieves excellent control results. However, there are many disadvantages to using this system: They are very expensive systems to design and are expensive to operate due to the large amounts of energy they require. Also, they tend to take up more space than passive monitors.

1.4.1 Active Tendon Systems

The active tensioner system generally consists of a set of prestressed tensioners (cables) whose tensions are controlled by electro-hydraulic servomechanisms [98,99]. Active tensioner control has been studied analytically in connection with the control of slender structures, tall buildings, bridges and offshore structures [100].

Figure 1.29 shows a schematic of a tendon controller. It consists of four cables and a hydraulic actuator. The cables are attached to the upper floor by one of their ends while the other ends are attached to a rigid horizontal frame by four pulleys. The structure is connected to the piston rod of a hydraulic actuator whose movement is controlled by a servo valve proportional to the difference between the analog signal and the actual displacement of the piston/rod. In this way, the cable tensions are actively modified, and produce horizontal control forces on the structure [101].

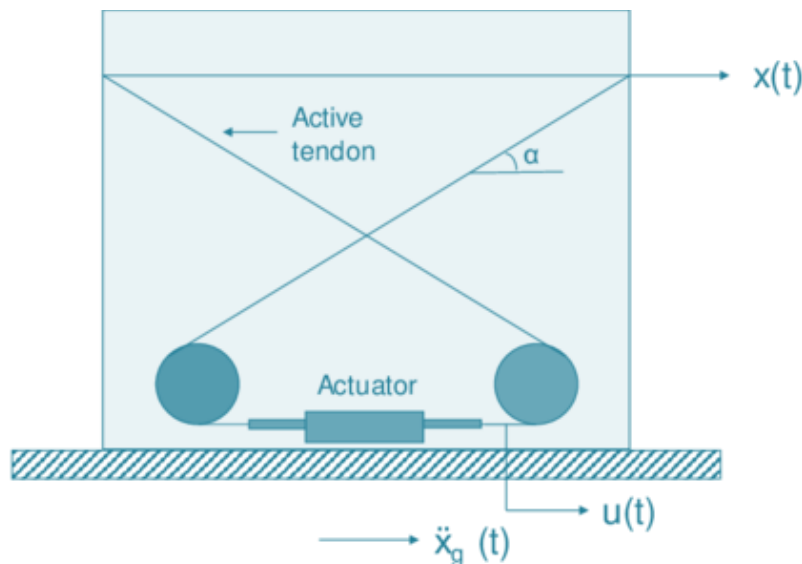


Figure 1.29 : Active tendon system.

1.4.2 Active Brace Damper

The active bracing system can make use of existing structural elements and thus minimize extensive additions or modifications to a built structure. This is attractive, for example, in the case of retrofitting or reinforcing an existing structure [16,102,103].

The control system allows the longitudinal expansion and contraction of the struts by hydraulic actuators. Inserted between the bracing elements and forming an internal part of the bracing system. The control system also includes hydraulic power force, analog and digital controller and analog sensors [104].

This system uses existing bracing elements to install an active control device on the structure. There are three types of bracing systems, either diagonal, K or V. A hydraulic actuator, is mounted above the bracing system and attached to the floor, is capable of generating a large control force. Figure 1.30 shows this system, which includes a servo valve, hydraulic actuator, external energy, sensors and control computer with a predetermined law. The sensors measure the movement of the structure due to seismic excitation. The control computer uses the control algorithm to process these measurements to generate the control signal. Then, the servo valve uses the control signal producing a pressure difference between the two chambers of the actuator.

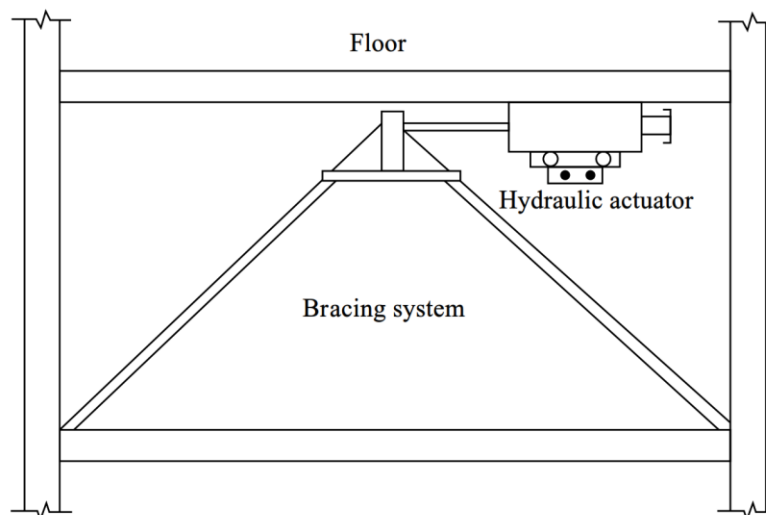


Figure 1.30 : Active bracing system with hydraulic actuator [16].

1.4.3 Active Tuned Mass Damper (ATMD)

Active Tuned Mass Dampers (ATMD) are widely used today for active control. They have been developed in many fields of application such as automotive, aeronautics, ships, buildings, and engineering structures.

The ATMD active tuned mass damper evolved from the TMD with the introduction of an active control mechanism. It is known that TMD dampers are only effective in structural response control when the first mode is dominant, such as wind-induced structural vibrations. The development of ATMDs focuses on the search for the control of the structural seismic response with a wide frequency band.

According to the literature, structures equipped with an active ATMD demonstrate increased efficiency compared to structures equipped with a passive TMD.

ATMD dampers were proposed in the early 1980s and were studied by *Yang et al.* [105], *Nishimura et al.* [106]. A conceptual model of an ATMD-controlled structure is shown in Figure 1.31, with a schematic comparison of ATMDs and TMDs. An actuator is installed between the primary system (structure) and the system (TMD). The movement of the secondary system can be controlled by the actuator to increase the efficiency of the device.

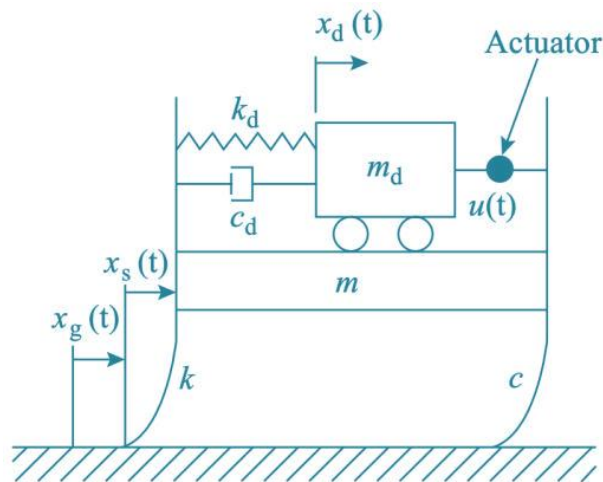


Figure 1.31 : An active tuned mass damper system [16].

The analytical study aims to know how to operate the actuator to attenuate the response of the primary system most efficiently with the optimal control law to find the appropriate feedback gain of the ATMD *Chang and Soong* [107].

Researchers have also conducted extensive shake table testing of ATMD dampers for seismic response control and their full-scale implementation *Soong T.T et al.* [108], *Soong and Spencer* [14], *Chung et al.* [109], *Aizawa et al.* [106].

The actuator in an ATMD is used to drive the auxiliary mass, while the actuator in other active systems usually acts directly on the structure. However, the controlling effectiveness of an ATMD is felt primarily at the fundamental frequency and less at higher Yang frequencies [105,110].

1.5 Hybrid control

Hybrid systems were developed in the early 1990s to overcome the main shortcoming of passive and active systems [111]. The term "hybrid control" generally refers to a combination of a passive and active control system [97,112,113,114]. Since part of the control goal is accomplished by the passive system, the active control effort is less, implying less energy requirement [115].

Like active systems, hybrid systems are computer controlled and information on the behavior of the structure is given by a set of sensors distributed throughout the building. Generally, they reduce the energy required, improve reliability, and reduce cost when compared to fully active systems.

Hybrid control strategies have been studied by many researchers. *Yang* and his collaborators have proposed the use of a hybrid system which consists of an elastomeric support and an active or passive mass damper. They showed that the combined system could become very efficient. *Reinhorn et al.* provided an extensive experimental study of the performance of active tendon and active shock absorbers. *Tadzbakhsh and Rofooei* as well as *Luco et al.*, performed the computer simulation of the performance of hybrid systems. The application of hybrid vibration control of aerospace structures has been reported by *Lee Glauser et al.* These studies have clearly shown the possibility of using a combination of passive and active control systems for optimal performance.

Research in the field of hybrid control systems has mainly focused on two categories of systems:

- hybrid mass damper systems.
- hybrid base insulation.

1.5.1 Hybrid Base Isolation

A class of hybrid control systems has been studied by several researchers. Given, an active base isolation system, consisting of a passive base isolation system combined with a control actuator to complement the effects of the base isolation system. Basic insulation systems have been applied worldwide on civil engineering structures for many years due to their simplicity, reliability, and efficiency [116].

Excellent articles on basic insulation systems are presented by *Kelly, Buckle and Mayes*, as well as *Soong and Constantinou*. However, basic isolation systems are passive systems and are limited in their ability to adapt to changing demands for reduced structural response. With the addition of an active monitoring device to a base isolated structure, a higher level of performance can possibly be achieved without a significant increase in cost, which is very attractive from a practical point of view.

Since the base isolation by itself can reduce the relative displacement of the stories and the absolute acceleration of the structure at the expense of the large displacement of the base, the combination with active control is able to achieve both low displacement and at the same time, to limit the maximum basic movement with a simple set of control forces.

Several small-scale experiments have been performed to verify the effectiveness of this class of systems in reducing structural responses. *Reinhorn and Riley* performed analytical and experimental studies of a small-scale bridge with a hybrid slip isolation system in which a control actuator was used between the sliding surface and floor to complete the basic insulation system.

1.5.2 Hybrid Mass Damper

The hybrid mass damper (HMD) is the most common control device used in large scale civil engineering applications. It is a combination of a tuned mass damper (TMD) and an active mass damper (AMD) [117,118]. The ability of this device to reduce structural responses relies primarily on the normal movement of the TMD. And its effectiveness depends on the forces of the control actuator. The forces of the control actuator are used to increase the efficiency of the HMD and to increase its reliability to changes in the dynamic characteristics of the structure. A typical HMD system requires less energy to operate than a fully active mass damper [113,116,119].

As depicted in Figure 1.32, they combine a TMD with an AMD. An AMD is linked to a TMD rather than the structure so that it can be small; its mass is between 10% and 15% of the TMD's. HMDs' ability to decrease vibration is its key feature.

A successful example of the execution of the HMD system is the Sendagaya INTES building in Tokyo in 1991. As shown in Figure 1.33, the HMD was installed at the top of the 11th floor and consists of two masses to control the movements transverse and torsion of the structure, while the hydraulic actuators provide the possibilities of active control.

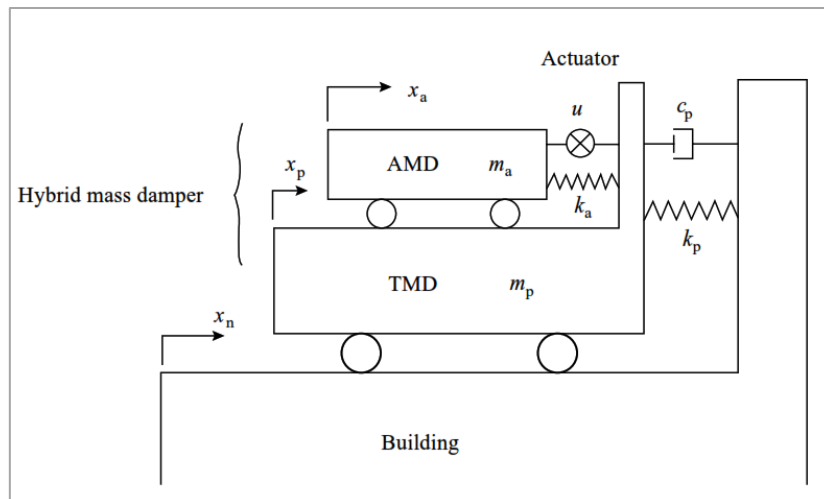


Figure 1.32 : Schematic of hybrid mass damper [16]



Figure 1.33 : Sendagaya INTES building (Tokyo, Japan)

1.6 Semi-Active control

Despite the challenge of applying vibration control in the field of civil engineering, particularly promising semi-active control strategies have emerged.

They offer the reliability of passive devices and the adaptability of active systems, without requiring a large source of energy. Semi-active control is able to develop suitable control forces using modern algorithms, using excitation measurement and/or response. Semi-active systems fall into three categories:

- With variable stiffness,
- With variable damping,
- With variable mass.

Some examples of semi-active control algorithms are:

- Semi-active LQR algorithm.
- Semi-active generalized LQR algorithm.
- Lyapunov algorithm.
- Bang Bang algorithm.
- Maximum Energy Dissipation Algorithm.
- Ground-hook algorithm.
- Skyhook algorithm.
- Variable stiffness algorithm.

1.6.1 Magnetorheological and Electrorheological Dampers

The discovery of the two fluids dates back to the end of the 1940s. The important property of these fluids is their ability to reversibly change their viscosities when they are exposed to variations in an electric field (case of the ER fluid) or magnetic field (case of MR). These dampers have shown efficiency in civil engineering applications and their applications are numerous and are still a subject of research [16,120-122].

Magneto-rheological dampers use smart MR fluid, which is a magnetic analog of ER fluid and typically consists of magnetically polarizable, micro-sized particles dispersed in a viscous fluid, such as silicone oil. When MR fluid is exposed to a magnetic field, the particles in the fluid become polarized and the fluid exhibits viscoelastic behavior, thus providing resistance to fluid flow. MR fluid is also characterized by its ability to undergo a reversible change from a linear viscous fluid to a semi-solid fluid in milliseconds when subjected to a magnetic field. By modifying the strength of the magnetic field according to a predefined algorithm, the control force generated by the MR damper can be adjusted accordingly. Compared to ER fluids, MR

fluids offer advantages of high yield strength (in the range of 50 to 100 kPa), insensitivity to contaminants and stable behavior over a wide range [123].

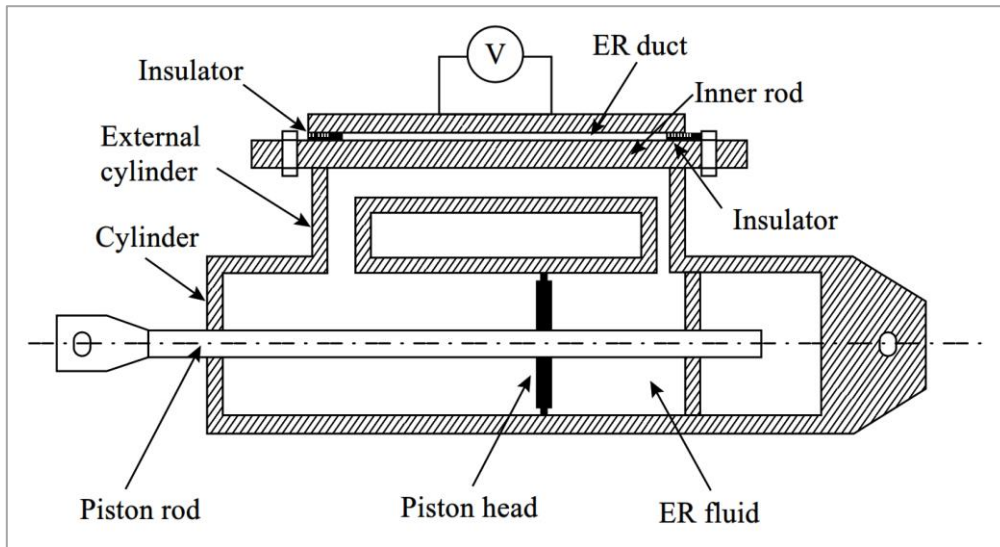


Figure 1.34 : Schematic of ER damper [16]

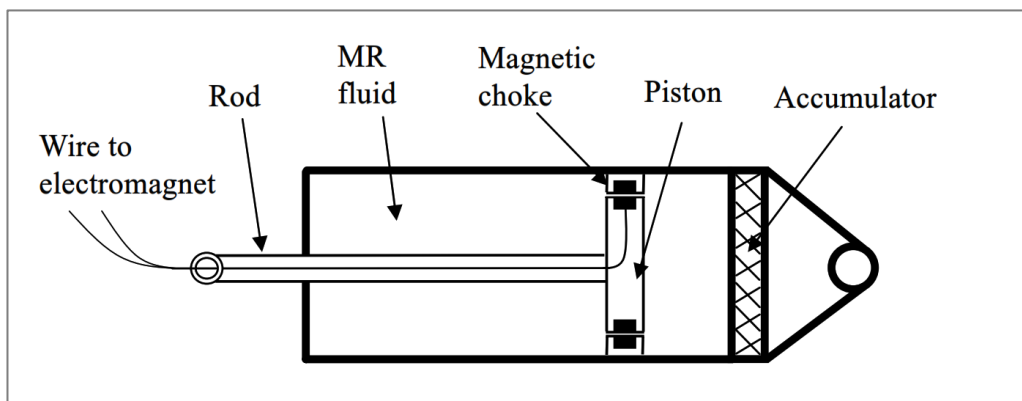


Figure 1.35 : Schematic of MR damper [16]

1.7 Conclusion

A classification and citation of the different vibration control mechanisms for civil engineering structures have been presented in this chapter. Passive, semi-active and active are given in detail specifying their advantages and disadvantages. The choice of system control must be done according to a well-defined objective considering the cost of each system.

Passive systems seem efficient and less expensive but with certain limits of performance. The limitations of passive systems can be overcome by adding an active system. The latter requires a source of energy for its operation. The equation of the control with the different mechanisms will be the subject of the next chapter.

In this chapter we have discussed the basic concepts and configurations of structural vibration control systems using passive, active, hybrid or semi-active systems. Smart structures that use active vibration control systems are fully adaptive against external forces like earthquakes, as they have a complete sensing and actuation system working together.

2

Chapter

Mathematical Formulation and Controlling algorithms

CHAPTER 2 MATHEMATICAL FORMULATION AND CONTROLLING ALGORITHMS

2.1 Introduction

For each control system, mathematical models and equations governing dynamic motion are required to simulate each system. In this chapter a presentation of the different dynamic equations and the different control systems ranging from structures without control to structures equipped with hybrid control systems are provided.

This chapter also aims to present the essential control algorithms that are commonly used in active vibration control. The first subsection presents a brief reminder of the basics to describe the principle of feedback control. These methods are often referred to as position or velocity feedback (ie. the system simply uses a fixed gain multiplied by the position, velocity, or acceleration signal to calculate an input signal, which is in turn provided to actuator). In this chapter more advanced control strategies are presented, such as the linear quadratic control (LQR), the proportional integral derivative (PID) and the fractional controllers, which are very commonly used in all areas of engineering, including active vibration control.

2.2 Equation of motion and mathematical representation

2.2.1 Structure without control

Most multi-story buildings can be modeled as multi-degree-of-freedom (MDOF) systems as shown in Figure 2.1. In this case, it is assumed that:

- the mass of the structure is concentrated at floor levels.
- the beams have infinite stiffness.
- the axial force in the columns does not cause the deformation of the structure.

The equation of motion for this MDOF system can be presented as follows [29]:

$$[M]\{\ddot{x}(t)\} + [C]\{\dot{x}(t)\} + [K]\{x(t)\} = -[M]\{r\}\{\ddot{x}_g\} \quad (2.1)$$

2.2.2 Structure with control

2.2.2.1 TMD parameters

Many researchers have developed different equations to obtain optimum values of the TMD's parameters using different methods or approaches. In this particular study we used the one given by R.Rana and T.T.Soong as a reference [124-126], The detailed literature survey for the passive TMDs was also presented by Elias and Matsagar [127]. where the following expression are used:

$$m_{atmd} = \mu \times M_T \quad (2.4)$$

$$f_{atmd} = \frac{f_s}{(\mu + 1)^2} \quad (2.5)$$

$$k_{atmd} = f_{atmd} \times m_{atmd} \quad (2.6)$$

$$c_{atmd} = \sqrt{\frac{3\mu}{8(\mu+1)^3}} \quad (2.7)$$

Where: $M_T = (m_b + \sum_{j=1}^n m_j)$ represents the base-isolated building total mass, m_{atmd} and m_b represents the active tuned mass damper and the base isolators mass, respectively, μ is the mass ratio of the structure, f_{atmd} and f_s are the ATMD frequency and building's first frequency, c_{atmd} is the damping of the ATMD, while k_{atmd} is the stiffness of the ATMD.

2.2.2.2 Building equipped with base isolators (LRB)

In this study an LRB (Lead Rubber Bearing) base isolation system is used, The LRB (Lead Rubber Bearing) system behaves like a hysteretic damper and the mathematical model is given in figure 2.3.

The basic principle of the base isolation system is to isolate the structure from the effect of ground excitation by installing a soft behavior isolator between the foundation and the superstructure. By using insulators, the superstructure behaves like a rigid body while the insulator experiences a relatively large deformation [128,192].

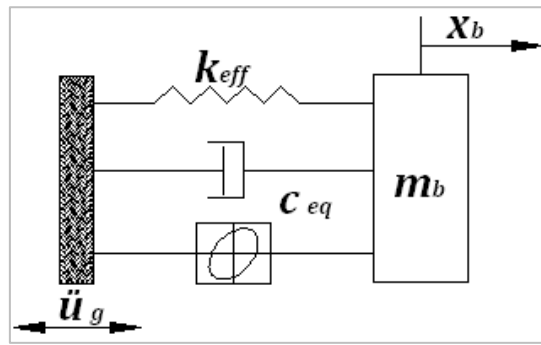


Figure 2.2 : Mathematical model for base isolation system [129].

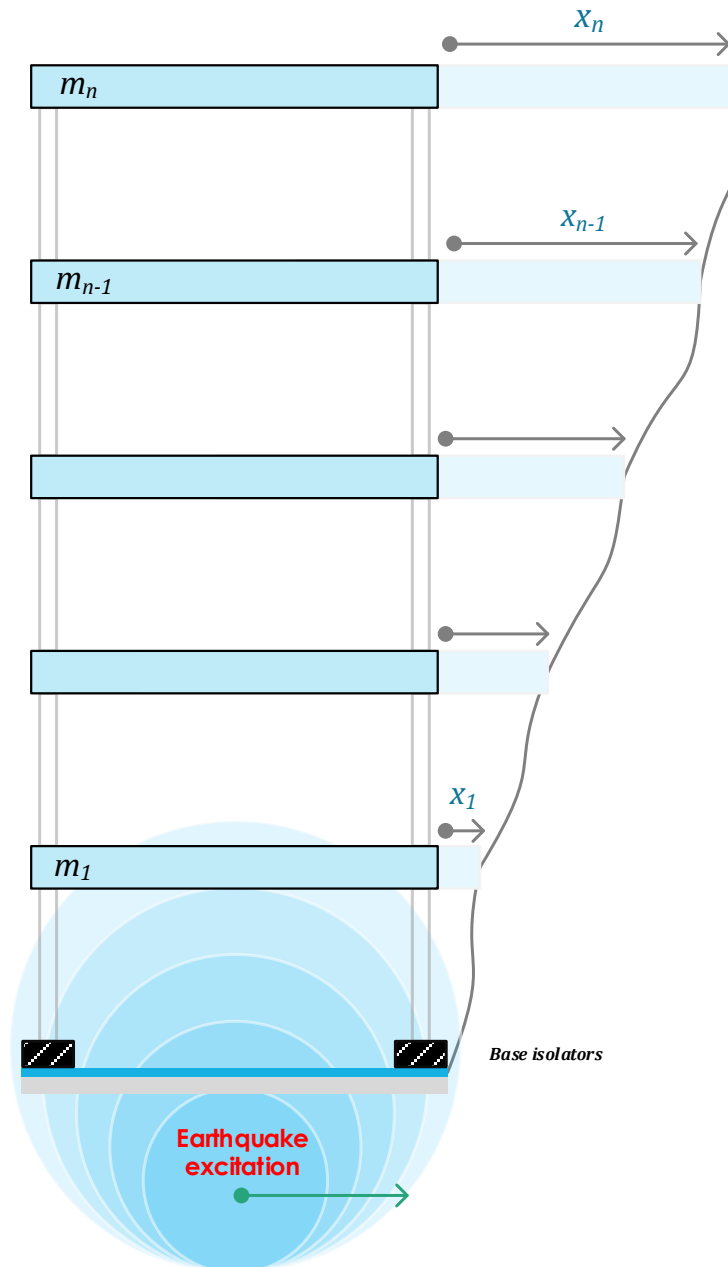


Figure 2.3 : Building structure with base isolation system.

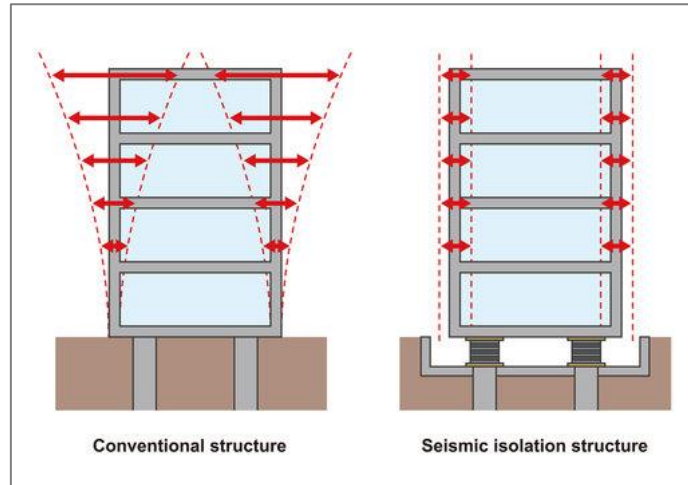


Figure 2.4 : 1DOF building structure with fixed and isolated base.

The equation of motion of the LRB system is given as follows [129]:

$$m_b(\ddot{x}_b + \ddot{u}_g) + c_{eq}\dot{x}_b + k_{eff}x_b = 0 \quad (2.8)$$

$$m_b\ddot{x}_b + c_{eq}\dot{x}_b + k_{eff}x_b = -m_b\ddot{u}_g \quad (2.9)$$

The equation of motion for a base-isolated building shown in Figure 2.3 can be written as:

$$[M] = \begin{bmatrix} m_b & & & & & \\ & m_1 & & & & \\ & & m_2 & & & \\ & & & \dots & & \\ & & & & m_{n-1} & \\ & & & & & m_n \end{bmatrix} \quad (2.10)$$

$$[C] = \begin{bmatrix} c_b + c_1 & -c_1 & & & & \dots \\ -c_1 & c_1 + c_2 & -c_2 & & & \\ & -c_2 & \ddots & \ddots & & \\ \vdots & & \ddots & \ddots & \ddots & \\ & & & & c_{n-1} + c_n & -c_n \\ & & & & -c_n & c_n \end{bmatrix} \quad (2.11)$$

$$[K] = \begin{bmatrix}
 k_b + k_1 & -k & 0 & 0 & 0 & \dots & 0 \\
 -k & k_1 + k_2 & -k_2 & 0 & 0 & 0 & 0 \\
 0 & -k_2 & \ddots & \ddots & 0 & 0 & 0 \\
 0 & 0 & \ddots & \ddots & \ddots & 0 & 0 \\
 \vdots & 0 & 0 & \ddots & \ddots & 0 & 0 \\
 0 & 0 & 0 & 0 & 0 & k_{n-1} + k_n & -k_n \\
 0 & 0 & 0 & 0 & 0 & -k_n & k_n
 \end{bmatrix} \quad (2.12)$$

Where $[M]$, $[C]$ and $[K]$ are $(n + 1) \times (n + 1)$ matrices of mass, damping and stiffness of the system.

2.2.2.3 Hybrid control (ATMD on the top floor + base isolation)

An earthquake-excited n -story shear building structure equipped with an ATMD at the top floor is shown in Figure 2.5.

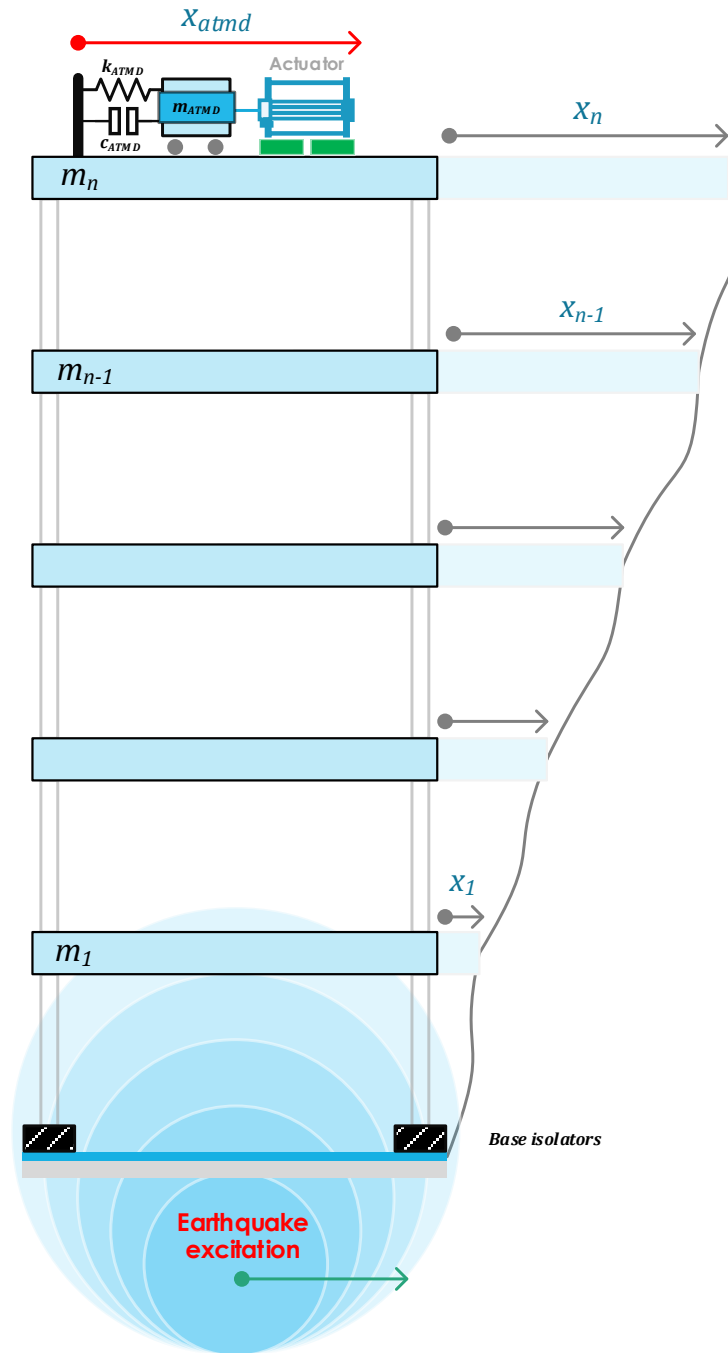


Figure 2.5 : A shear building structure equipped with an ATMD at the top floor

The mass of the ATMD adds one more Degree of Freedom to the system, which means that the relative displacement of the ATMD with respect to the top floor displacement is given as follows:

$$\Delta_d(t) = x_d(t) - x_n(t) \quad (2.13)$$

And then the system becomes an \$(n + 1)\$ order, that means the displacement vector will be defined as:

2.2.2.4 Hybrid control (ATMD on the first floor + base isolation)

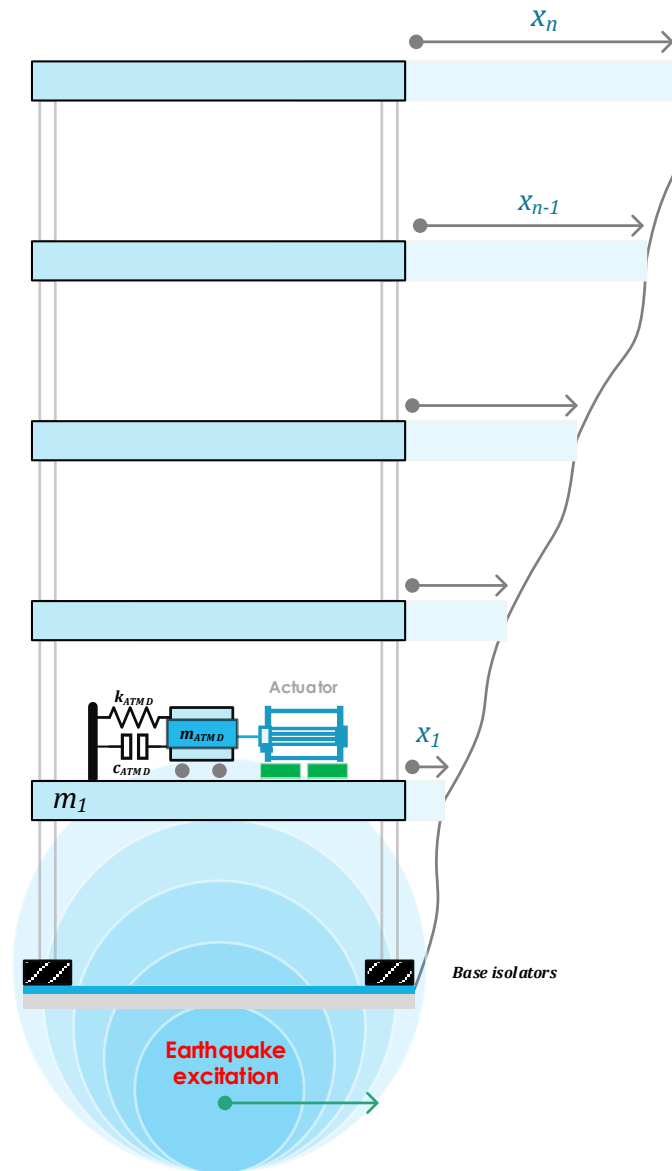


Figure 2.6 : A shear building structure equipped with an ATMD on the first floor

In this case the matrices $[M]$, $[C]$ and $[K]$ will be presented as follows:

$$[M] = \begin{bmatrix} m_b & & & & \\ & m_1 & & & \\ & & \dots & & \\ & & & m_{n-1} & \\ & & & & m_n & \\ & & & & & m_{atmd} \end{bmatrix} \quad (2.22)$$

$$[C] = \begin{bmatrix} c_b + c_1 + c_{atmd} & -c_1 & & & \dots & -c_{atmd} \\ -c_1 & c_1 + c_2 & -c_2 & & & \\ & -c_2 & \ddots & \ddots & & \\ \vdots & & \ddots & \ddots & c_{n-1} + c_n & -c_n \\ -c_{atmd} & & & -c_n & c_n & c_{atmd} \end{bmatrix} \quad (2.23)$$

$$[K] = \begin{bmatrix} k_b + k_1 + k_{atmd} & -k & & & \dots & -k_{atmd} \\ -k & k_1 + k_2 & -k_2 & & & \\ & -k_2 & \ddots & \ddots & & \\ \vdots & & \ddots & \ddots & k_{n-1} + k_n & -k_n \\ -k_{atmd} & & & -k_n & k_n & -k_{atmd} \end{bmatrix} \quad (2.24)$$

And since the ATMD is installed on the first floor, The vector where the control forces are applied equals:

$$\{d\} = [0, 1, \dots, 0, 0]^t \quad (2.25)$$

2.3 State-space representation

2.3.1 Introduction

In control engineering, a state space representation is a mathematical model of a physical system as a set of input, output and state variables related by first-order differential equations. To abstract from the number of inputs, outputs and states, the variables are expressed as vectors. Additionally, if the dynamical system is linear and time invariant, the differential and algebraic equations may be written in matrix form. The state space representation (also known as the "time-domain approach") provides a convenient and compact way to model and analyze systems with multiple inputs and outputs. Unlike the frequency domain approach, the use of the state space representation is not limited to systems with linear components and zero initial conditions. "State space" refers to the space whose axes are the state variables. The state of the system can be represented as a vector within that space [130].

The most general state-space representation of a linear system with \mathbf{u} inputs, \mathbf{y} outputs and n state variables is written in the following form (Fig. 2.7):

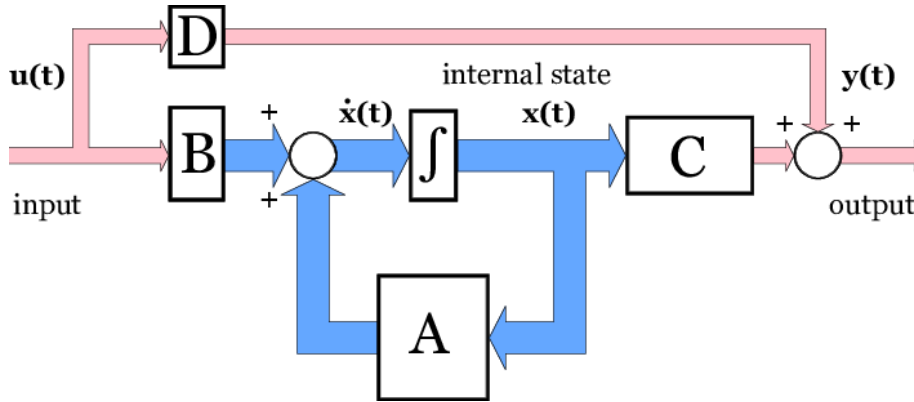


Figure 2.7 : Block diagram representation of the State-Space equations [130].

In this study, the dynamic system is represented with a state-space representation, where \mathbf{x} represents the state vector, and \mathbf{u}, \mathbf{y} represents the input and the output vectors respectively [131].

$$\begin{cases} \dot{\mathbf{x}}(t) = \mathbf{A}\mathbf{x}(t) + \mathbf{B}\mathbf{u}(t) \\ \mathbf{y}(t) = \mathbf{C}\mathbf{x}(t) + \mathbf{D}\mathbf{u}(t) \end{cases} \quad (2.26)$$

$$\mathbf{A} = \begin{bmatrix} \mathbf{0}_{n \times n} & \mathbf{I}_{n \times n} \\ -\mathbf{M}^{-1}\mathbf{K}_{n \times n} & -\mathbf{M}^{-1}\mathbf{C}_{n \times n} \end{bmatrix} \quad (2.27)$$

$$\mathbf{B} = \begin{bmatrix} \mathbf{0}_{n \times n} & \mathbf{I}_{n \times n} \\ -\mathbf{r}_{n \times n} & \mathbf{M}^{-1}\mathbf{d}_{n \times n} \end{bmatrix} \quad (2.28)$$

$$\mathbf{C} = [\mathbf{I}_{n \times n}] \quad (2.29)$$

$$\mathbf{D} = [\mathbf{0}_{n \times n}] \quad (2.30)$$

$\mathbf{A}, \mathbf{B}, \mathbf{C}$, and \mathbf{D} are the system, input, output, and feedthrough matrices in that order.

$\mathbf{x}, \mathbf{u}, \mathbf{y}$ are state, input, and output vectors.

2.3.2 Why use state-space representations

State-space models:

- are numerically efficient to solve,
- can handle complex systems,
- allow for a more geometric understanding of dynamic systems and form the basis for much of modern control theory.

2.4 Classic Feedback control

A controller is classified as a classic feedback controller, when the vibration signal measured by the sensors is simply amplified by gain and fed back to the actuators. To demonstrate the mathematical concept, we consider a vibrating system described by the following state equation [16,132]:

$$\begin{cases} \dot{x}(t) = Ax(t) + Bu(t) \\ y(t) = Cx(t) + Du(t) \end{cases} \quad (2.31)$$

With x the vector of state variables, u the vector of commands, and y the vector of outputs. This very powerful formalism in fact makes it possible to treat SISO (Single Input Single Output) or MIMO (Multiple-Input Multiple-Output) systems with many degrees of freedom in the same way. In addition, terms modeling the various noises that may exist in the system are easily integrated [16,132].

The idea in classic control by direct position feedback is very simple: it consists of sending the signal from the amplified sensor to the actuator. The control law can be described as:

$$u(t) = -Ky(t) \quad (2.32)$$

Where: K is the control gain.

In the case of direct speed feedback control, the control law is given by:

$$u(t) = -K\dot{y}(t) \quad (2.33)$$

In addition, it is also possible to use the acceleration measurement to formulate the control input:

$$u(t) = -K\ddot{y}(t) \quad (2.34)$$

2.5 Linear Quadratic Regulator (LQR)

Linear quadratic control belongs to the family of optimal control algorithms. In optimal control, a cost function indicating a performance index is chosen which is then minimized to obtain an optimal input.

Let us consider the system in the state equation form in equation 2.31, stationary and invariant in time. The cost function in the quadratic optimal control problem can be chosen to be quadratically dependent on the command input and the output state or response [133]:

$$J = \frac{1}{2} \int_{t_0}^{t_f} (x^T Q x + u^T R u) dt \quad (2.35)$$

The terms $x^T Q x$ and $u^T R u$ can be interpreted as a measure of the vibrational energy of the system and the control energy. Q and R are respectively the weighting matrix (output), the control vector (input) [134,135].

$$u(t) = -Kx(t) \quad (2.36)$$

K (LQR gain vector) is given by the relation:

$$K = R^{-1} B^T P \quad (2.37)$$

Where P is the solution matrix of Riccati's equation:

$$-PA - A^T P + PBR^{-1}B^T P - Q = 0 \quad (2.38)$$

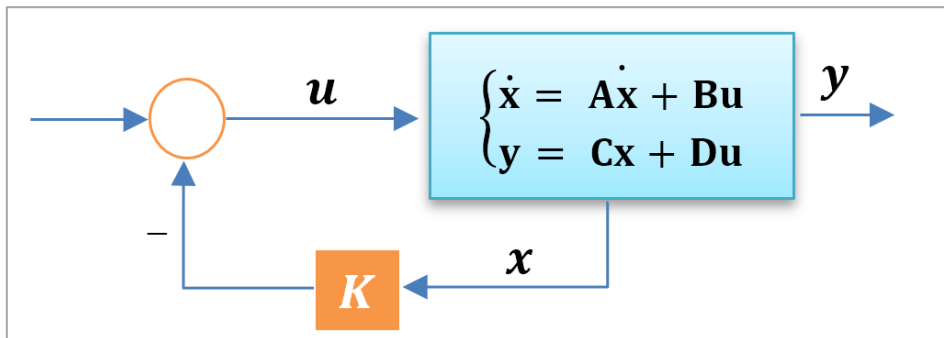


Fig.2.8 : LQR controller

This method applies to any linear dynamic system. In the general case, all the matrices intervening in the expression 2.38 can vary according to time. The matrix of control gains K minimizing the quadratic index J is called the optimal matrix. Several methods, generally iterative, exist to solve the RICCATI equation. In practice, software tools of the MATLAB type have appeared to directly calculate the optimal matrix K from the state system and the chosen criterion.

The methodology for designing an optimal quadratic control, presented previously, can be summarized by the following steps:

- Definition of the Q and R weighting matrices to achieve the desired performance with the available control effort.
- Calculation of the matrix P , solution of the algebraic equation of Riccati equation 2.38 from the matrices of the system A and B , and of weightings Q and R .
- Calculation of the gain matrix (constant) K from P equation 2.37.

If we return to equation 2.31, with u satisfying $u(t) = -Kx(t)$, we have the following control system:

$$\begin{cases} \dot{x}(t) = (A - BK)x(t) \\ y(t) = Cx(t) \end{cases} \quad (2.39)$$

Since K is a matrix that multiplies all state variables, it is necessary to measure all state variables. In the case of an active suspension, some state variables are difficult to measure. Adding an optimal observer circumvents the problem but makes the control system more complex.

The creativity of the human mind is limitless, and this is also true for the design of control strategies that can be used in active vibration control (AVC).

The reader interested in this field can consult the reference *Takács and Rohal-Ilkiv 2012* [136].

2.6 PID controller

An example of control widely used in industry and belonging to the classic control family is the control method using a PID (Proportional-Integral-Derivative) regulator or corrector. This feedback control method makes it possible to obtain a control signal from the measured signal, its integral and its derivative. This type of control makes it possible to make a compromise between the precision, the speed and the robustness of the system. It is adaptable to many cases [137,138].

A PID controller essentially performs three functions:

- It provides a command signal $u(t)$ considering the evolution of the output signal $y(t)$ in relation to the setpoint $r(t)$.
- It eliminates the static error thanks to the term integrator.
- It anticipates the variations of the output thanks to the derivative term.

The behavior of the standard proportional integral derivative (PID) controller can be described by the following equation:

$$u(t) = K_p e(t) + K_i \int e(t) dt + K_d \frac{de}{dt} \quad (2.40)$$

The error signal $e(t)$ is obtained by the following equation:

$$e(t) = r(t) - y(t) \quad (2.41)$$

Where:

- $r(t)$ is the reference signal.
- $y(t)$ is the feedback signal obtained from the responses of the structure (displacement, acceleration).

The control signal resulting from the algorithm described above is composed of the sum of three distinct terms which, by virtue of the function performed, are logically referred to respectively as the proportional K_p , integral K_i and derivative term K_d . The controller parameters associated with these different terms are the proportional gain, the integration constant and the derivative constant. A diagram of the PID controller block is shown in Figure 2.9.

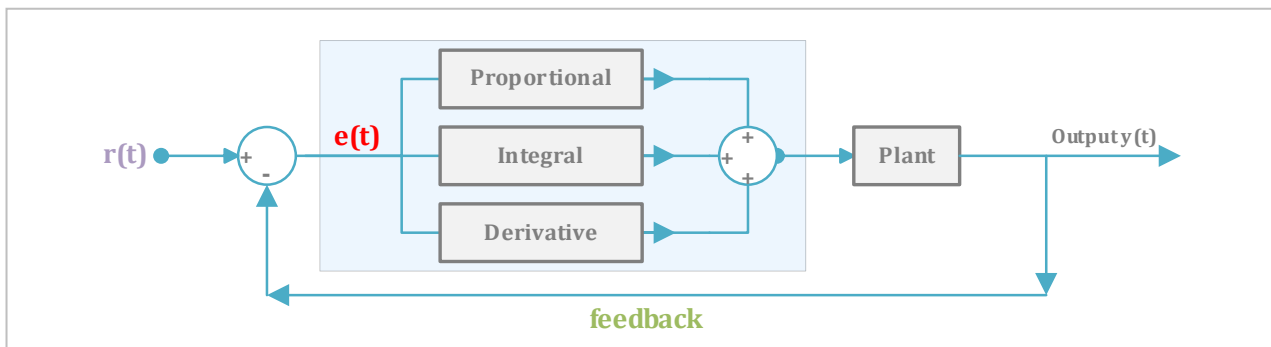


Figure 2.9 : Block diagram of the PID controller.

The algorithm of the PID regulator as described in equation 2.40 can be represented by the following transfer function:

$$G(s) = K_p + \frac{K_i}{s} + K_d s = \frac{K_d s^2 + K_p s + K_i}{s} \quad (2.42)$$

Other variations of the standard formulation are commonly used in order to increase the closed loop performance of the PID controller. Adding a filter in the derived term is often adopted in practice. This results in the following transfer function:

$$G(s) = K_p \left(1 + \frac{1}{T_i s} + \frac{T_d s}{\frac{T_d}{N} s + 1} \right) \quad (2.43)$$

The integration gain T_i and derivation gains T_d are related to the parameters of the standard form by the following relations:

$$\begin{cases} T_i = \frac{K_p}{K_i} \\ T_d = \frac{K_d}{K_p} \end{cases} \quad (2.44)$$

where the additional term $\frac{T_d}{N} s + 1$ is a low-pass filter introduced on the derivative action.

2.7 Fractional Order PID controller

An FO-PID controller is a type of control instrument that enables closed-loop regulation of an industrial process. The FO-PID controller seeks to rectify a process-measured value using a setpoint. [35]. The "FO-PID" represents the abbreviations of the three actions it uses to make its corrections, a Proportional action, an Integral action, and a Derivative action. The adjustment of this sort of controller is frequently a matter of experience. When applied to known, linear, and little-variant systems, his independence from a system model guarantees robustness. [139].

$$u(t) = K_p e(t) + K_i \frac{d^{-\lambda}}{dt^{-\lambda}} e(t) + K_d \frac{d^{\mu}}{dt^{\mu}} e(t) \quad (2.45)$$

Where:

K_p is the proportional gain, K_i is the integral gain and K_d is the derivative gain and $e(t)$ represents the error signal.

The FO-PID controller is defined as an extension and generalization of the classical or conventional PID controller. The FO-PID controller has two more parameters than the classical PID controller μ , which is called the differential order, and λ , which is called the integral order [14]. Therefore, this can enhance and improve the performance of the controlling system and give robust control. The block diagram of the FO-PID controller is shown in Figure 2.10.

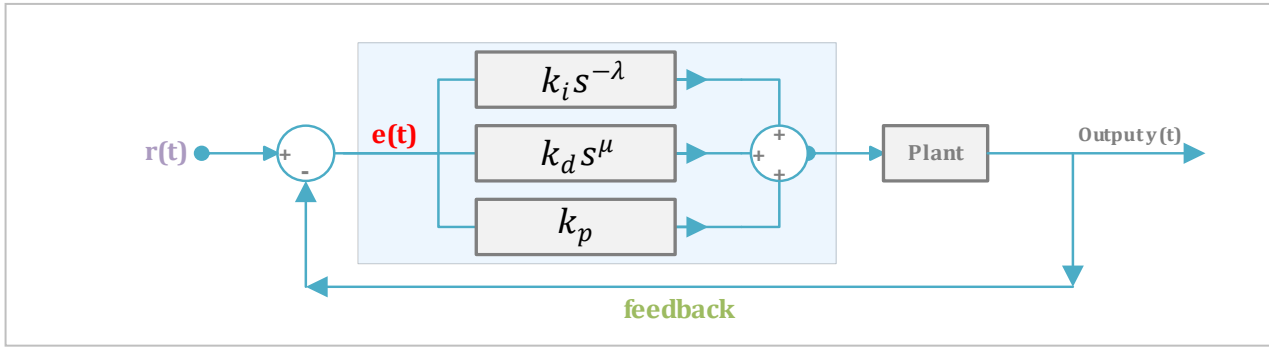


Figure 2.10 : Block diagram of an FO-PID controller.

The error signal $e(t)$ is obtained by the following equation:

$$e(t) = x_r(t) - x(t) \quad (2.46)$$

Where x_r is the reference signal (equals zero), and x is the feedback signal obtained from the responses of the structure (displacement, acceleration).

2.8 Optimization Algorithms

2.8.1 Introduction

In this work, the optimum tuning of the FO-PID and PID controllers has been accomplished by using a new meta-heuristic bio-inspired optimization algorithm called the artificial hummingbird algorithm (AHA) [140]. To evaluate the performance of the FO-PID, A comparison study is carried out against the conventional PID controller under the influence of five different earthquake excitations. After tuning the FO-PID/PID controllers, these last ones ensure the structural response control with an active tuned mass damper (ATMD) mounted on the top floor of a 5-story building.

2.8.2 Artificial Hummingbird Algorithm

The artificial hummingbird algorithm is a novel meta-heuristic optimization approach inspired by hummingbirds' natural flying abilities and intelligence. Because of its unique biological foundation, the AHA algorithm differs significantly from other current optimization algorithms. This program models these birds' three flying abilities: axial, diagonal, and omnidirectional flight. [140]. Comparing AHA to other meta-heuristic algorithms in this study reveals that AHA is more competitive owing to its high-quality solutions employing fewer control parameters. (inputs).

Hummingbirds are thought to be the world's tiniest birds. If intelligence is measured by brain-to-body ratio, hummingbirds would be among the most intellectual species on the planet. There

are over 360 different species of this bird located around the world, and what makes these birds so extraordinary is their ability to beat their wings swiftly and at a high frequency, usually up to 80 times per second. They feed on a variety of insects, including mosquitoes and aphids, to provide energy for flight. They also consume flower nectar and the tasty liquid found there in [141].

Another astounding talent of these birds is their flight capacity; their tiny bodies and fast-beating wings allow them to fly in any direction with accuracy; they can fly backward and forwards, left and right, up and down, with ease [142].

Hummingbirds have a hippocampus in their brain, which aids with foraging memory and learning speed; in fact, they can remember information about flowers such as location, nectar quality, and the last time they visited these flowers [143].

The three primary components of the Artificial Hummingbird algorithm are as follows:

Food sources: Food source is the solution vector in AHA, whereas nectar-refilling of a certain bloom represents the fitness function.

Hummingbirds: Each hummingbird is always assigned a single food source from which to feed, and both the hummingbird and the food supply live in the same area.

Visit Table: This table is updated with each loop iteration, and it tracks how many times a certain hummingbird visits a specific food source.

The visit table of six hummingbirds for six distinct food sources is shown in Figure 2.11 below.

		<i>Food Source</i>					
		x_1	x_2	x_3	x_4	x_5	x_6
<i>Hummingbird</i>	x_1	-	5	6	4	3	1
	x_2	4	-	4	5	9	4
	x_3	3	7	-	3	4	5
	x_4	4	2	5	-	6	2
	x_5	2	2	7	4	-	1
	x_6	6	1	6	1	5	-

Figure 2.11 : Visit table of a hummingbird’s population.

The structure of the AHA is represented in Figure 2.12.

Initialization
While stop criterion is not satisfied
Guided foraging
Territorial foraging
Migration foraging
End

Figure 2.12 : Artificial Hummingbird algorithm structure.

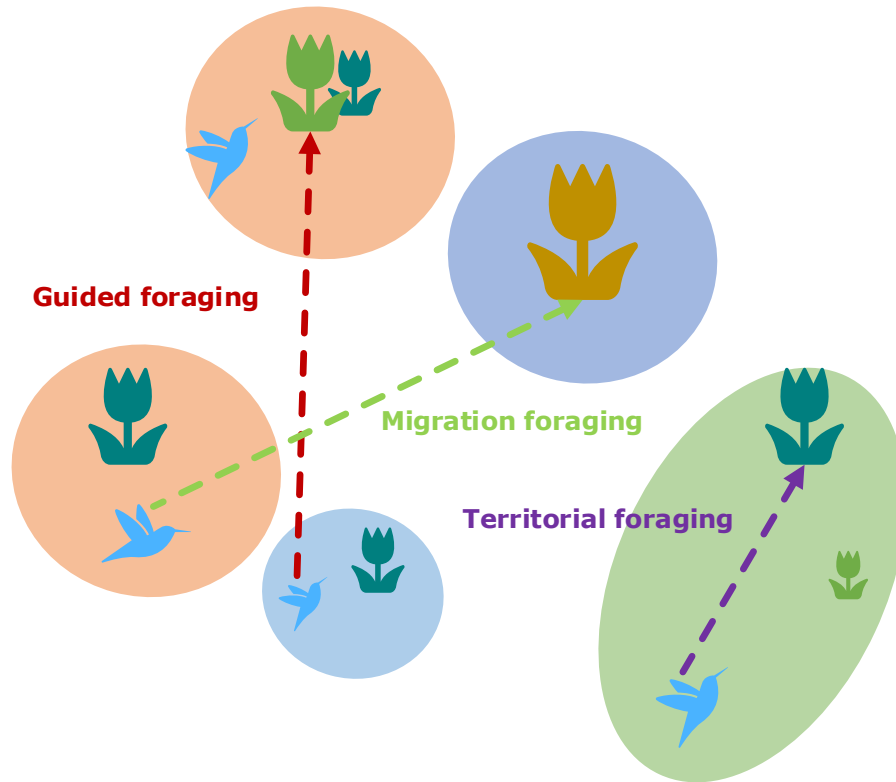


Figure 2.13 : Foraging behaviors of AHA.

2.8.2.1 Initialization

A random number n of hummingbirds are put on n food sources.

$$x_i = Low + r.(Up - Low) \quad i = 1, \dots, n$$

Where: Low : lower bound, Up : upper bound, r : random numbers within $[0, 1]$, x_i : position of the i^{th} food source.

The visit table initialization:

$$VT_{i,j} = \begin{cases} 0 & \text{if } i \neq j \\ \text{null} & \text{if } i = j \end{cases} \quad i = 1, \dots, n ; j = 1, \dots, n$$

2.8.2.2 Guided foraging

In guided foraging behavior, a hummingbird is meant to discover the most frequently visited food source and then select the ones with the highest nectar content.

A hummingbird will use three separate flying talents when foraging: axial, diagonal, and omnidirectional flight. Figure 2.14 depicts the three flight talents in 3D space. A hummingbird travels along one axis in axial flight and can shift corners in diagonal flight. Any two axes can define this style of flying. The omnidirectional flight demonstrates how any flying direction may be projected to any of the three coordinate axes. In other words, all birds can fly in all directions, but only hummingbirds can fly axially and diagonally [140].

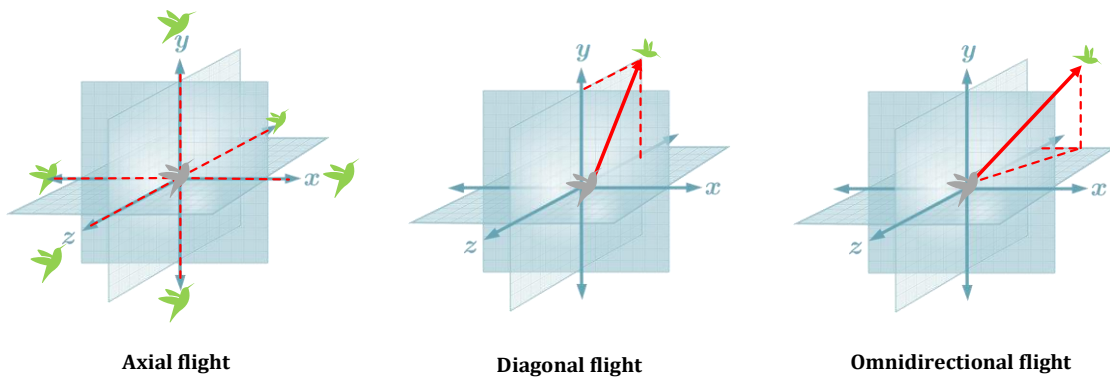


Figure 2.14 : Three flight behaviors of hummingbirds.

In a d -D space, axial flying can be characterized as follows:

$$D^{(i)} = \begin{cases} 1 & \text{if } i = \text{randi}([1, d]) \\ 0 & \text{else} \end{cases} \quad i = 1, \dots, d$$

Diagonal flight:

$$D^{(i)} = \begin{cases} 1 & \text{if } i = P(j), j \in [1, k], P = \text{randperm}(k) \quad k \in [2, [r_1 \cdot (d - 2) + 1]] \\ 0 & \text{else} \end{cases} \quad i = 1, \dots, d$$

Omnidirectional flight:

$$D^{(i)} = 1 \quad i = 1, \dots, d$$

The $\text{randi}([1, d])$ instruction creates a random integer number in $[1, d]$, $\text{randperm}(k)$ generates a random permutation of integers, r_1 is a random number ranging from 0 to 1, and d represents the problem dimension.

2.8.2.3 Territorial foraging

When the present food source is consumed, a hummingbird will begin looking for another. A hummingbird will migrate to a nearby place within the same territory if a new and better food source becomes available. The visit table may be updated by utilizing the mathematical equation that represents the territorial foraging-seeking strategy, which is shown below [140]:

$$v_i(t + 1) = x_i(t) + b \cdot D \cdot x_i(t)$$

Where b is the territorial factor, and v_i is the visiting table.

2.8.2.4 Migration foraging

When a hummingbird notices a shortage of food in one area, it will generally travel to another area where food is plenty. A migration coefficient will be defined in the Artificial Hummingbird algorithm, and if the number of iterations exceeds the value of this coefficient, it means that the hummingbird is located at a food source with a low nectar-refilling, and a migration to a new food source is required, and this food source will be presented randomly in the search space. This entire process is known as hummingbird migratory foraging, and it may be expressed mathematically as follows [140]:

$$x_{wor}(t + 1) = Low + r \cdot (Up - Low)$$

Where x_{wor} represents the worst nectar-refiling rate of a food source in the population. The AHA pseudo-code is presented in Figure 2.15 [140].

<p>Procedure Artificial Hummingbird Optimizer (AHA) Input: $n, d, f, Max_iteration, Low, Up$ Output: $Globalminimum, Globalminimizer$ Initialization: For i^{th} hummingbird from 1 to n, Do $x_i = Low + r(Up - Low)$, For j^{th} food source from 1 to n, Do If $i \neq j$ Then $Visit_table_{i,j} = 1$, Else $Visit_table_{i,j} = null$, End If End For End For While $t \leq Max_iteration$ Do For i^{th} hummingbird from 1 to n, Do If $rand \leq 0.5$ Then If $r < 1/3$ Then perform equation (3), Else If $r > 2/3$ Then perform equation (4), Then perform equation (5), End If End If Then perform equation (6), If $f(v_i(t + 1)) < f(x_i(t))$ Then $x_i(t + 1) = v_i(t + 1)$, For j^{th} food source from 1 to n ($j \neq tar, i$), Do $Visit_table_{i,j} = Visit_table_{i,j} + 1$, End For $Visit_table_{i,tar} = 0$,</p>	<p>$Visit_table_{i,j} = Visit_table_{i,j} + 1$, End For $Visit_table_{i,tar} = 0$, End Else Perform equation (9), If $f(v_i(t + 1)) < f(x_i(t))$ Then $x_i(t + 1) = v_i(t + 1)$, For j^{th} food source from 1 to n ($j \neq i$), Do $Visit_table_{i,j} = Visit_table_{i,j} + 1$, End For For j^{th} food source from 1 to n, Do $Visit_table_{j,i} = \max_{i \in n \text{ and } i \neq j}(Visit_table_{i,j}) + 1$, End For Else For j^{th} food source from 1 to n ($j \neq i$), Do $Visit_table_{i,j} = Visit_table_{i,j} + 1$, End For End If End If End For If $mod(t, 2n) == 0$, Then perform equation (11), For j^{th} food source from 1 to n ($j \neq wor$), Do $Visit_table_{wor,j} = Visit_table_{wor,j} + 1$, End For For j^{th} food source from 1 to n, Do $Visit_table_{j,wor} = \max_{i \in n \text{ and } i \neq j}(Visit_table_{i,j}) + 1$,</p>
---	--

<pre> For j^{th} food source from 1 to n, Do Visit_table$_{j,i}$ = max$_{l \in n \text{ and } l \neq j}$(Visit_table$_{l,j}$) + 1, End For Else For j^{th} food source from 1 to $n(j \neq tar, i)$, Do </pre>	<pre> End For End If End While </pre>
---	--

Figure 2.15 : Pseudocode of the AHA [140].

2.8.3 Genetic Algorithms

Genetic algorithms are a general, powerful mechanism for solving problems for which:

- There are a very large number of more or less good solutions.
- There is no deterministic algorithm to calculate the best solution(s).
- The universe of the problem is not formalized.

Genetic algorithms consist of using the principle of evolution to an optimization problem. According to Darwin's theory of evolution, each living being has genes that determine its characteristics. The most successful beings have a greater chance of survival, therefore more likely to transfer their genes to the next generation. Unlike traditional algorithms, the search starts with a population of starting points and not just one. Different mechanisms make it possible to explore the space of solutions and find the optimum. Like traditional algorithms, there is no certainty about the optimality of the solution, but the explored space is much larger [144]. The genetic algorithm process has four essential steps Figure 2.16:

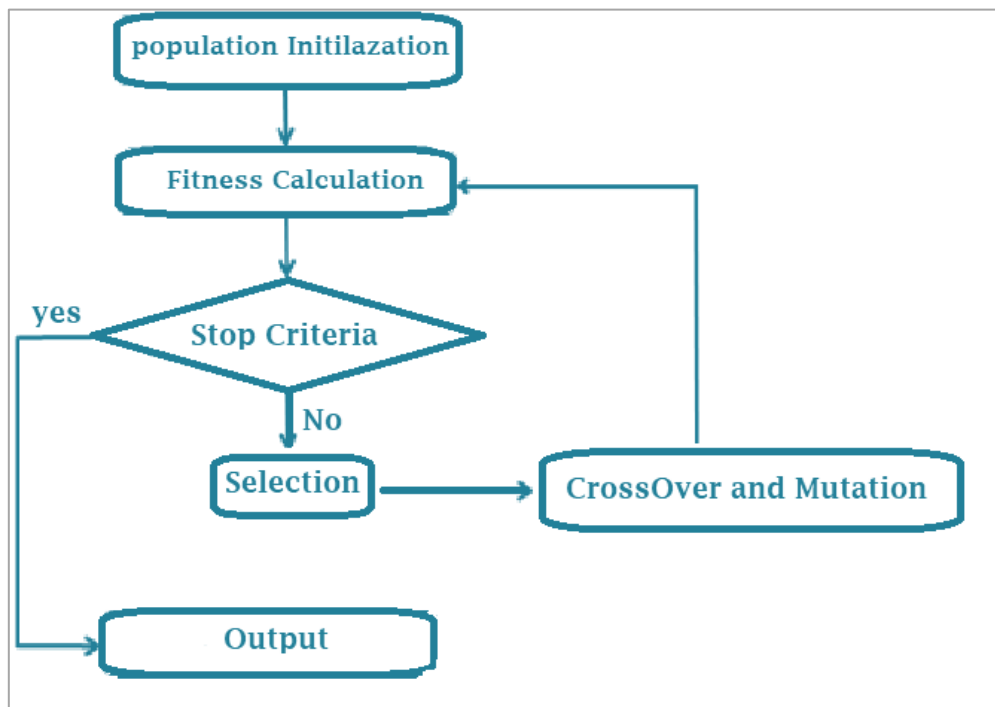


Figure 2.16 : Genetic algorithm Flow Chart

There are five stages involved in genetic algorithm [145] :

1. Population Initialization.
2. Calculation of Fitness value.
3. Selection.
4. Crossover.
5. Mutation.
6. Termination.

1. Population Initialization: Genetic algorithm starts with the initialization of the population. The population represents the subset of all the possible solutions to our problem. Initialization is usually done randomly.

2. Calculation of Fitness value: The fitness value is calculated from the initialized population using the fitness function. On the basis of fitness value calculated the section of the individual is done. From the population, the individuals with high fitness values are selected for the next steps i.e. crossover and mutation.

3. Selection: Selection is the process of selecting the fittest individuals and lets them pass their genes to the next generation. Selection is performed on the basis of fitness value. A pair of individuals from the selected ones undergo further phases i.e. crossover and mutation.

4. Crossover: Crossover also called recombination is the process of exchange of genetic materials (genes) between the parents. For the pair of individuals (or parents) to be recombined, a random crossover point is chosen. Then the genes are exchanged between the parents beyond the crossover point.

4.1. One Point Crossover: A random crossover point is chosen and the part beyond the crossover point is swapped between the parents to get new offspring.

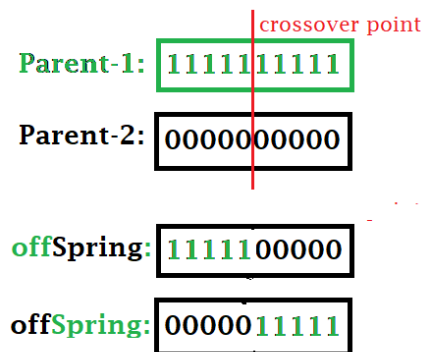


Figure 2.17 : One Point Crossover

4.2. Multipoint Crossover: In the multipoint crossover, multiple crossover points are chosen randomly and the genes between the crossover points are swapped between the parents.

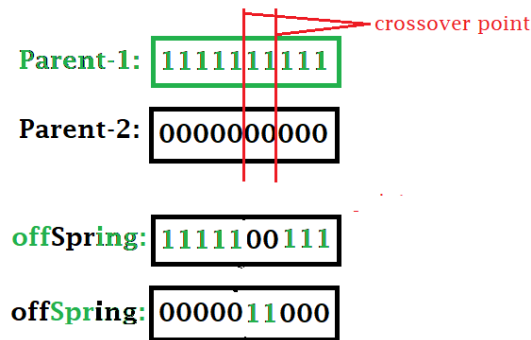


Figure 2.18 : Multipoint Crossover

4.3. Uniform Crossover: In this type of crossover each gene can take part in the crossover as a separate entity. To decide which gene to swap, we opt for some selection techniques like the tossing of a coin.

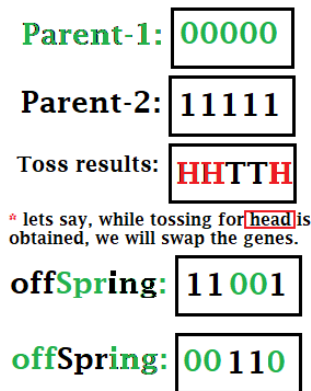


Figure 2.19 : Uniform Crossover

5. Mutation: It is analogous to biological mutation. Mutation maintains the genetic diversity from one generation of the population to the next. In mutation some of the genes of the obtained off-springs are altered from its previous state, thus creating an entirely new solution. Hence mutation can help to get a better solution.

6. Termination: The termination condition in the genetic algorithm decides how long the looping in the algorithm will run. The GA produces better results in every loop, therefore, to have the right number of loops, the termination criteria should be selected wisely. Usually, the algorithm terminates when the population converges (means, when the offspring generated, are not significantly different from the previous ones). In some cases, we may also terminate the algorithm if the value of the objective function has reached some predefined value.

2.8.4 Grey Wolf Algorithm

Grey wolf (*Canis lupus*) belongs to Canidae family. Grey wolves are considered as apex predators, meaning that they are at the top of the food chain. Grey wolves mostly prefer to live in a pack. The group size is 5–12 on average. Of particular interest is that they have a very strict social dominant hierarchy as shown in Figure 2.20. The leaders are a male and a female, called alphas. The alpha is mostly responsible for making decisions about hunting, sleeping place, time to wake, and so on. The alpha's decisions are dictated to the pack. However, some kind of democratic behavior has also been observed, in which an alpha follows the other wolves in the pack. In gatherings, the entire pack acknowledges the alpha by holding their tails down. The alpha wolf is also called the dominant wolf since his/her orders should be followed by the pack. The alpha wolves are only allowed to mate in the pack. Interestingly, the alpha is not necessarily the strongest member of the pack but the best in terms of managing the pack. This shows that the organization and discipline of a pack is much more important than its strength [146].

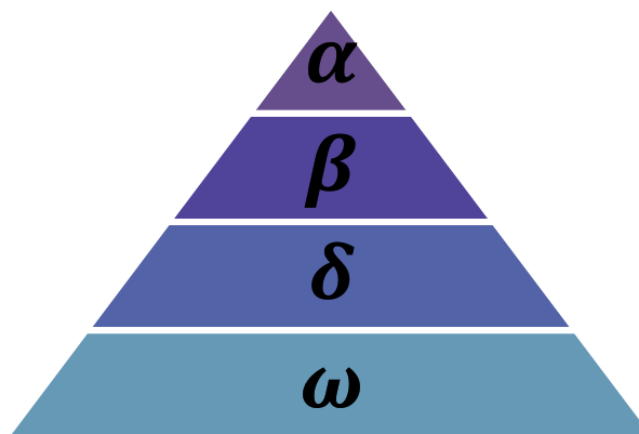


Figure 2.20 Hierarchy of grey wolf [146].

2.9 Conclusion

These active control algorithms are used by the controller to determine the control force from the information measured by the sensors. As well as these algorithms will have produced a control law.

A citation of the works carried out in this field presented in the literature for the control of the vibrations of the structures isolated at the base allows to have a precise idea on the context of work of this thesis. The variants of the structures to be studied will be detailed in the next chapters with the results obtained and their analysis.

Chapter

3

**Hybrid Vibration Control for Structures :
Simulation & Numerical Results.**

CHAPTER 3 HYBRID VIBRATION CONTROL FOR STRUCTURES: SIMULATION AND NUMERICAL RESULTS

3.1 Introduction

In this Chapter, the performance hybrid vibration control system (ATMD + Base isolation system) is evaluated using different controlling algorithm. A comparative study between LQR algorithm and a classical, none tuned PID controller is done in the first section. After that a classical PID controller will be compared to an optimized PID controller using well known state-of-art meta-heuristic optimization algorithms such as Artificial Hummingbird Algorithms, Grey Wolf Algorithm, Whale Optimization Algorithm, Dragonfly Algorithm, and Ant Lion Algorithm.

In the last section the optimum tuning of the FO-PID and PID controllers has been accomplished by using a new meta-heuristic bio-inspired optimization algorithm called the artificial hummingbird algorithm (AHA). To evaluate the performance of the FO-PID, A comparison study is carried out against the conventional PID controller under the influence of five different earthquake excitations. After tuning the FO-PID/PID controllers, these last ones ensure the structural response control with an active tuned mass damper (ATMD) mounted on the top floor of a 5-story building.

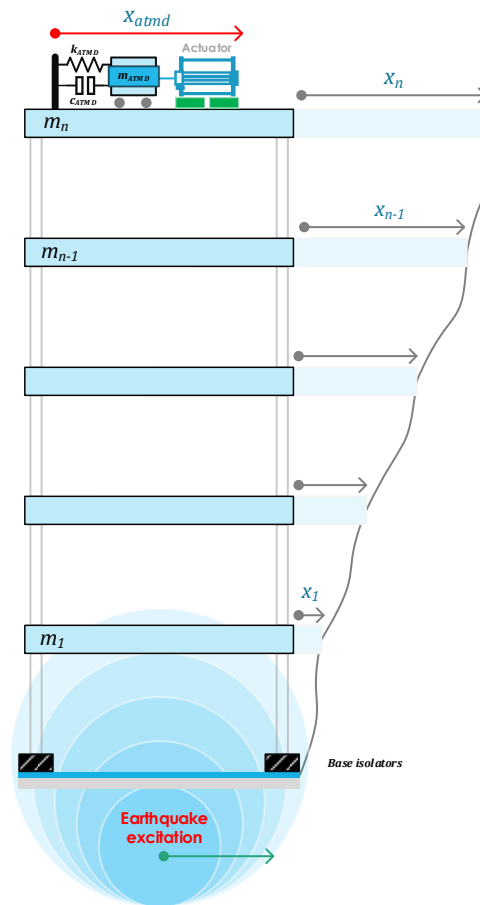
3.2 Comparative study on hybrid vibration control of base-isolated buildings equipped with ATMD

In this section, the performance of a hybrid control system (base isolators + ATMD) is investigated. The active force is obtained by a PID controller and by an LQR controller. In this study, a 5-story base-isolated building is used. In both control systems (PID & LQR) the top floor displacement was used as 'feedback'. The damping and stiffness of the ATMD are determined assuming a passive TMD device adjusted to the structure's first mode, The building structure parameters are shown in Table 3.1. The proportional, integral, and derivative values selected for the PID controller are as follows:

$K_p = -20, K_i = -1, K_d = -300$. And coefficient filter (N) = 100 .

Table 3.1 : Building Parameters

Floor	Mass (Kg)	Stiffness (KN/m)	Damping (KN.s/m)
Base isolators	1.5×10^3	2.16×10^2	2.7
1	1.5×10^3	2.1×10^6	34
2	1.5×10^3	2.1×10^6	34
3	1.5×10^3	2.1×10^6	34
4	1.5×10^3	2.1×10^6	34
5	1.5×10^3	2.1×10^6	34
ATMD (active tuned mass damper)	900	7.85	0.689

**Figure 3.1** : Base isolated building equipped with ATMD on the top floor

The simulation was done using MATLAB software. Three strong historically known earthquakes were used in this study. El Centro earthquake (1940), Northridge earthquake (1994), and Kobe earthquake (1995).

The response results of the isolated, uncontrolled structure are compared to the same structure equipped with an ATMD, using two different types of PID and LQR control algorithms.

Figures 3.2 to 3.4 show the building's top floor displacement comparison during El Centro, Kobe, and Northridge earthquakes respectively.

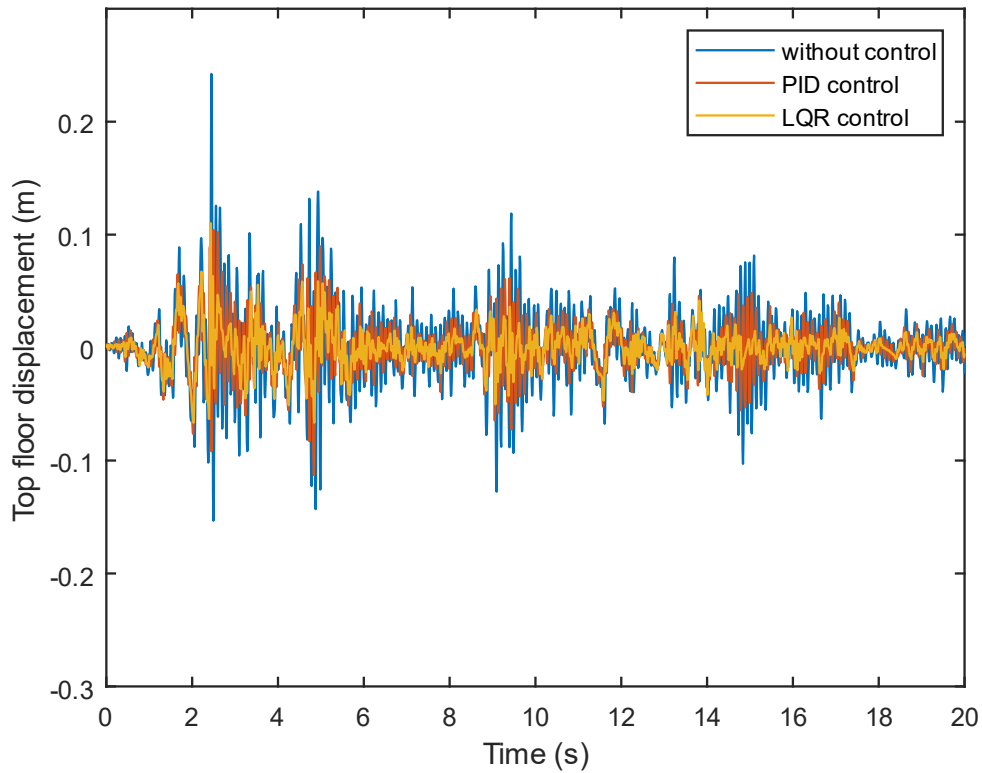


Figure 3.2 : Top floor response under El Centro seismic excitation

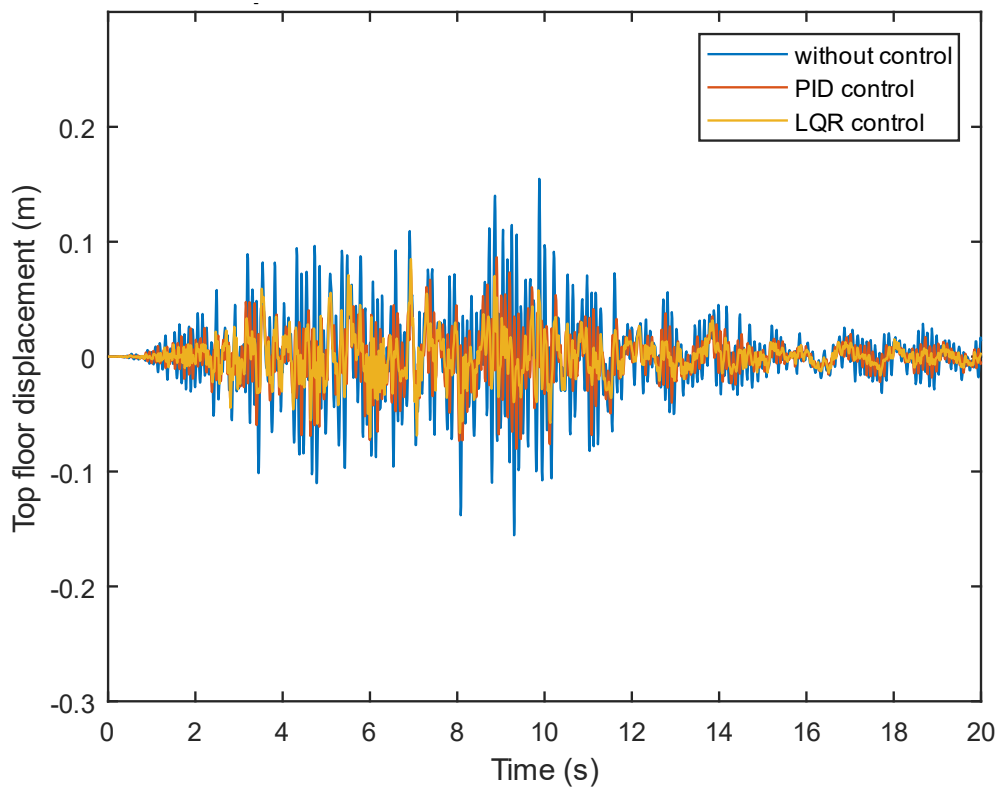


Figure 3.3 : Top floor response under Kobe seismic excitation

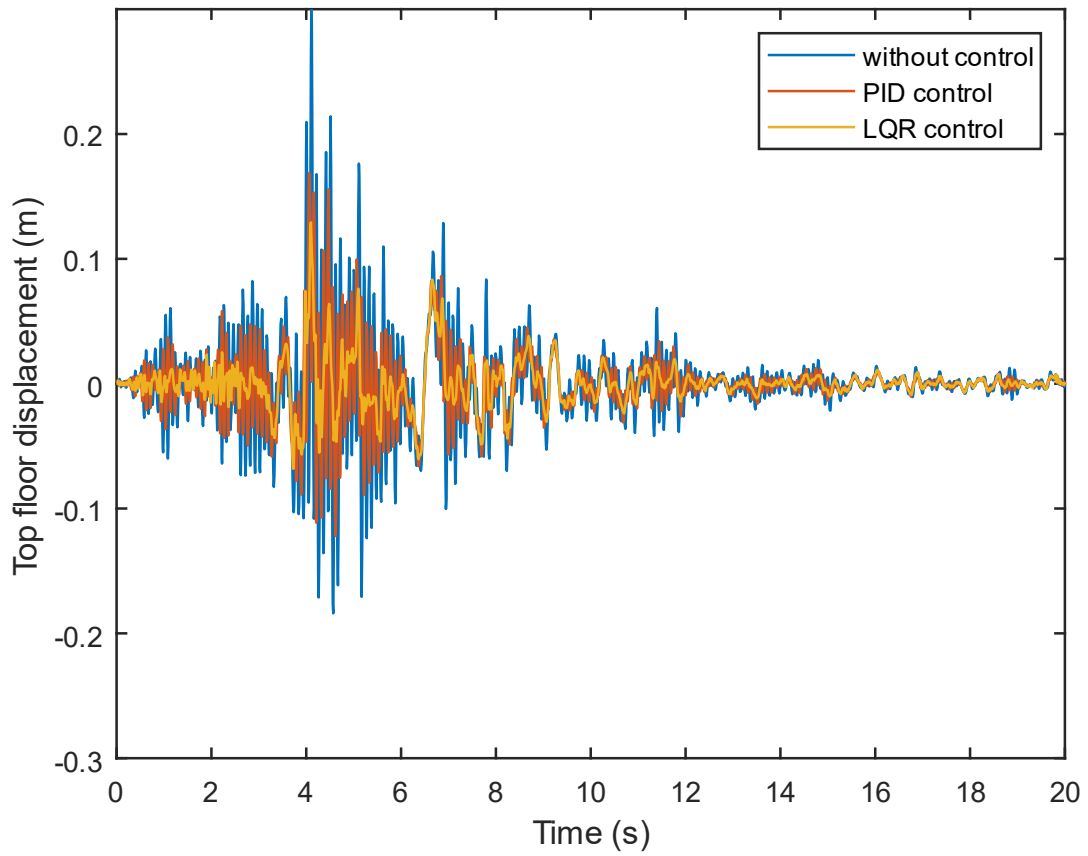
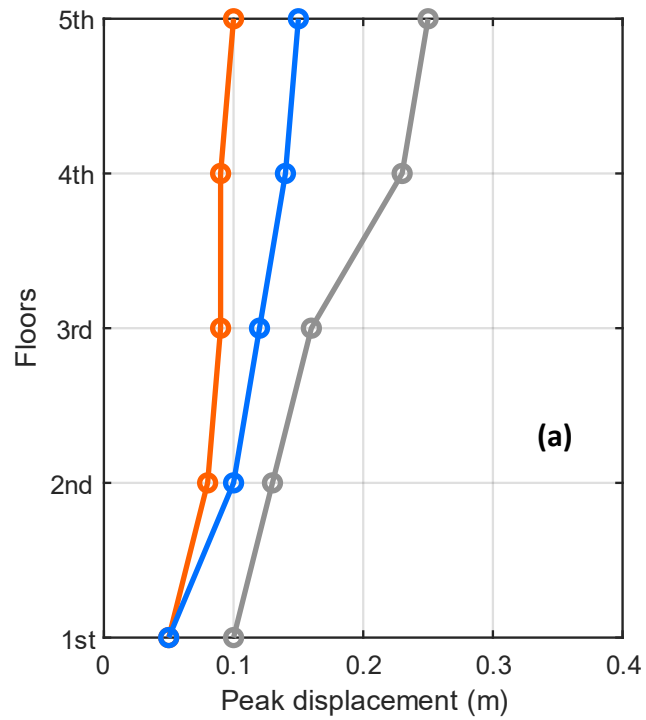


Figure 3.4 : Top floor response under Northridge seismic excitation.



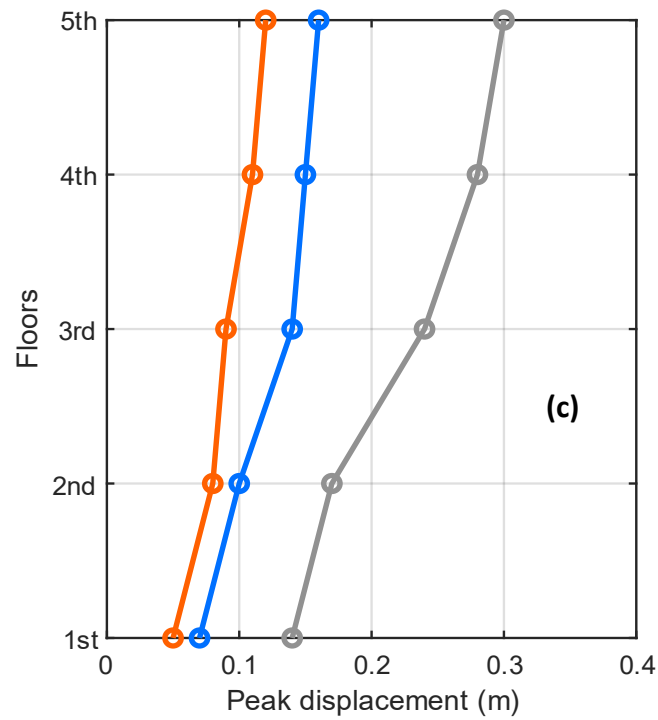
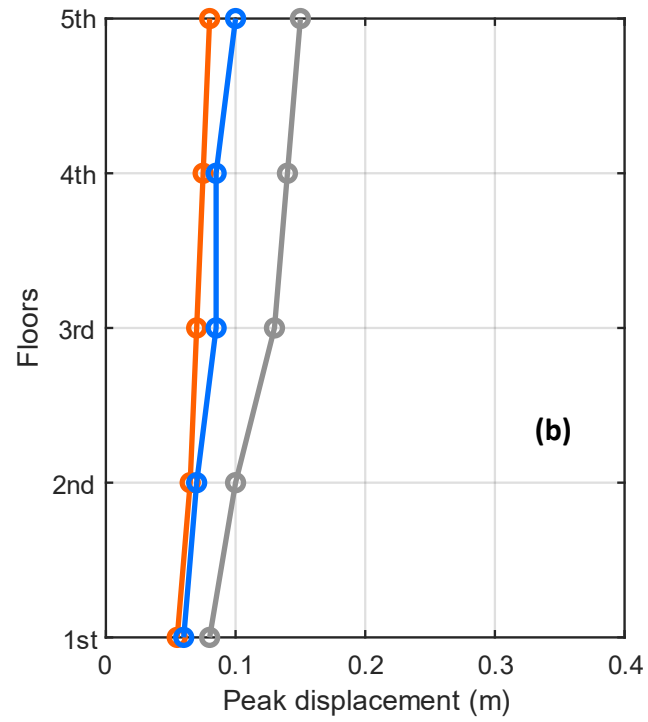


Figure 3.5 : Maximum story drift for the structure under the different earthquake excitations. (a) El Centro, (b) Kobe, and (c) Northridge.

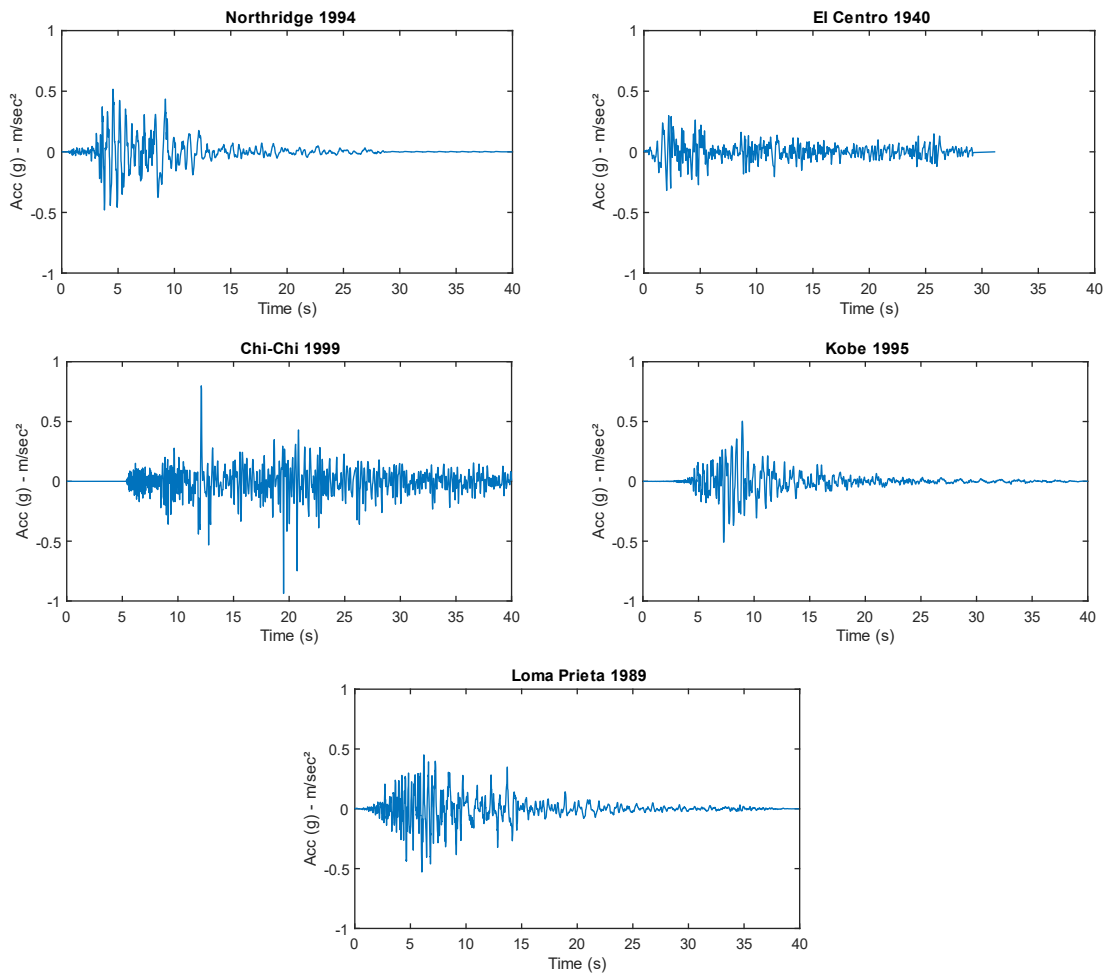
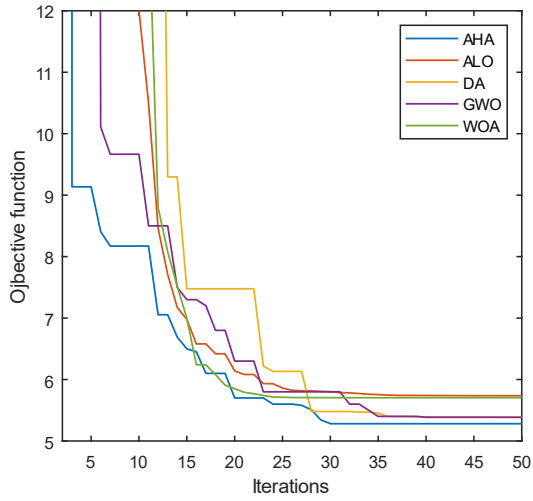


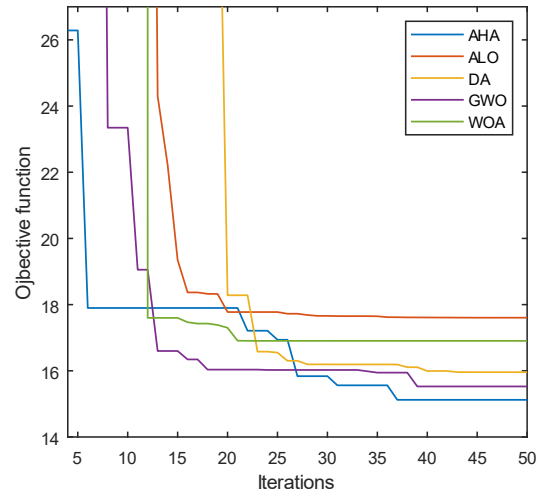
Figure 3.6 : Time histories for the considered earthquake ground motion records.

Table 3.3 : Parameters of the AHA.

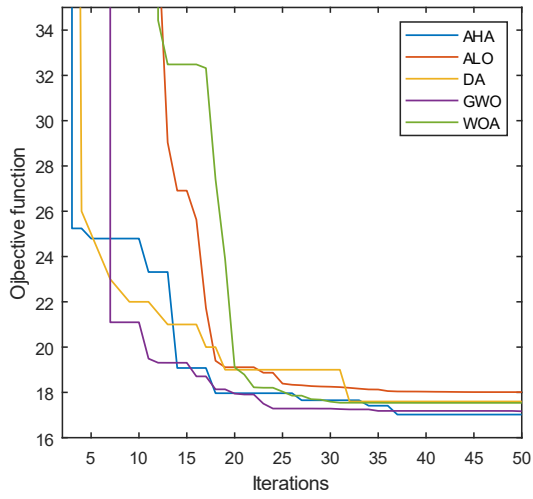
No	Parameter	Values
1	Lower bound [Kp, Ki, Kd]	[-50,-50,-50]
2	Upper bound [Kp, Ki, Kd]	[50,50,50]
3	Population size	25
4	No of iteration	50



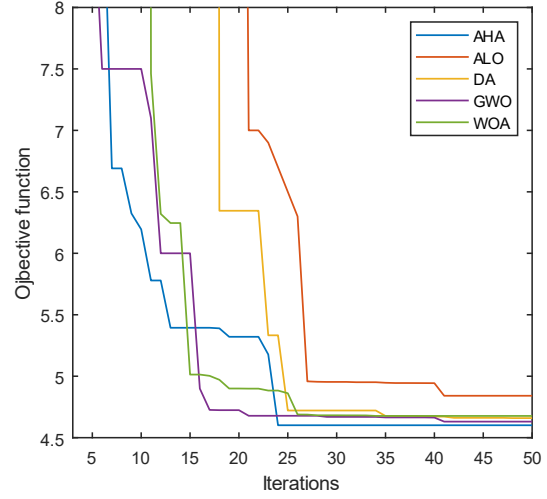
(a)



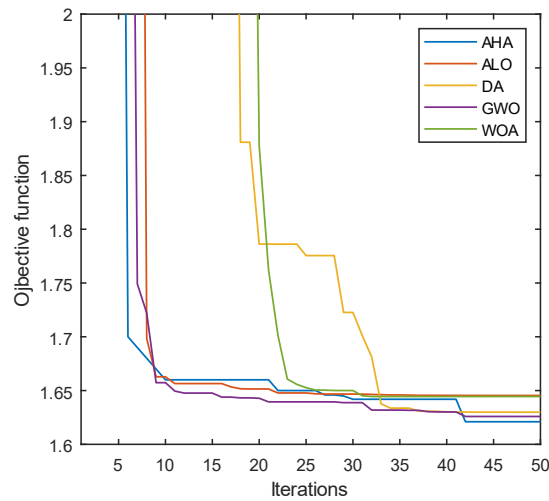
(b)



(c)



(d)



(e)

Artificial Hummingbird Algorithm

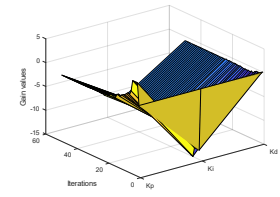
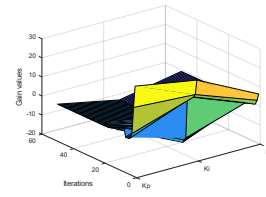
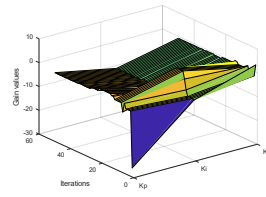
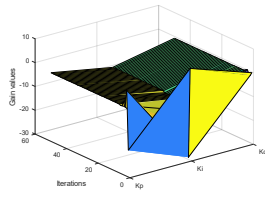
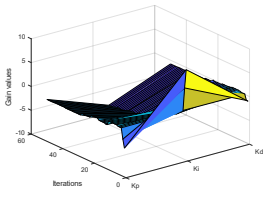
Grey Wolf Optimization Algorithm

Dragonfly Algorithm

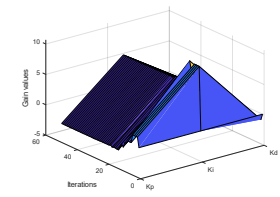
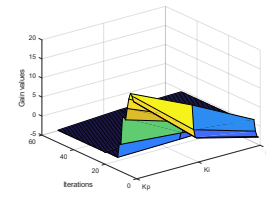
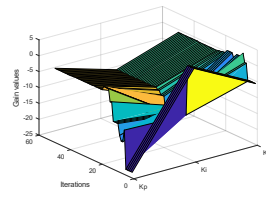
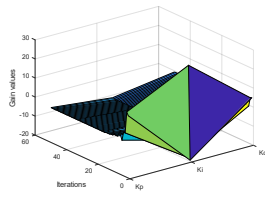
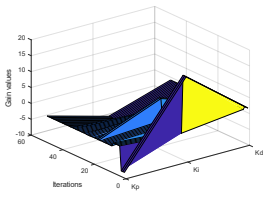
Whale Optimization Algorithm

Ant Lion Optimization Algorithm

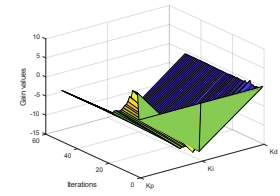
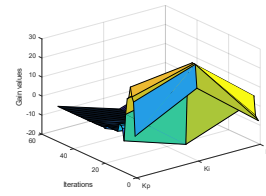
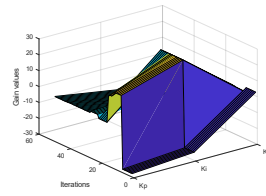
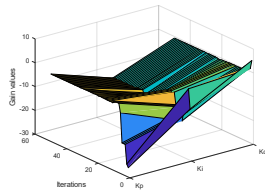
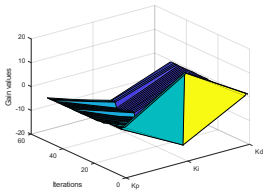
Northridge



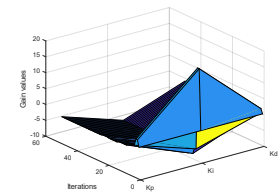
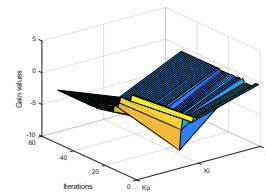
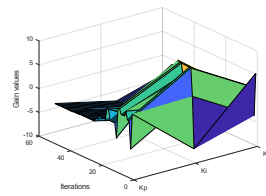
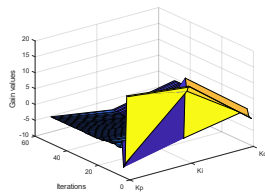
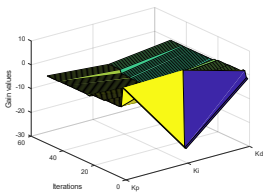
El Centro



Chi-Chi



Kobe



Loma Prieta

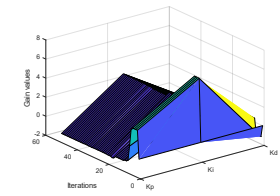
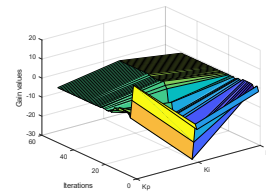
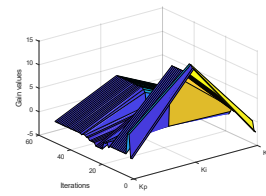
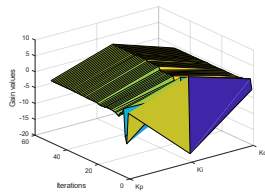
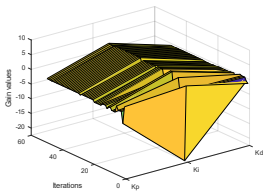
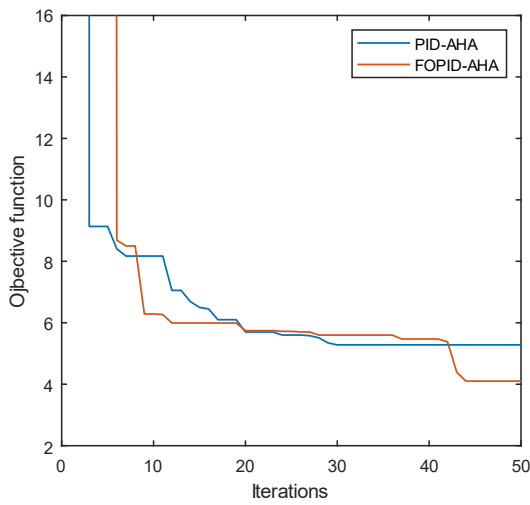
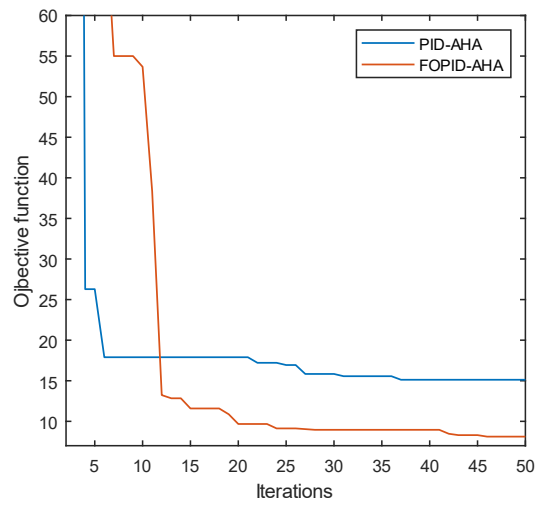


Figure 3.8 : PID controller parameters evolution for all algorithms.

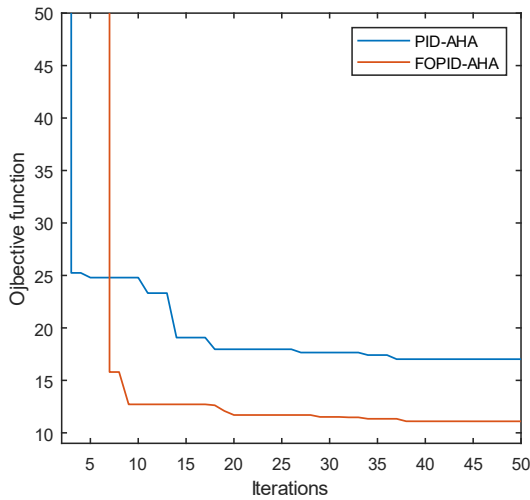
PID and the FO-PID controllers. Table 3.9 shows the optimum values obtained for the objective functions. It can be seen that the FO-PID performs much better than the classical PID controller in every case. Under Northridge earthquake excitation, the FO-PID controller finds a better solution $J=4.1013$, while the classical PID controller finds a value of $J=5.2811$, which means the FO-PID gives a better controlling performance, and it is more significant in the structural vibration control. Under El Centro, Chi-Chi, Kobe, and Loma Prieta, the FO-PID again gives better objective function results which are equal to $J=8.1183$, $J=11.0972$, $J=3.4119$, and $J=2.5307$ respectively.



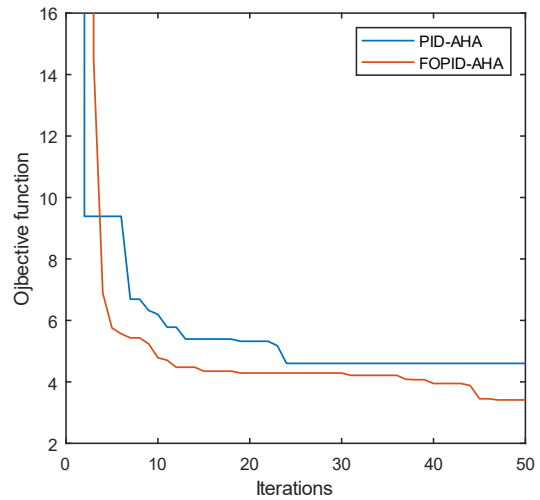
(a)



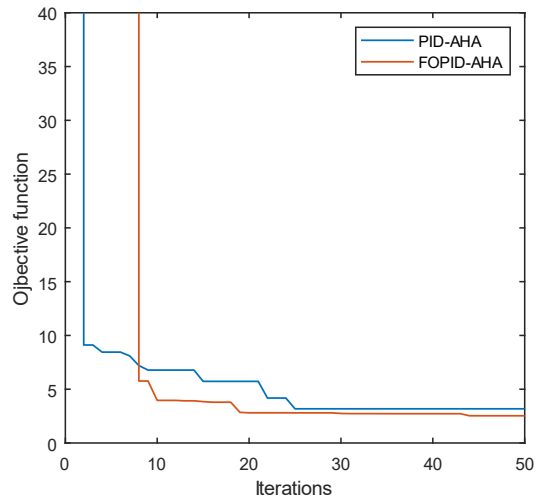
(d)



(c)



(d)



(e)

Figure 3.21 : The convergence history of the objective function for the AHA, GWO, DA, WOA, and ALO algorithms under the different earthquake excitations. (a) Northridge, (b) El Centro, (c) Chi-Chi, (d) Kobe and (e) Loma Prieta.

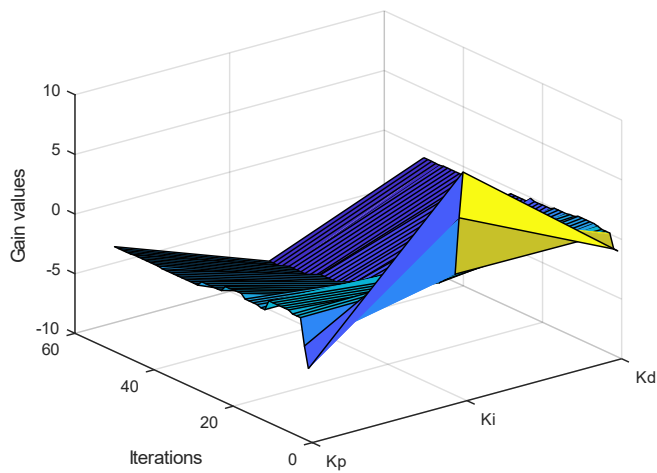


Figure 3.22 : PID gains evolution (K_p, K_i, K_d) under Northridge earthquake.

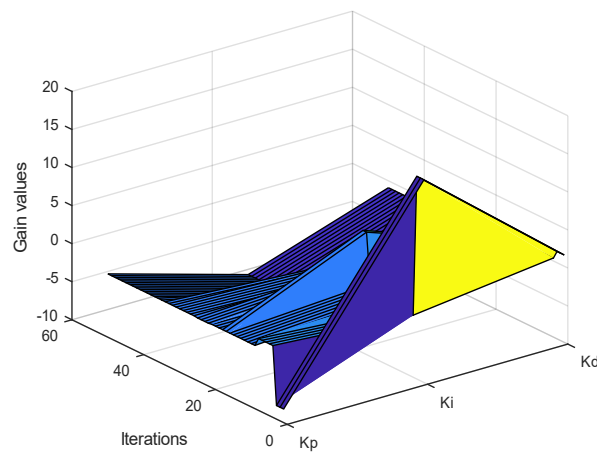


Figure 3.23 : PID gains evolution (K_p, K_i, K_d) under El Centro earthquake.

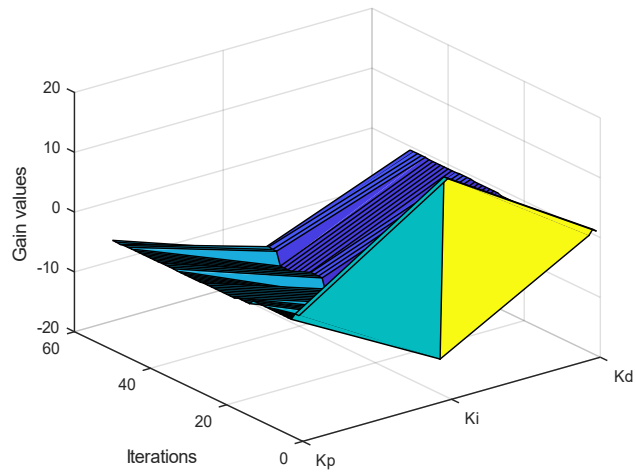


Figure 3.24 : PID gains evolution (K_p, K_i, K_d) under Chi-Chi earthquake.

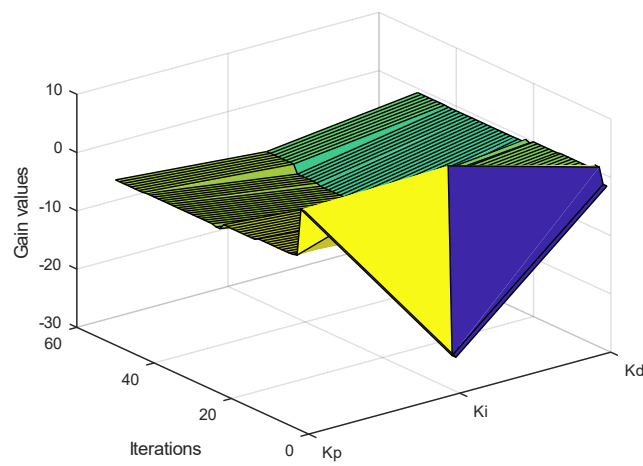


Figure 3.25 : PID gains evolution (K_p, K_i, K_d) under Kobe earthquake.

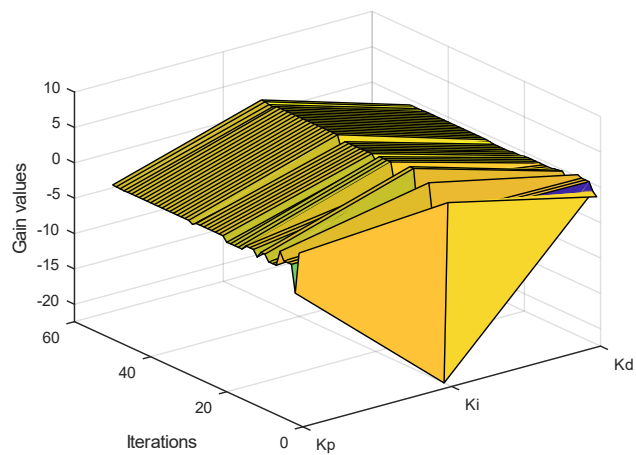


Figure 3.26 : PID gains evolution (K_p, K_i, K_d) under Loma Prieta earthquake.

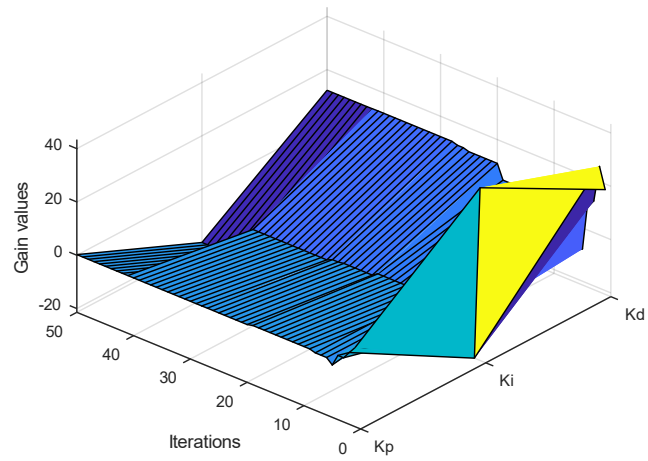


Figure 3.27 : FO-PID gains evolution (K_p, K_i, K_d) under Northridge earthquake.

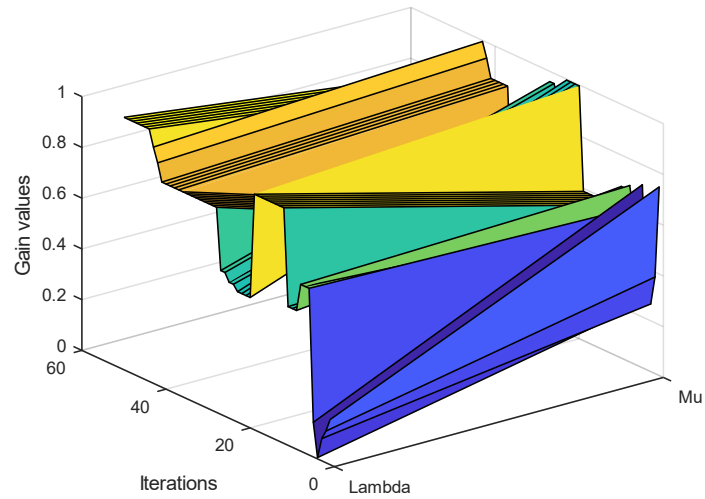


Figure 3.28 : FO-PID gains evolution (λ, μ) under Northridge earthquake.

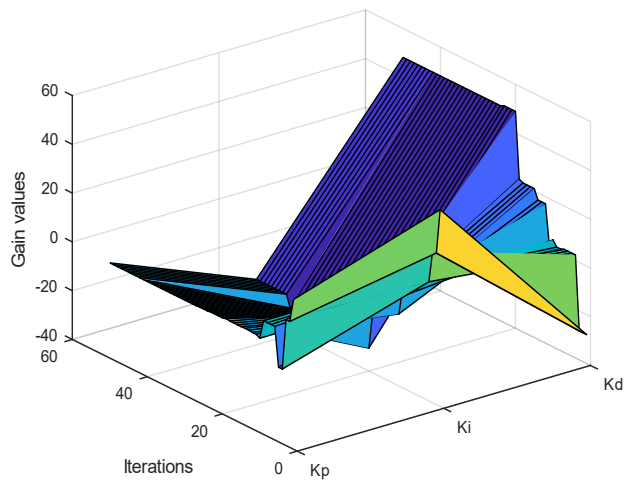


Figure 3.29 : FO-PID gains evolution (K_p, K_i, K_d) under El Centro earthquake.

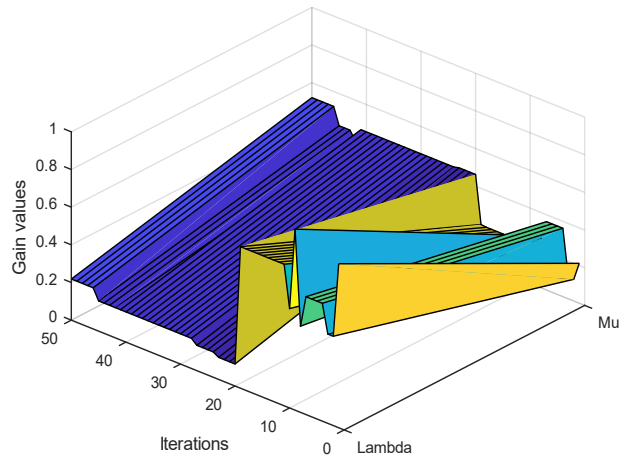


Figure 3.30 : FO-PID gains evolution (λ, μ) under El Centro earthquake.

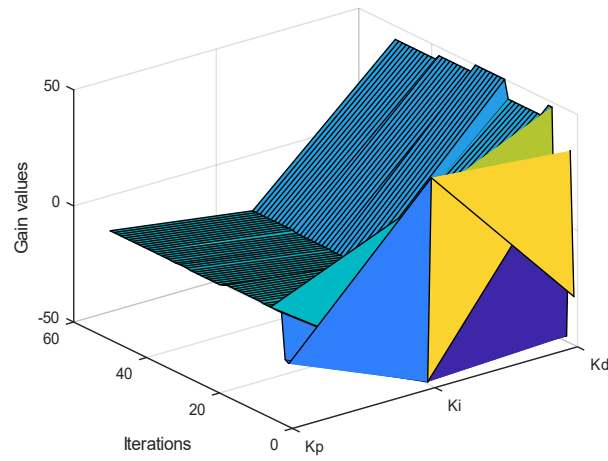


Figure 3.31 : FO-PID gains evolution (K_p, K_i, K_d) under Chi-Chi earthquake.

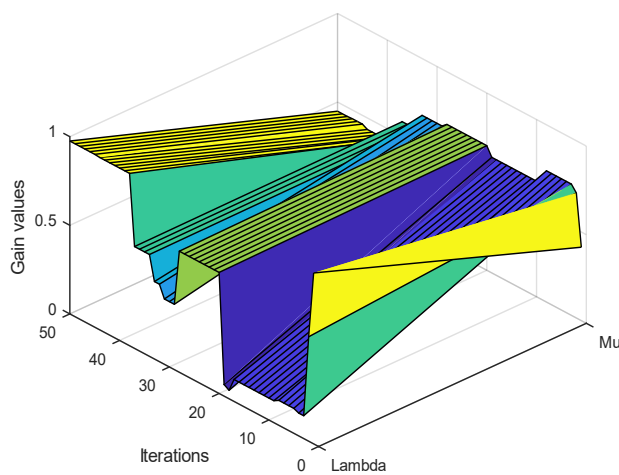


Figure 3.32 : FO-PID gains evolution (λ, μ) under Chi-Chi earthquake.

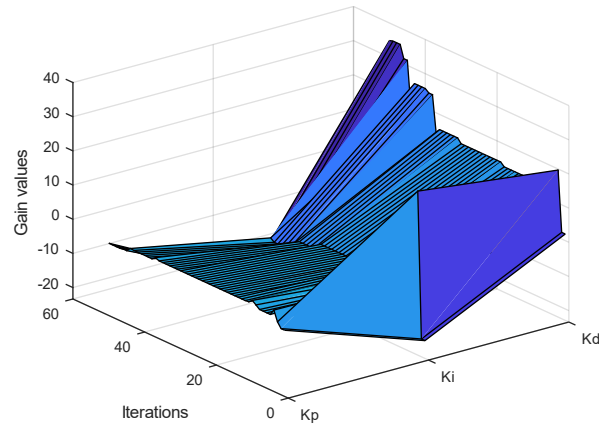


Figure 3.33 : FO-PID gains evolution (K_p, K_i, K_d) under Kobe earthquake.

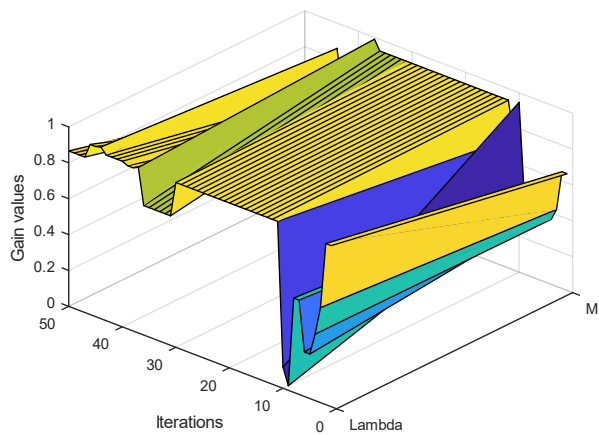


Figure 3.34 : FO-PID gains evolution (λ, μ) under Kobe earthquake.

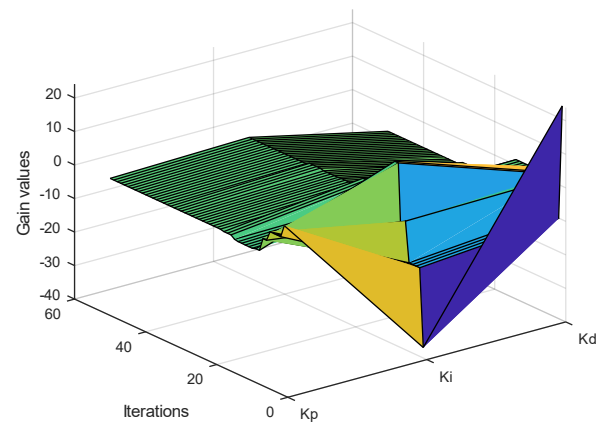


Figure 3.35 : FO-PID gains evolution (K_p, K_i, K_d) under Loma Prieta earthquake.

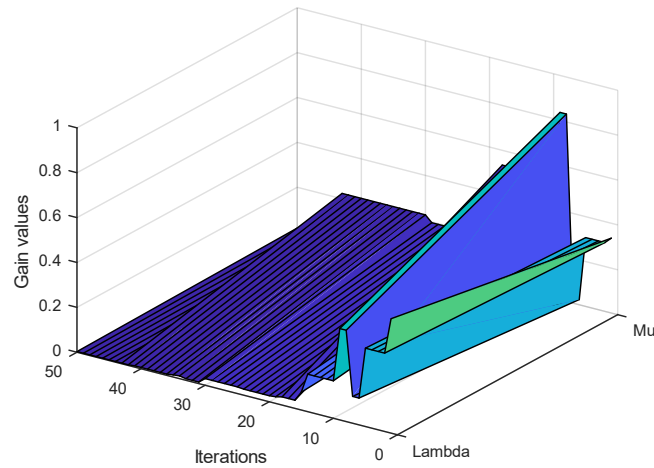


Figure 3.36 : FO-PID gains evolution (λ, μ) under Loma Prieta earthquake.

Figures 3.22 to 3.26 shows the evolution of the parameters gain of the classical PID controller (K_p, K_i, K_d) during the AHA algorithm under several earthquakes: Northridge, El Centro, Chi-Chi, Kobe and Loma Prieta respectively. On the other hand, the figures from 3.27 to 3.36 show the evolution of the parameters gain of the FO-PID controller (K_p, K_i, K_d, λ and μ), under the same previous algorithm and earthquakes. Based on the obtained results presented in Table 3.9, the FO-PID controller gives optimum values of the objective function compared with the classical PID, which mean minimum displacement in the top floor under all earthquake excitations.

Table 3.10 : The optimum parameters of the PID and FO-PID controllers obtained by different used earthquakes.

Earthquake ground motions	Artificial Hummingbird Algorithm (PID)			Artificial Hummingbird Algorithm (FO-PID)				
	K_p	K_i	K_d	K_p	K_i	K_d	λ	μ
Northridge	-1.2109	-5.9405	-0.7796	0.2387	-20.0300	12.2625	0.9948	0.8248
El Centro	-1.6831	-7.0496	-0.9066	-0.9673	-25.3107	48.1543	0.2184	0.5205
Chi-Chi	-1.6722	-10.3402	-0.6354	-3.0592	-12.0348	44.2058	0.9754	0.4485
Kobe	-1.6419	-3.8140	-0.7171	-2.1816	-23.3380	34.8575	0.8663	0.5327
Loma Prieta	-0.6652	5.6568	-0.7508	0.8828	1.8741	-7.5443	0.0029	0.0182

Table 3.10 shows the optimum parameters of the FO-PID and PID controllers obtained using the Artificial Hummingbird optimization algorithm. These parameters were obtained using five

different earthquake excitations. The AHA algorithm is used to find the best parameters of the FO-PID and PID in which the maximum top floor displacement is minimized.

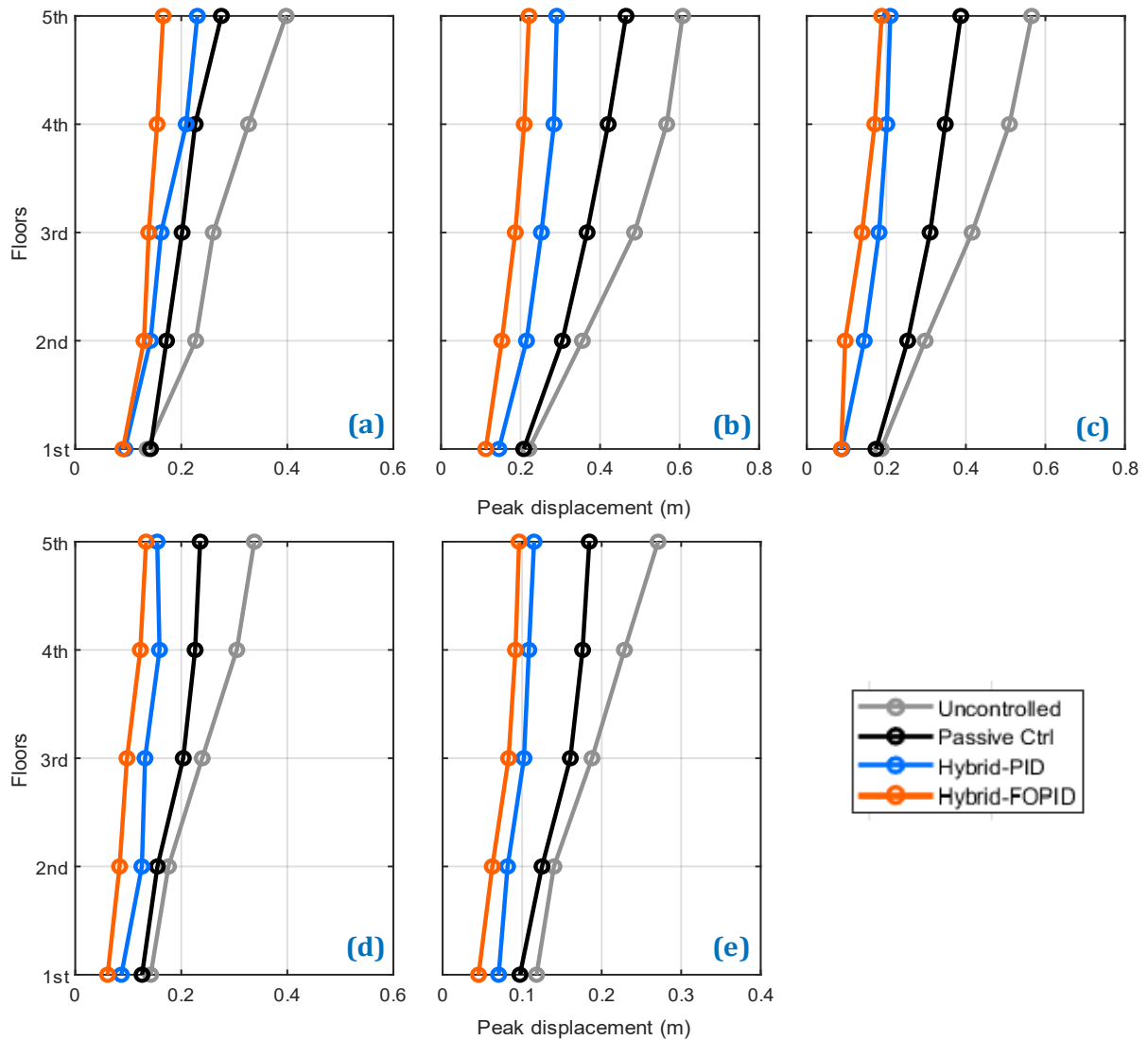


Figure 3.37 : Maximum story drift for the structure under the different seismic excitations, (a) Northridge, (b) El Centro, (c) Chi-Chi, (d) Kobe and (e) Loma Prieta.

According to Fig. 3.37, which shows the maximum story drift for the structure under the different used seismic excitations, it can be seen that for the five scenarios, the Hybrid FO-PID control system gives the best performance compared to Hybrid-PID and obviously performs better than the passive control system or the uncontrolled system. The hybrid control system using an optimized FO-PID controller gives good results in reducing the maximum displacement on every single floor of the building structure.

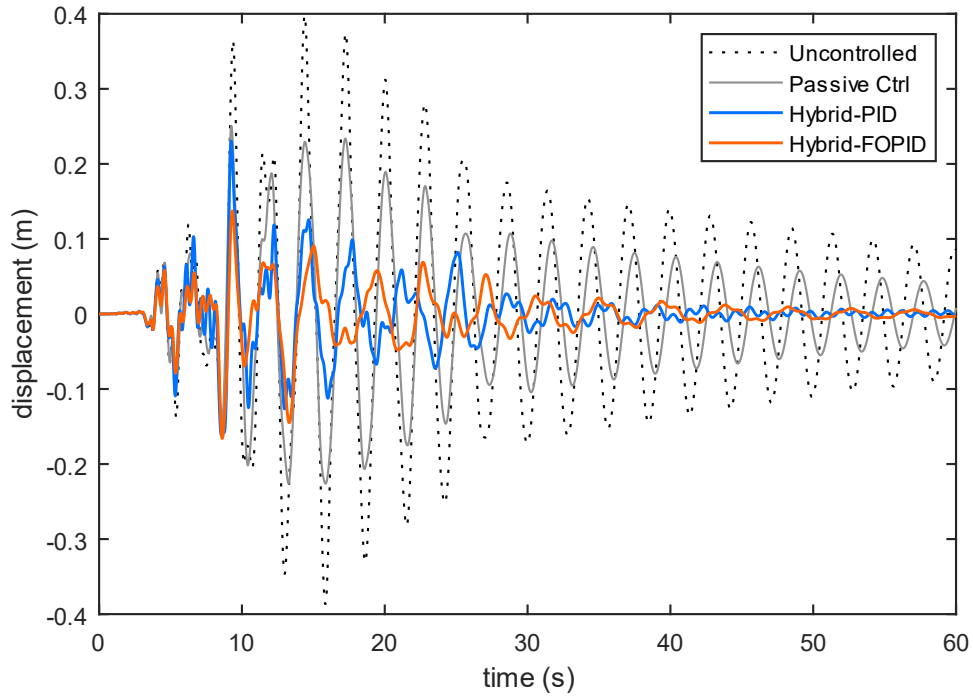


Figure 3.38 : Time history displacement of the top story of the structure during Northridge earthquake excitation using the different optimization algorithms.

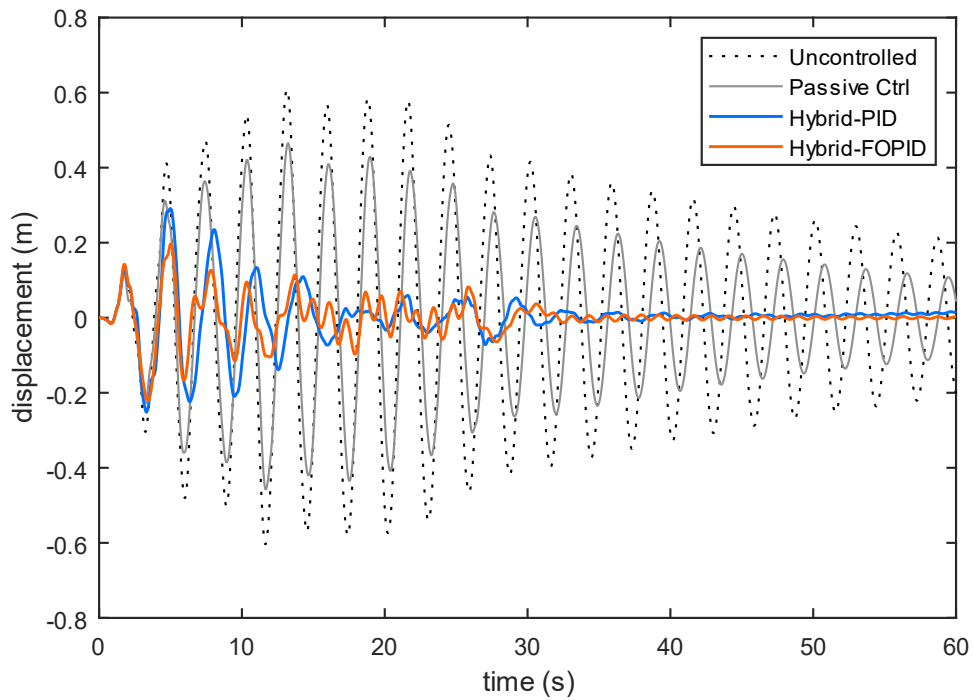


Figure 3.39 : Time history displacement of the top story of the structure during El Centro earthquake excitation using the different optimization algorithms.

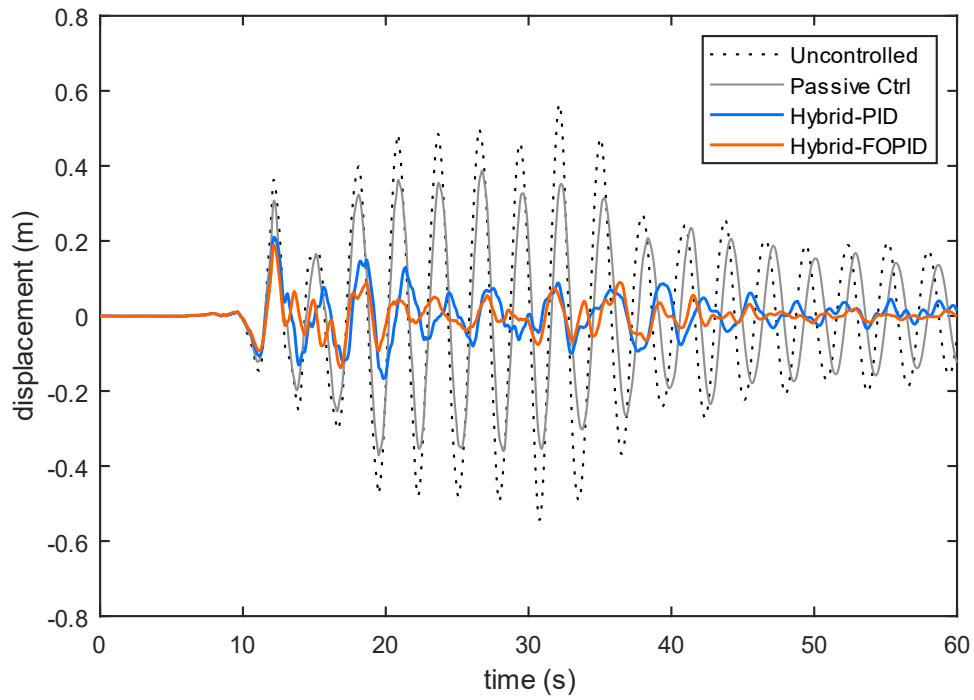


Figure 3.40 : Time history displacement of the top story of the structure during Chi-Chi earthquake excitation using the different optimization algorithms.

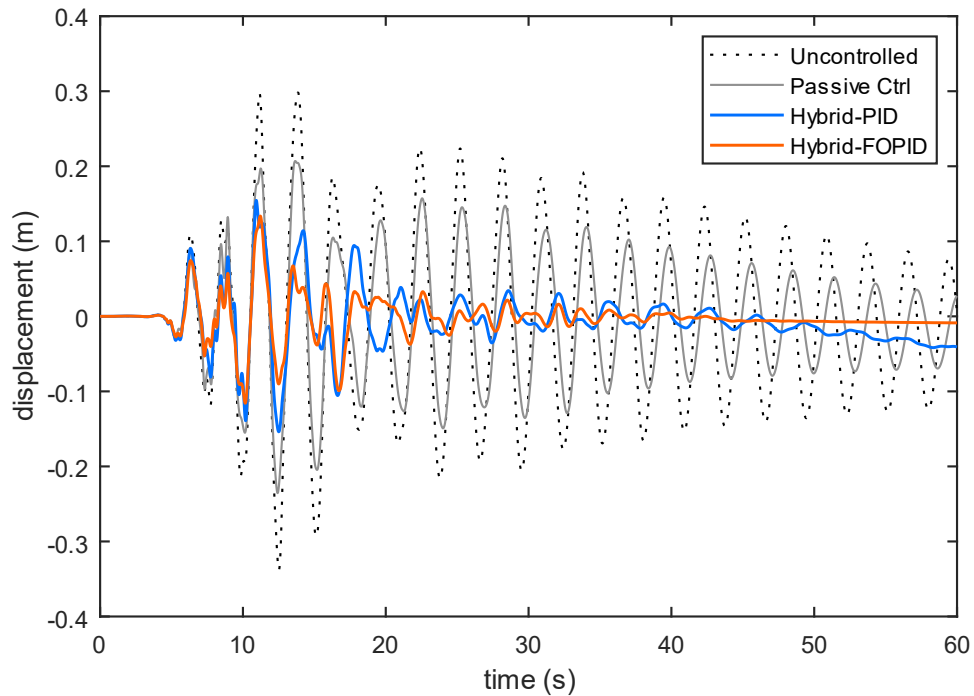


Figure 3.41 : Time history displacement of the top story of the structure during Kobe earthquake excitation using the different optimization algorithms.

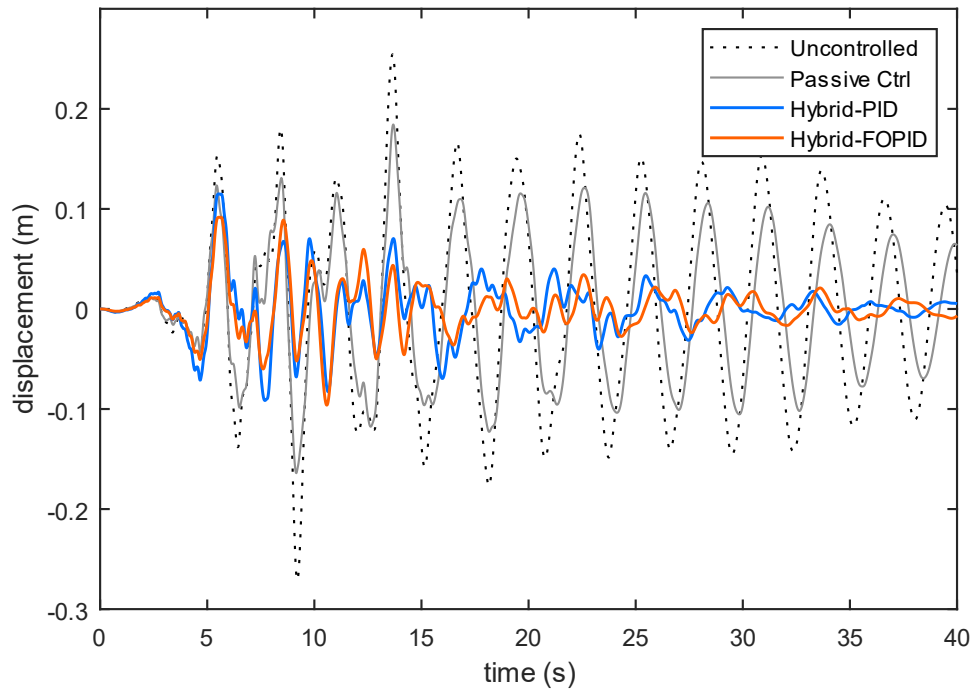


Figure 3.42 : Time history displacement of the top story of the structure during Loma Prieta earthquake excitation using the different optimization algorithms.

Table 3.11 : Maximum responses under different earthquake excitation.

Story	Peak Displacement (m)				Response reduction (%)		
	Uncontrolled response	Passive Ctrl	Hybrid Control		Passive Ctrl	Hybrid Control	
			PID	FO-PID		AHA	FO-PID
Northridge							
1	0.1454	0.142	0.0937	0.0901	2.34	35.56	38.03
2	0.2271	0.1722	0.1419	0.1296	24.17	37.52	42.93
3	0.2604	0.2016	0.162	0.1386	22.58	37.79	46.77
4	0.3271	0.2263	0.2094	0.1544	30.82	35.98	52.8
5	0.3977	0.2757	0.2303	0.1659	30.68	42.09	58.29
El Centro							
1	0.2210	0.2082	0.1456	0.1125	5.79	34.12	49.1
2	0.3555	0.3053	0.2150	0.1529	14.14	39.53	57
3	0.4867	0.3673	0.2525	0.1867	24.53	48.12	61.64
4	0.5676	0.4204	0.2840	0.2092	25.94	49.97	63.15
5	0.6077	0.4652	0.2911	0.2211	23.45	52.1	63.62
Chi-Chi							
1	0.1873	0.1739	0.0886	0.0866	7.15	52.71	53.76
2	0.2977	0.2537	0.1443	0.0964	14.77	51.53	67.61
3	0.4157	0.3101	0.1816	0.1388	25.41	56.32	66.61
4	0.5096	0.3482	0.2013	0.1709	31.67	60.5	66.46
5	0.5655	0.3482	0.2099	0.1883	38.42	62.89	66.7
Kobe							
1	0.1423	0.1260	0.0870	0.0611	11.45	38.86	57.06
2	0.1758	0.1550	0.1257	0.0836	11.85	28.5	52.45
3	0.2395	0.2037	0.1316	0.0976	14.93	45.05	59.25
4	0.3047	0.2261	0.1590	0.1228	25.80	47.82	59.7
5	0.3378	0.2355	0.1546	0.1337	30.28	54.24	60.43
Loma Prieta							
1	0.1181	0.0973	0.0705	0.0452	17.61	40.3	61.73
2	0.1400	0.1250	0.0817	0.0625	10.71	41.64	55.36
3	0.1878	0.1606	0.1023	0.0830	14.49	45.53	55.8
4	0.2286	0.1759	0.1085	0.0916	23.03	52.54	59.93
5	0.2710	0.1844	0.1150	0.0961	31.96	57.56	64.54

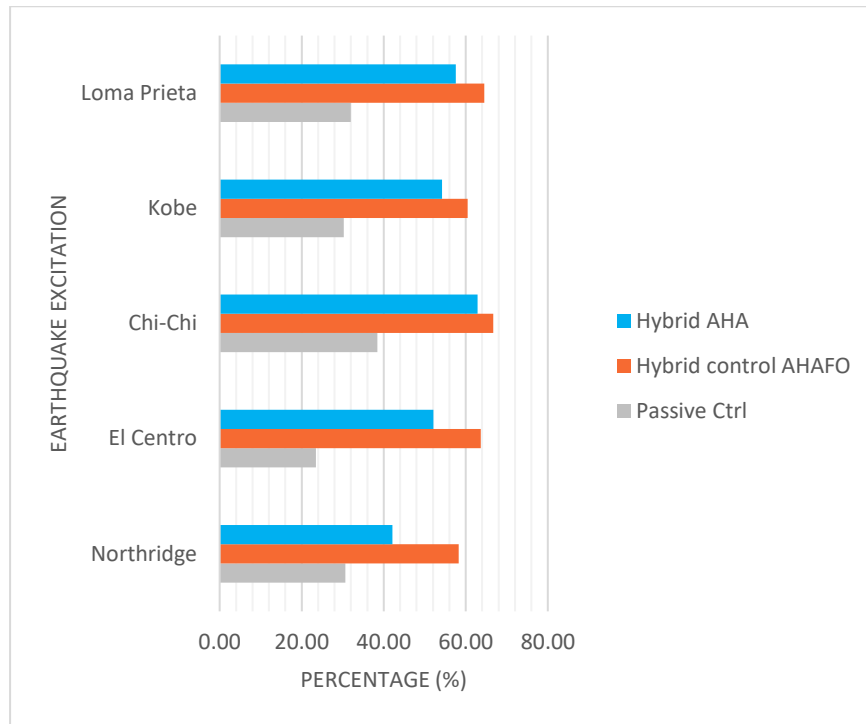


Figure 3.43 : The reduction of maximum response for the top story.

The maximum displacement of every floor for uncontrolled, passive, and hybrid-controlled systems and the percentage of response reduction against different earthquake excitations using Optimized FO-PID and PID controllers are shown in Table 3.11 and in Fig. 3.43.

Looking at Fig. 3.38 shows the top floor displacement during the Northridge earthquake excitation. It can be seen that the Hybrid control system using an optimized FO-PID controller reduces the maximum displacement by 58%, while the PID controller by 42%. In Fig. 3.39 again, the FO-PID controller outperforms the classical PID controller in reducing the maximum displacement by almost 63% during El Centro earthquake excitation, while the classical PID controller reduces the top story peak response by 52%. Fig. 3.40 shows the top floor displacement during Chi-Chi earthquake excitation. In this case, the hybrid control using the optimized FO-PID controller reduces the maximum displacement by almost 67%, while the classical PID controller by only 62%. As shown in Fig. 3.41 and Fig. 3.42, the hybrid control system using the optimized FO-PID gives better performance compared to the classical PID controller by reducing the peak displacement by 60% and 64%, respectively. These previous figures show that all controllers can reduce the structural response, but the FO-PID controller reduces the displacement of the top floor more significantly and gives better performance overall.

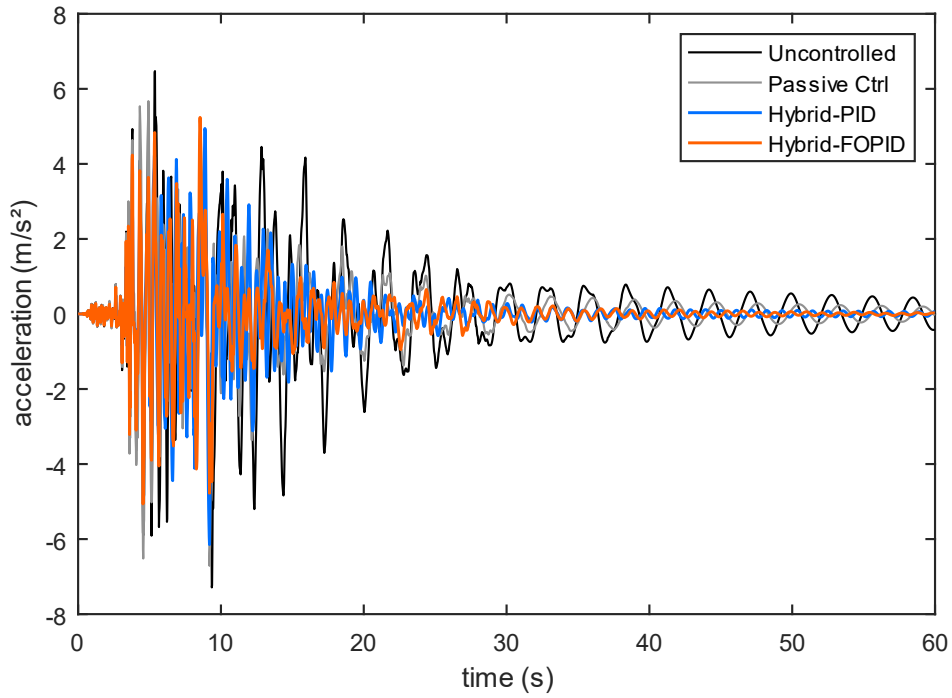


Figure 3.44 : Top story acceleration during Northridge earthquake excitation using the different optimization algorithms.

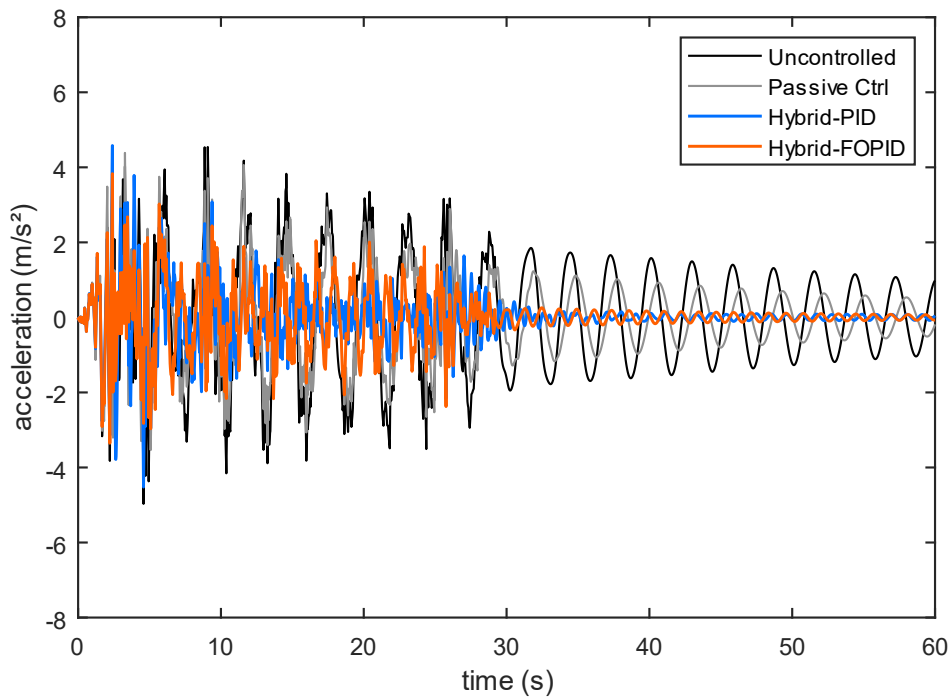


Figure 3.45 : Top story acceleration during El Centro earthquake excitation using the different optimization algorithms.

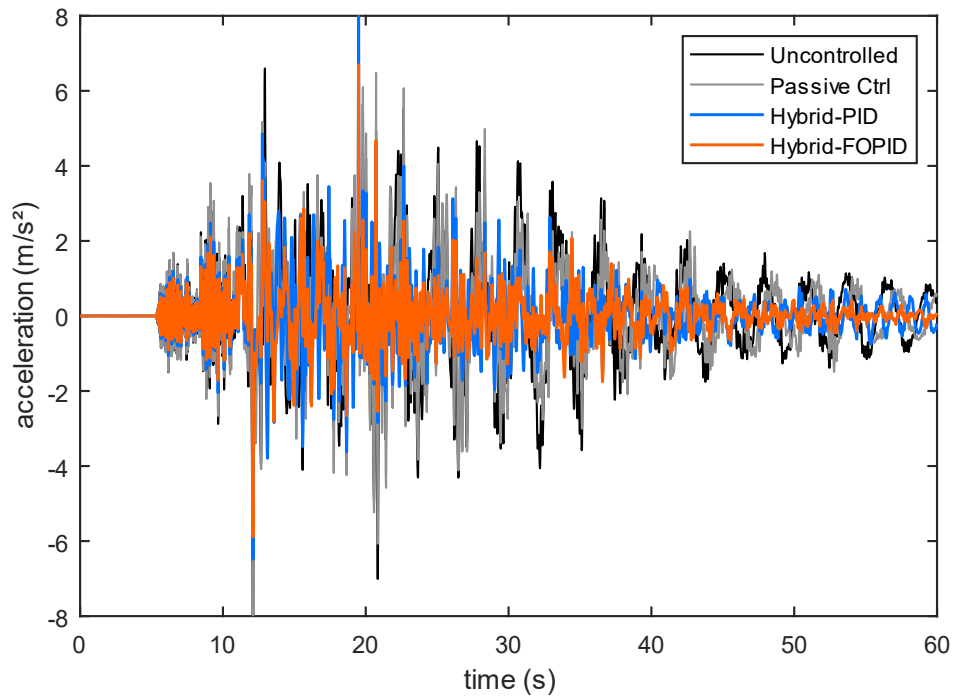


Figure 3.46 : Top story acceleration during Chi-Chi earthquake excitation using the different optimization algorithms.

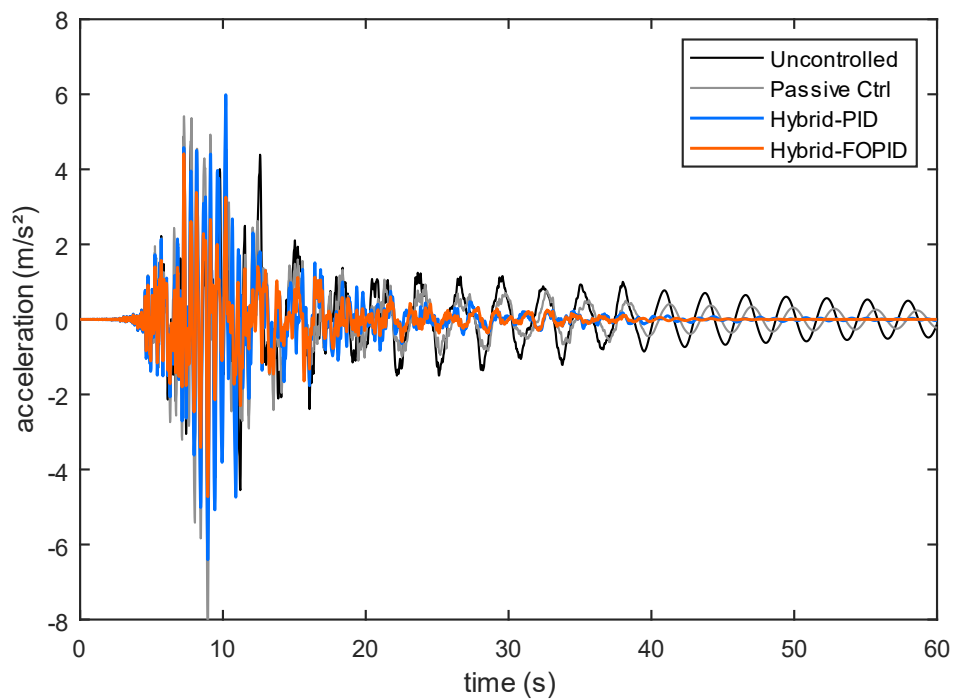


Figure 3.47 : Top story acceleration during Kobe earthquake excitation using the different optimization algorithms.

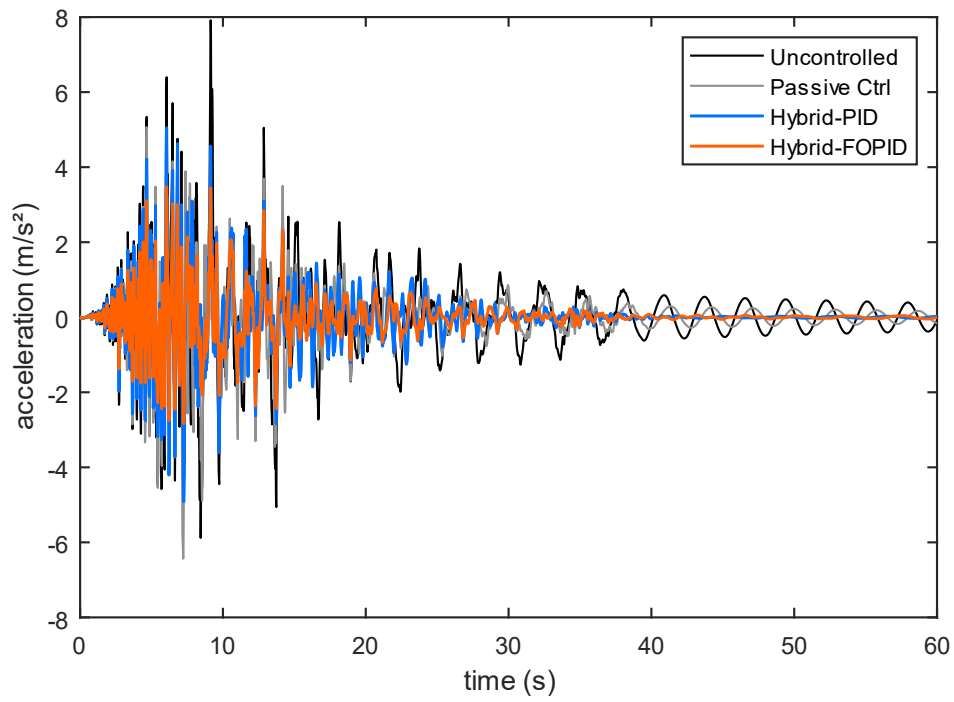


Figure 3.48 : Top story acceleration during Loma Prieta earthquake excitation using the different optimization algorithms.

Table 3.12 : Average accelerations under different earthquake excitation.

Story	Average Acceleration (m/s ²)				Average Acceleration reduction (%)		
	Uncontrolled response	Passive Ctrl	Hybrid Control		Passive Ctrl	Hybrid Control	
			PID	FO-PID		AHA	FO-PID
Northridge							
1	0.5625	0.3715	0.5051	0.3013	33.96	10.21	46.43
2	0.7832	0.3752	0.7036	0.4325	52.10	10.16	44.78
3	0.6867	0.5911	0.3895	0.3385	13.92	43.27	50.70
4	0.6583	0.5471	0.5548	0.3204	16.90	15.72	51.32
5	0.8921	0.5638	0.4303	0.3654	36.80	51.76	59.04
El Centro							
1	0.5032	0.4398	0.4576	0.4483	12.60	9.06	10.92
2	0.7805	0.5928	0.4902	0.3921	24.05	37.19	49.76
3	0.9864	0.7432	0.3458	0.2572	24.66	64.94	73.93
4	1.1468	0.8395	0.4147	0.3111	26.80	63.83	72.87
5	1.2771	0.8616	0.3594	0.4164	32.54	71.86	67.39
Chi-Chi							
1	0.6816	0.4123	0.6350	0.4272	39.50	6.84	37.32
2	0.8028	0.7511	0.6977	0.3795	6.44	13.08	52.72
3	0.8815	0.8411	0.4857	0.3624	4.58	44.90	58.89
4	0.9614	0.9132	0.5682	0.3671	5.02	40.90	61.82
5	1.0526	0.8900	0.5556	0.4086	15.44	47.22	61.18
Kobe							
1	0.4014	0.2868	0.2644	0.2085	28.57	34.14	48.07
2	0.5156	0.3789	0.3155	0.2541	26.53	38.82	50.72
3	0.5364	0.5049	0.3246	0.2221	5.86	39.48	58.59
4	0.5980	0.5919	0.3564	0.2143	1.02	40.40	64.16
5	0.6432	0.5156	0.3493	0.2424	19.83	45.70	62.32
Loma Prieta							
1	0.5207	0.3133	0.2496	0.2751	39.83	52.07	47.16
2	0.5904	0.3746	0.2545	0.2618	36.55	56.89	55.66
3	0.6520	0.4755	0.4323	0.2440	27.07	33.70	62.58
4	0.6570	0.5011	0.4091	0.2550	23.73	37.73	61.18
5	0.7067	0.4971	0.3681	0.2782	29.67	47.91	60.64

To evaluate the performance of the different controlling systems, the average accelerations of every floor for uncontrolled, passive, and hybrid-controlled systems and the percentage of average acceleration reduction against different earthquake excitations using FO-PID and PID controllers are shown in Table 3.12.

From Fig. 3.44, Fig. 3.45, Fig. 3.46, Fig. 3.47, and Fig. 3.48, the performance of FO-PID controlled system performs better than the classical PID in reducing the top floor average acceleration by 59%, 67%, 61%, 62%, and 60%, in comparison, to the uncontrolled structure, for Northridge, El Centro, Chi-Chi, Kobe, and Loma Prieta earthquakes.

In this work and based on the obtained results, we succeeded pretty much to maintain the safe displacement responses of a 5-story building against different earthquake excitations based on the proposed hybrid vibration control system. Where, the parameters gain of the FO-PID were chosen in an optimal way using the AHA metaheuristic algorithm, the examined building structure system is represented mathematically using a state-space representation, two inputs (earthquake excitation and the control force signal) and the outputs are the displacements, and the accelerations responses. The effect of the fractional-order derivative and integration of the FO-PID is clearly visible in the comparative study with the integer-order PID controller. The maximum displacement of all the floors under the applied force control of the proposed FO-PID ranging between $2 \leq x \leq 11$, the classical PID force control ranging between $3 \leq x \leq 17$, from the both displacement interval, the positive effect of the two fractional-order actions is clearly visible. In the side of control force, i.e. the energy consumed by the actuators, we see that interval search of the selected FO-PID controller gains are more suitable in economical point of view where: $0.9 \leq K_p \leq -3$, $-25 \leq K_i \leq 2$ **and** $48 \leq K_d \leq -8$.

Chapter

4

Hybrid Vibration Control for Structures with soil-structure interaction : Simulation & Numerical Results.

CHAPTER 4 HYBRID VIBRATION CONTROL FOR STRUCTURES WITH SOIL-STRUCTURE INTERACTION: SIMULATION AND NUMERICAL RESULTS

4.1 Introduction

The dynamic response of structures equipped with vibration control systems are usually investigated without taking soil-structure interaction (SSI) effects into consideration. Taking the SSI effects can significantly and drastically impact the dynamic properties of the studied structure. Many studies have shown that the SSI effect cannot be ignored if we want to obtain the best performance from the active vibration control system.

This chapter aims to show and discuss the impacts of SSI on the seismic performance of the structures and the effectiveness of the implemented controllers. A mathematical model is created, or the time domain examination of tall buildings equipped with ATMD and including SSI effects. The numerical analyses are conducted on a 5-story building structure subjected to various historically well-known seismic excitations, taking into account the fixed base case and three types of soil states: soft, medium, and dense soil.

An optimized PID controller is used for tuning control force of ATMD in different conditions of ground state. Also, the Artificial Hummingbird algorithm (AHA) is used for the gain parameters of the controller in both cases without and with SSI effects.

Mathematical Formulation:

The equation of motion for the system can be expressed as follows:

$$[M]\{\ddot{x}\} + [C]\{\dot{x}\} + [K]\{x\} = -[M]\{r\}\{\ddot{x}_g\} - \{d\}f(t) \quad (4.1)$$

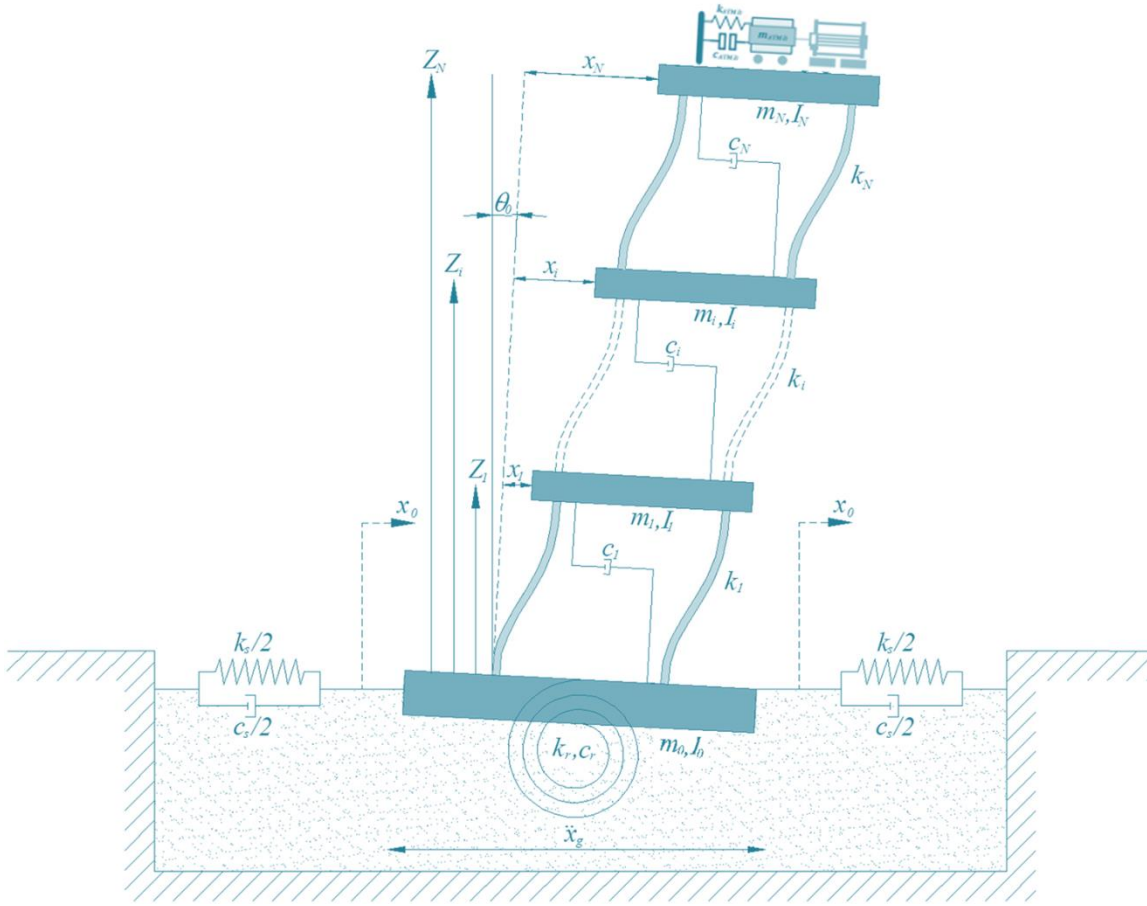


Figure 4.1 : Building structure equipped with ATMD including SSI effects.

Figure 15 shows a 5-story building structure with ATMD considering the SSI effect. The AMTD parameters mass, viscous damping and stiffness are represented by M_{ATMD} , C_{ATMD} and K_{ATMD} , while the stiffness and damping between the different floors are assumed to be $[M]$, $[C]$ and $[K]$ respectively. Also $\{\ddot{x}\}$, $\{\dot{x}\}$ and $\{x\}$ are the acceleration, velocity, and displacement vectors of the system respectively.

Displacement vector: $\{x\} = [x_b, x_1, \dots, x_n, x_{atmd}]^T$,

velocity vector: $\{\dot{x}\} = [\dot{x}_b, \dot{x}_1, \dots, \dot{x}_n, \dot{x}_{atmd}]^T$,

acceleration vector: $\{\ddot{x}\} = [\ddot{x}_b, \ddot{x}_1, \dots, \ddot{x}_n, \ddot{x}_{atmd}]^T$.

x_b : the displacement of the base.

x_{atmd} : the ATMD displacements.

$\{r\}$: is called influence vector, wherein this study $\{r\} = [1, 1, \dots, 1, 1]^t$.

$\{d\}$: is a vector, this vector locates where the control forces are applied

$$[K] = \begin{bmatrix} k_b + k_1 & -k & 0 & & \dots & & 0 \\ -k & k_1 + k_2 & -k_2 & & & & \\ 0 & -k_2 & \ddots & \ddots & & & \vdots \\ \vdots & & \ddots & \ddots & \ddots & & \\ & & & & k_n + k_{atmd} & -k_{atmd} & \\ & & & & -k_{atmd} & k_{atmd} & \\ 0 & & & & & & K_s & 0 \\ & & & & & & 0 & K_r \end{bmatrix} \quad (4.4)$$

In this study, the dynamic system is represented with a state-space representation, where x represents the state vector and u represents the input vector.

$$\begin{cases} \dot{x} = Ax + Bu \\ y = Cx + Du \end{cases} \quad (4.5)$$

A , B , C , and D are the system, input, output, and feedthrough matrices in that order.

x , u , y are state, input, and output vectors.

The properties of the building are shown in previous chapter. Two different ground acceleration are used in this numerical simulation: Northridge and El Centro (as indicated in Table 4.2), with magnitudes ranging from 6.7 to 6.9.

Table 4.2 : Earthquakes are considered in the numerical study.

Eq.	Location	Date of occurrence	Station	PGA (g)	Moment magnitude
EQ1	Northridge	1994	Beverly Hills-Mulhol	0.52	6.7
EQ2	El Centro	1940	USGS station 0117	0.38	6.9

4.2 Results and discussion

The hybrid vibration control system is evaluated from two points of view, the safety of the structural building and the residential comfort, the criteria used for the optimization of the PID controller is the maximum horizontal displacement of the building's top story.

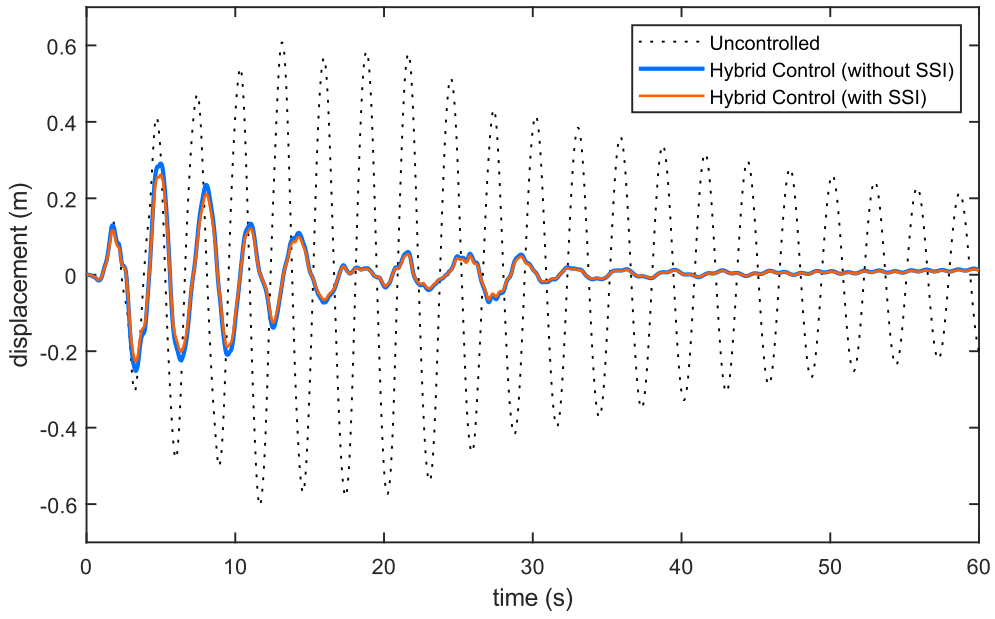


Figure 4.2 : Top story displacement with and without SSI effect, El Centro earthquake, Dense Soil.

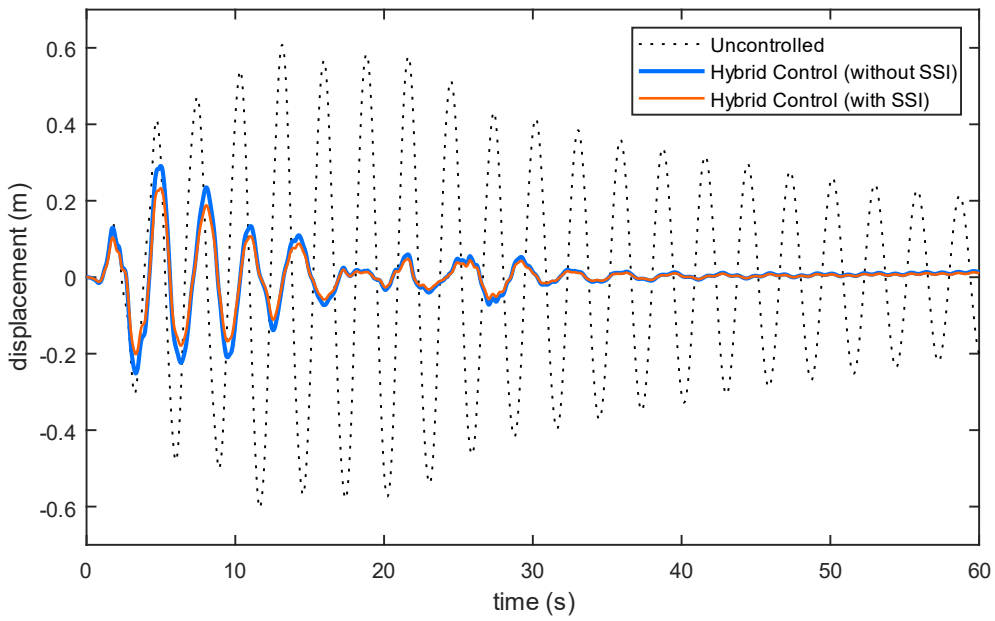


Figure 4.3 : Top story displacement with and without SSI effect, El Centro earthquake, Medium Soil.

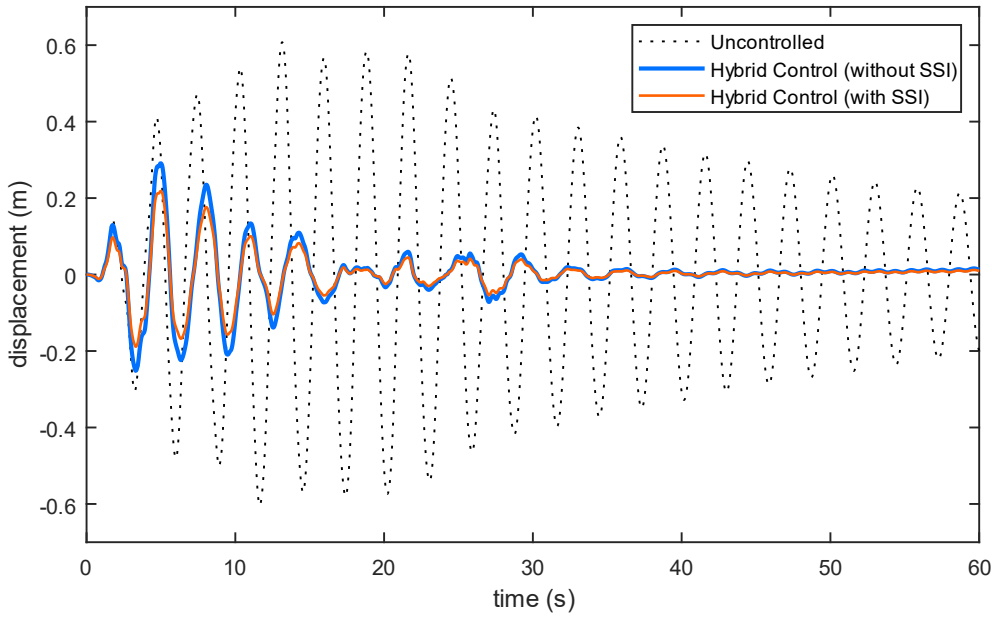


Figure 4.4 : Top story displacement with and without SSI effect, El Centro earthquake, Soft Soil.

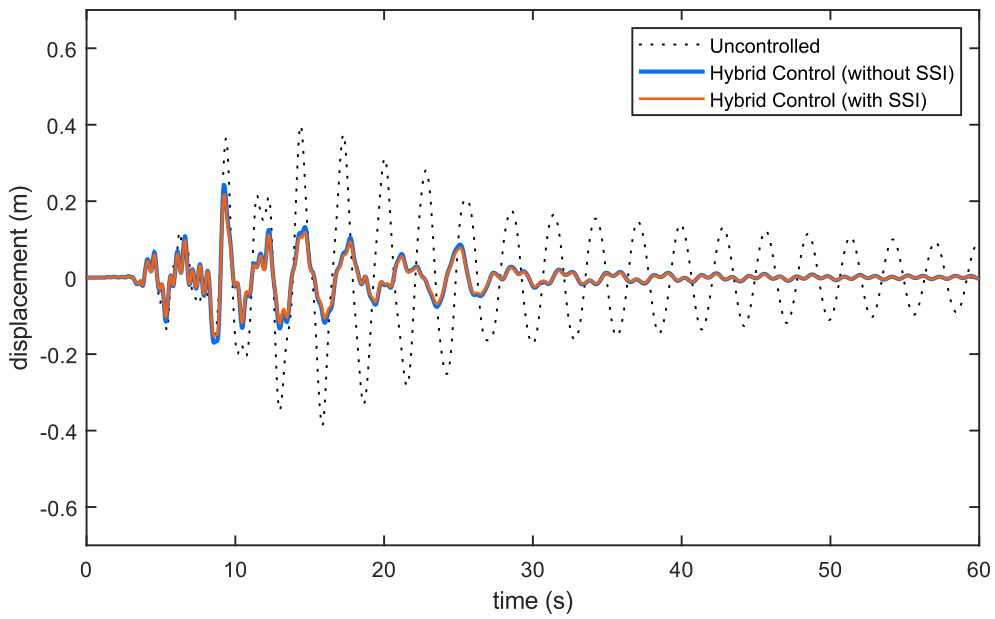


Figure 4.5 : Top story displacement with and without SSI effect, Northridge earthquake, Dense Soil.

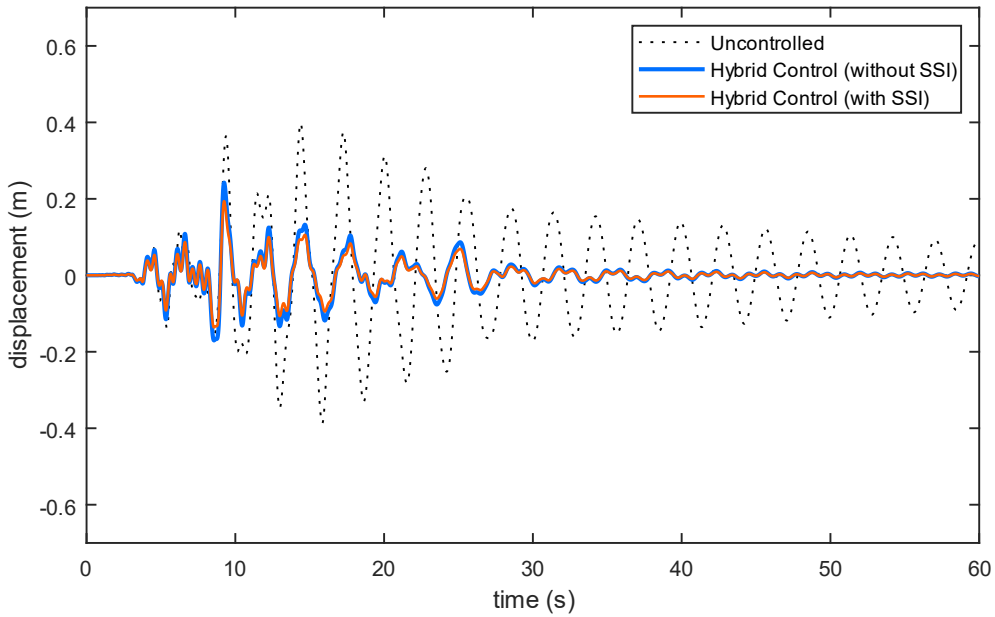


Figure 4.6 : Top story displacement with and without SSI effect, Northridge earthquake, Medium Soil.

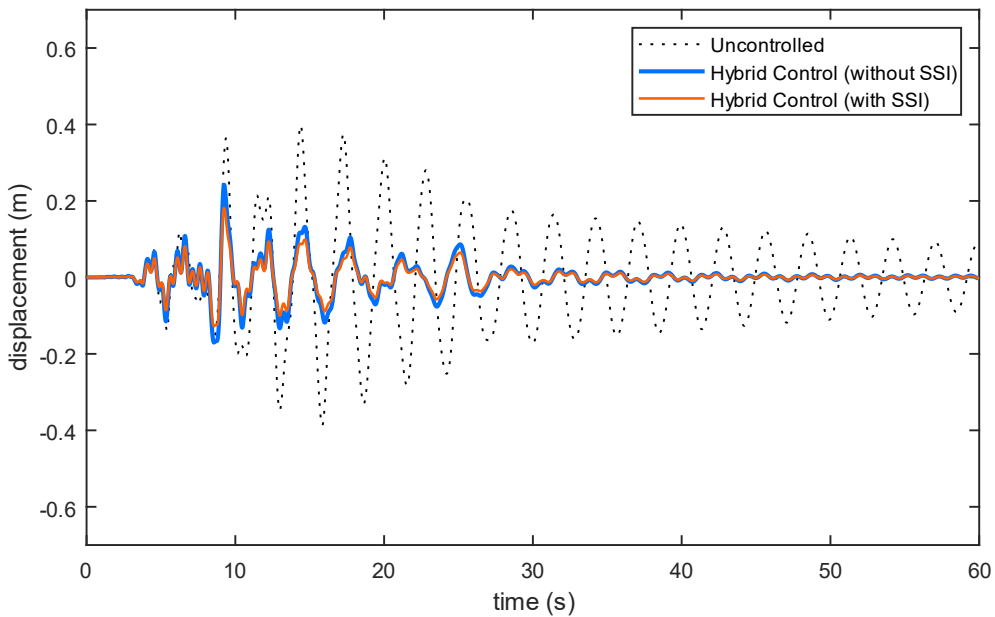


Figure 4.7 : Top story displacement with and without SSI effect, Northridge earthquake, Soft Soil.

The time history analyses of the building structures are carried out using two well-known strong earthquake excitations, El Centro (1940) and Northridge (1994). The structure equipped with hybrid vibration control system controlled by an FO-PID controller is simulated without and with SSI effect and also without control. These three cases will be compared together. In case where SSI effect is considered, three types of soil (dense, medium, and soft) are used.

As shown in Figures 4.2, 4.3 and 4.4, it can be seen that the response of the building lying on dense soil is very close to the response of the fixed base structure. Also, it can be observed that the soft soil has important effect on the response of the building in such way that the structure with soft soil can help the hybrid control system to decrease the uncontrolled peak response of the top floor of the fixed base structure under the El Centro earthquake excitation. The same observations can be seen on Figures 4.5, 4.6 and 4.7.

From all the previous results, it can be seen that when the foundation stiffness decreases, the structure's dynamic response also decreases, energy, so the dynamic response of the structure on soft soil is generally smaller than that on hard soil. This is so because soft soil can absorb more energy compared to hard soil. Therefore, ignoring the SSI effect may result in significant errors in the seismic analysis of high-rise structures, which is consistent with the obtained results.

4.3 Conclusion

Neglecting the SSI impacts could lead to inaccurate and unrealistic results of the structure's seismic behavior.

The optimum hybrid vibration control for different support conditions is very different. For fixed based and dense soil, the controlling results, but compared to the soft soil the performance can be completely different. In that case, the fixed based assumptions can be only accepted for very dense soil.

It is found that hybrid vibration control is more effective for the higher soil stiffness and their efficiencies are degraded in soft soils. Furthermore, the SSI significantly effects on the optimum design of the PID controller. The adopted controller is significantly able to mitigate the peak top floor displacement of the tall building, compared to uncontrolled building. The performance of the controllers decreases with increasing soil softness, so that the ignoring the SSI effects may result in incorrect and unrealistic results of the seismic behavior of the structures.



General conclusion

General Conclusion

The earthquake remains the number one enemy of structures because it presents the most destructive phenomenon in urbanized areas. It is unfortunately certain that earthquakes will continue to surprise man and because of the impossibility of predicting them, the only valid prevention is to build earthquake-resistant because prevention is better than cure. Among the seismic construction methods is structural vibration control technology.

This study presents the results of the analysis of the hybrid control of the vibrations of buildings, the result of the coupling of the insulation at the base with a TMD or ATMD damper in order to compensate for the deficiencies of the seismic insulation against high intensity earthquakes, such as reduced travel at the base and high accelerations at the top of the building.

In which, three control algorithms have been studied, which are: open loop control law, closed loop control law and closed open loop control law. These algorithms have been used, on structures with 1 and n DOF , to calculate the force necessary to apply.

Base on the numerical study carried out in this study, the following conclusions can be made:

- A state of the art has about the different methods of structural vibration control as well as a historical overview of these methods and their importance in controlling building vibration is presented.
- The behavior of isolated structures differs from one earthquake to another, and from one base isolation system to another.
- The numerical study must be driven over a wide range of seismic excitations recordings and many structural configurations in order to be able to validate the results and to properly judge the proposed vibration control systems.
- All controlled systems reduce the displacements and the accelerations of the different floors.
- Based on the structural response reduction percentage, it is clear that the hybrid (Base isolators + ATMD) control system is far more efficient than the passive control.
- The FO-PID controller can give a remarkable and better controlling performance of the system compared to the classical PID controller.
- All control systems can lead to reduced structural responses.

- The hybrid control system (Base isolators + ATMD) is significantly better and more efficient than the passive control system based on the structural response reduction percentages.
- It is found that hybrid vibration control is more effective for the higher soil stiffness and their efficiencies are degraded in soft soils. Furthermore, the SSI significantly effects on the optimum design of the PID controller. The adopted controller is significantly able to mitigate the peak top floor displacement of the tall building, compared to uncontrolled building. The performance of the controllers decreases with increasing soil softness, so that the ignoring the SSI effects may result in incorrect and unrealistic results of the seismic behavior of the structures.
- The essence of this work has been assembled into an interactive graphical interface using MATLAB, to make this work available and easy to exploit for all concerned in the field of the active vibration control of a multi-story building structure. The Artificial Hummingbird algorithm outperforms the other optimization algorithms in reducing the displacements and accelerations of the 5-story building during the different earthquake excitations.

Further works

- More than one active control can be placed on different building floors. This is known as the multi-variable active control.
- Adding uncertainty in a mathematical model of building structure to check the robustness of proposed controllers.
- Generalized this work in discrete-time and frequency domain.
- Stability study of the building structure under different earthquake excitations in time and frequency domain.

References

- [1] Aiken, Ian D., Douglas K. Nims, and James M. Kelly. "Comparative study of four passive energy dissipation systems." *Bulletin of the New Zealand Society for Earthquake Engineering* 25, no. 3 (1992): 175-192.
- [2] Kelly, James M., R. I. Skinner, and A. J. Heine. "Mechanisms of energy absorption in special devices for use in earthquake resistant structures." *Bulletin of the New Zealand Society for Earthquake Engineering* 5, no. 3 (1972): 63-88.
- [3] Meirovitch, Leonard. *Dynamics and control of structures*. John Wiley & Sons, 1991.
- [4] Martelli, Alessandrol Forni, and Hyun Min Koh. "Main features and conclusions of the 1999 international post-SMiRT conference seminar on seismic isolation, passive energy dissipation and active control of vibrations of structures." (2001).
- [5] Cheng, F., and C. Pantelides. "Algorithm development for using optimal control in structural optimization subjected to seismic and wind forces." NSF Report, US Department of Commerce, *National Technical Information Service*, NTIS No. PB90-1333471 (1998).
- [6] Cheng, Franklin Y., Peter Tian, V. Rao, K. Martin, Frank W. Liou, and Jung-Hua Yeh. "Theoretical and experimental studies on hybrid control of seismic structures." (1996).
- [7] Soong, T. T., and B. F. Spencer. "Active, semi-active and hybrid control of structures." *Bulletin of the New Zealand Society for Earthquake Engineering* 33, no. 3 (2000): 387-402.
- [8] Casciati, Fabio, and Georges Magonette. *Structural Control for Civil and Infrastructure Engineering: Proceedings of the 3rd International Workshop on Structural Control: Paris, France 6-8 July 2000*. World Scientific, 2001.
- [9] Kelly, James M. "State-of-the-art and state-of-the-practice in base isolation." In *Seminar on Seismic Isolation, Passive Energy Dissipation and Active Control (ATC-17-1)*, Applied Technology Council, Redwood City. 1993.
- [10] Kobori, Takuji. "Future Direction on Research and Development of Seismic-Response-Controlled Structures." *Computer-Aided Civil and Infrastructure Engineering* 11, no. 5 (1996): 297-304.
- [11] Soong, T. T., and B. F. Spencer Jr Reviewer. "Active structural control: theory and practice." *Journal of Engineering Mechanics* 118, no. 6 (1992): 1282-1285.
- [12] Soong, Tsu T., and Michalakis C. Costantinou, eds. *Passive and active structural vibration control in civil engineering*. Vol. 345. Springer, 2014.
- [13] Soong, Tsu T., and Gary F. Dargush. * *Passive Energy Dissipation Systems in Structural Engineering*. Wiley, 1997.
- [14] Soong, T.T. and Spencer Jr, B.F., 2002. Supplemental energy dissipation: state-of-the-art and state-of-the-practice. *Engineering structures*, 24(3), pp.243-259.

- [15] Liu, S. C., M. Tomizuka, and A. G. Ulsoy. "Challenges and opportunities in the engineering of intelligent systems." In *Proc. of the 4th International Workshop on Structural Control*, New York, pp. 295-300. 2004.
- [16] Cheng, Franklin Y. *Smart structures: innovative systems for seismic response control*. CRC press, 2008.
- [17] Casciati, Fabio, Jose Rodellar, and Umut Yildirim. "Active and semi-active control of structures—theory and applications: A review of recent advances." *Journal of Intelligent Material Systems and Structures* 23, no. 11 (2012): 1181-1195.
- [18] Aiken, Ian D., Douglas K. Nims, and James M. Kelly. "Comparative study of four passive energy dissipation systems." *Bulletin of the New Zealand Society for Earthquake Engineering* 25, no. 3 (1992): 175-192.
- [19] Aiken, Ian D., Douglas K. Nims, Andrew S. Whittaker, and James M. Kelly. "Testing of passive energy dissipation systems." *Earthquake spectra* 9, no. 3 (1993): 335-370.
- [20] Arima, Fumiaki, Mitsuo Miyazaki, Hisaya Tanaka, and Yutaka Yamazaki. "A study on buildings with large damping using viscous damping walls." In *Proceedings of the 9th world conference on earthquake engineering*, vol. 821. 1988.
- [21] El-Khoury, Omar, and Hojjat Adeli. "Recent advances on vibration control of structures under dynamic loading." *Archives of Computational Methods in Engineering* 20, no. 4 (2013): 353-360.
- [22] Cheng, Franklin Y., and Hongping Jiang. "Optimum control of a hybrid system for seismic excitations with state observer technique." *Smart materials and structures* 7, no. 5 (1998): 654.
- [23] Ruge, Arthur C. "Earthquake Resistance of Elevated Water-Tanks." *Transactions of the American Society of Civil Engineers* 103, no. 1 (1938): 889-938.
- [24] Kobori, Takuji. "Active seismic response control." *Proceedings of the 9th WCEE, Tokyo-Kyoto, Japan* (1988): 2-9.
- [25] Yao, James TP. "Concept of structural control." *Journal of the Structural Division* 98, no. 7 (1972): 1567-1574.
- [26] Kobori, Takuji, Norihide Koshika, Kazuhiko Yamada, and Yoshiki Ikeda. "Seismic-response-controlled structure with active mass driver system. Part 2: Verification." *Earthquake engineering & structural dynamics* 20, no. 2 (1991): 151-166.
- [27] Liu, S. C., M. Tomizuka, and A. G. Ulsoy. "Challenges and opportunities in the engineering of intelligent systems." In *Proc. of the 4th International Workshop on Structural Control*, New York, pp. 295-300. 2004.
- [28] Kobori, Takuji, Norihide Koshika, Kazuhiko Yamada, and Yoshiki Ikeda. "Seismic-response-controlled structure with active mass driver system. Part 1: Design." *Earthquake Engineering & Structural Dynamics* 20, no. 2 (1991): 133-149.
- [29] Buckle, Ian G. "Passive control of structures for seismic loads." *Bulletin of the New Zealand Society for Earthquake Engineering* 33, no. 3 (2000): 209-221.

- [30] Iemura, H. "Principles of TMD and TLD—Basic principles and design procedure." In *Passive and active structural vibration control in civil engineering*, pp. 241-253. Springer, Vienna, 1994.
- [31] Sadek, Fahim, Fahim Sadek, Andrew W. Taylor, and Riley M. Chung. *Passive energy dissipation devices for seismic applications*. US Department of Commerce, *National Institute of Standards and Technology*, 1996.
- [32] Stanton, John Francis, and Charles W. Roeder. "Elastomeric bearings design, construction, and materials." NCHRP report 248 (1982).
- [33] Roeder, Charles W., and John F. Stanton. "Elastomeric bearings: state-of-the-art." *Journal of Structural Engineering* 109, no. 12 (1983): 2853-2871.
- [34] Koh, Chan Ghee, and James M. Kelly. "A simple mechanical model for elastomeric bearings used in base isolation." *International journal of mechanical sciences* 30, no. 12 (1988): 933-943.
- [35] Roeder, Charles W., John F. Stanton, and Andrew W. Taylor. *Performance of elastomeric bearings*. No. 298. 1987.
- [36] Hameed, Asif, Min-Se Koo, Thang Dai Do, and Jin-Hoon Jeong. "Effect of lead rubber bearing characteristics on the response of seismic-isolated bridges." *KSCE Journal of Civil Engineering* 12, no. 3 (2008): 187-196.
- [37] Salic, Radmila B., Mihail A. Garevski, and Zoran V. Milutinovic. "Response of lead-rubber bearing isolated structure." In *The 14th World Conference on Earthquake Engineering*. 2008.
- [38] Robinson, William H. "Lead-rubber hysteretic bearings suitable for protecting structures during earthquakes." *Earthquake engineering & structural dynamics* 10, no. 4 (1982): 593-604.
- [39] Wu, Yi-feng, Hao Wang, Ai-qun Li, Dong-ming Feng, Ben Sha, and Yu-ping Zhang. "Explicit finite element analysis and experimental verification of a sliding lead rubber bearing." *Journal of Zhejiang University-SCIENCE Hwang, J. S., and S. W. Ku. "Analytical modeling of high damping rubber bearings." Journal of Structural Engineering* 123, no. 8 (1997): 1029-1036. A 18, no. 5 (2017): 363-376.
- [40] Hwang, J. S., and S. W. Ku. "Analytical modeling of high damping rubber bearings." *Journal of Structural Engineering* 123, no. 8 (1997): 1029-1036.
- [41] Kelly, Trevor E. *Base isolation of structures: Design guidelines*. Wellington, New Zealand: Holmes Consulting Group Ltd (2001).
- [42] Mokha, Anoop, M. C. Constantinou, A. M. Reinhorn, and Victor A. Zayas. "Experimental study of friction-pendulum isolation system." *Journal of Structural Engineering* 117, no. 4 (1991): 1201-1217.
- [43] Wang, Yen-Po, Lap-Loi Chung, and Wei-Hsin Liao. "Seismic response analysis of bridges isolated with friction pendulum bearings." *Earthquake Engineering & Structural Dynamics* 27, no. 10 (1998): 1069-1093.

- [44] Wang, Yen-Po, Min-Cheng Teng, and Kuo-Whie Chung. "Seismic isolation of rigid cylindrical tanks using friction pendulum bearings." *Earthquake engineering & structural dynamics* 30, no. 7 (2001): 1083-1099.
- [45] Jangid, R. S. "Optimum friction pendulum system for near-fault motions." *Engineering structures* 27, no. 3 (2005): 349-359.
- [46] Fenz, Daniel M., and Michael C. Constantinou. "Behaviour of the double concave friction pendulum bearing." *Earthquake engineering & structural dynamics* 35, no. 11 (2006): 1403-1424.
- [47] Fenz, Daniel M., and Michael C. Constantinou. "Behaviour of the double concave friction pendulum bearing." *Earthquake engineering & structural dynamics* 35, no. 11 (2006): 1403-1424.
- [48] Constantinou, Michalakis C., Tsu T. Soong, and Gary F. Dargush. "Passive energy dissipation systems for structural design and retrofit." (1998).
- [49] Aiken, Ian D., Douglas K. Nims, Andrew S. Whittaker, and James M. Kelly. "Testing of passive energy dissipation systems." *Earthquake spectra* 9, no. 3 (1993): 335-370.
- [50] Ramirez, Oscar Manuel. Development and evaluation of simplified procedures for the analysis and design of buildings with passive energy dissipation systems. State University of New York at Buffalo, 2001.
- [51] Symans, M. D., F. A. Charney, A. S. Whittaker, M. C. Constantinou, C. A. Kircher, M. W. Johnson, and R. J. McNamara. "Energy dissipation systems for seismic applications: current practice and recent developments." *Journal of structural engineering* 134, no. 1 (2008): 3-21.
- [52] Sadek, Fahim, and Bijan Mohraz. Semiactive control algorithms for structures with variable dampers. US Department of Commerce, Technology Administration, National Institute of Standards and Technology, 1997.
- [53] Spiteri, Shaun. "Shock Absorber Applications." *European Journal of Engineering and Technology Research* 4, no. 1 (2019): 37-41.
- [54] Pocanschi, A., and Marios C. Phocas. "Earthquake isolator with progressive nonlinear deformability." *Engineering Structures* 29, no. 10 (2007): 2586-2592.
- [55] Skinner, R. Ivan, James M. Kelly, and A. J. Heine. "Hysteretic dampers for earthquake-resistant structures." *Earthquake engineering & structural dynamics* 3, no. 3 (1974): 287-296.
- [56] Aiken, Ian D., Douglas K. Nims, and James M. Kelly. "Comparative study of four passive energy dissipation systems." *Bulletin of the New Zealand Society for Earthquake Engineering* 25, no. 3 (1992): 175-192.
- [57] Aiken, Ian D., Douglas K. Nims, Andrew S. Whittaker, and James M. Kelly. "Testing of passive energy dissipation systems." *Earthquake spectra* 9, no. 3 (1993): 335-370.
- [58] Martinez-Romero, Enrique. "Experiences on the use of supplementary energy dissipators on building structures." *Earthquake spectra* 9, no. 3 (1993): 581-625.

- [59] Cherry, S., and A. Filiatrault. "Seismic response control of buildings using friction dampers." *Earthquake Spectra* 9, no. 3 (1993): 447-466.
- [60] Moreschi, L. M., and M. P. Singh. "Design of yielding metallic and friction dampers for optimal seismic performance." *Earthquake engineering & structural dynamics* 32, no. 8 (2003): 1291-1311.
- [61] Shen, K. L., and T. T. Soong. "Modeling of viscoelastic dampers for structural applications." *Journal of Engineering Mechanics* 121, no. 6 (1995): 694-701.
- [62] Crosby, Patrick, James Kelly, and J. P. Singh. "Utilizing visco-elastic dampers in the seismic retrofit of a thirteen story steel framed building." In *Structures congress XII*, pp. 1286-1291. ASCE, 1994.
- [63] Tsai, C. S., and H. H. Lee. "Applications of viscoelastic dampers to high-rise buildings." *Journal of structural engineering* 119, no. 4 (1993): 1222-1233.
- [64] Chang, Kuei-Chung, T. T. Soong, S-T. Oh, and M. L. Lai. "Effect of ambient temperature on viscoelastically damped structure." *Journal of Structural Engineering* 118, no. 7 (1992): 1955-1973.
- [65] Park, S. W. "Analytical modeling of viscoelastic dampers for structural and vibration control." *International Journal of Solids and structures* 38, no. 44-45 (2001): 8065-8092.
- [66] Kareem, Ahsan, Tracy Kijewski, and Yukio Tamura. "Mitigation of motions of tall buildings with specific examples of recent applications." *Wind and structures* 2, no. 3 (1999): 201-251.
- [67] Housner, GWea, Lawrence A. Bergman, T. Kf Caughey, Anastassios G. Chassiakos, Richard O. Claus, Sami F. Masri, Robert E. Skelton, T. T. Soong, B. F. Spencer, and James TP Yao. "Structural control: past, present, and future." *Journal of engineering mechanics* 123, no. 9 (1997): 897-971.
- [68] Council, Building Seismic Safety. "NEHRP guidelines for the seismic rehabilitation of buildings." *FEMA-273, Federal Emergency Management Agency, Washington, DC* (1997): 2-12.
- [69] Riley, Michael A., Fahim H. Sadek, and Bijan Mohraz. "Guidelines for testing passive energy dissipation devices." (1999).
- [70] FEMA 356, FEDERAL EMERGENCY. "Prestandard and commentary for the seismic rehabilitation of buildings." *Federal Emergency Management Agency: Washington, DC, USA* (2000).
- [71] Hüffmann, Günter K. "Full base isolation for earthquake protection by helical springs and viscodampers." *Nuclear engineering and design* 84, no. 3 (1985): 331-338.
- [72] Makris, Nicos, and M. C. Constantinou. "Fractional-derivative Maxwell model for viscous dampers." *Journal of Structural Engineering* 117, no. 9 (1991): 2708-2724.
- [73] Rama Raju, K., M. Ansu, and Nagesh R. Iyer. "A methodology of design for seismic performance enhancement of buildings using viscous fluid dampers." *Structural Control and Health Monitoring* 21, no. 3 (2014): 342-355.

- [74] Symans, M. D., and M. C. Constantinou. "Passive fluid viscous damping systems for seismic energy dissipation." *ISET Journal of Earthquake Technology* 35, no. 4 (1998): 185-206.
- [75] Mekki, Othman Ben. "Amortissement semi-actif des structures flexibles." PhD diss., Ecole des Ponts ParisTech, 2006.
- [76] Krishnamoorthy, Agrahara, and Kiran Kumar Shetty. "Seismic response control of structure using tuned mass dampers." *Journal of the Institution of Engineers (India): Civil Engineering Division* 86, no. AUG. (2005): 58-61.
- [77] Kaynia, Amir M., Daniele Veneziano, and John M. Biggs. "Seismic effectiveness of tuned mass dampers." *Journal of the Structural Division* 107, no. 8 (1981): 1465-1484.
- [78] Hoang, Nam, Yozo Fujino, and Pennung Warnitchai. "Optimal tuned mass damper for seismic applications and practical design formulas." *Engineering structures* 30, no. 3 (2008): 707-715.
- [79] DJELLOULI, Lynda. "Modélisation de système d'isolation parasismique pour le contrôle de la réponse dynamique des structures." PhD diss., Université Mohamed Khider-Biskra, 2012.
- [80] Mansfield, Neil J. *Human response to vibration*. CRC press, 2004.
- [81] McNamara, Robert J. "Tuned mass dampers for buildings." *Journal of the Structural Division* 103, no. 9 (1977): 1785-1798.
- [82] Kareem, A. "The next generation of tuned liquid dampers." In *Proceedings of the first world conference on structural control*, vol. 1, pp. 19-28. 1994.
- [83] Fujino, Yozo, Limin Sun, Benito M. Pacheco, and Piyawat Chaiseri. "Tuned liquid damper (TLD) for suppressing horizontal motion of structures." *Journal of Engineering Mechanics* 118, no. 10 (1992): 2017-2030.
- [84] Banerji, Pradipta, Mohan Murudi, Arvind H. Shah, and Neil Popplewell. "Tuned liquid dampers for controlling earthquake response of structures." *Earthquake engineering & structural dynamics* 29, no. 5 (2000): 587-602.
- [85] Yalla, Swaroop K., and Ahsan Kareem. "Optimum absorber parameters for tuned liquid column dampers." *Journal of Structural Engineering* 126, no. 8 (2000): 906-915.
- [86] Hoang, Nam, Yozo Fujino, and Pennung Warnitchai. "Optimal tuned mass damper for seismic applications and practical design formulas." *Engineering structures* 30, no. 3 (2008): 707-715.
- [87] Fujino, Yozo, Limin Sun, Benito M. Pacheco, and Piyawat Chaiseri. "Tuned liquid damper (TLD) for suppressing horizontal motion of structures." *Journal of Engineering Mechanics* 118, no. 10 (1992): 2017-2030.
- [88] Hsieh, Meng-Chang, Guan-Lee Huang, Haijun Liu, Shih-Jiun Chen, and Bang-Fuh Chen. "A numerical study of hybrid tuned mass damper and tuned liquid damper system on structure motion control." *Ocean Engineering* 242 (2021): 110129.

- [89] Shin, Ji-Hwan, Moon K. Kwak, Soo-Min Kim, and Kwang-Hyun Baek. "Vibration control of multi-story building structure by hybrid control using tuned liquid damper and active mass damper." *Journal of Mechanical Science and Technology* 34, no. 12 (2020): 5005-5015.
- [90] Symans, Michael D., and Michael C. Constantinou. "Semi-active control systems for seismic protection of structures: a state-of-the-art review." *Engineering structures* 21, no. 6 (1999): 469-487.
- [91] Asgari, B., and S. A. Osman. "Application of isolation systems in the seismic control of cable-stayed bridges: A state-of-the-art review. Latest Trends on Engineering Mechanics, Structures." In *Engineering Geology, International Conference on Geography and Geology*. 2010.
- [92] Symans, Michael D., and Michael C. Constantinou. "Semi-active control systems for seismic protection of structures: a state-of-the-art review." *Engineering structures* 21, no. 6 (1999): 469-487.
- [93] Lee, Brian L. CIV. "DEPARTMENT OF THE ARMY US ARMY CORPS OF ENGINEERS." (2021).
- [94] Lynch, Jerome Peter. "Active structural control research at Kajima Corporation." *The National Science Foundation's Summer Institute in Japan Program, Research Project* 17, no. 11 (1998).
- [95] Spencer Jr, B. F., S. J. Dyke, and H. S. Deoskar. "Benchmark problems in structural control: part II—active tendon system." *Earthquake engineering & structural dynamics* 27, no. 11 (1998): 1141-1147.
- [96] Zhang, L., C. Y. Yang, M. J. Chajes, and AH-D. Cheng. "Stability of active-tendon structural control with time delay." *Journal of engineering mechanics* 119, no. 5 (1993): 1017-1024.
- [97] Betti, R., and G. F. Panariello. "Active tendon control systems for structures subjected to multiple support excitation." *Smart Materials and Structures* 4, no. 3 (1995): 153.
- [98] Achkire, Younes, and André Preumont. "Active tendon control of cable-stayed bridges." *Earthquake engineering & structural dynamics* 25, no. 6 (1996): 585-597.
- [99] Nigdeli, Sinan Melih. "Active brace control of frame structures under earthquake excitation." *Nat. Cataclysms Glob. Prob. Mod. Civilization* 102 (2011).
- [100] Soong, Tsu T. "Active structural control." *Longman Scientific and Technical* (1990).
- [101] Soong, T. T., and A. M. Reinhorn. "Case studies of active control and implementational issues." In *Proceedings of ATC-17-1 Seminar of Seismic Isolation, Passive Energy Dissipation, and Active Control*, vol. 2, pp. 701-713. 1993.
- [102] Yang, J. N. "Control of tall buildings under earthquake excitation." *Journal of the Engineering Mechanics Division* 108, no. 5 (1982): 833-849.
- [103] Nishimura, Isao, Takuji Kobori, Mitsuo Sakamoto, Norihide Koshika, Katsuyasu Sasaki, and Satoshi Ohru. "Active tuned mass damper." *Smart Materials and Structures* 1, no. 4 (1992): 306.

- [104] Chang, James CH, and Tsu T. Soong. "Structural control using active tuned mass dampers." *Journal of the Engineering Mechanics Division* 106, no. 6 (1980): 1091-1098.
- [105] Soong, Tsu T. "Active structural control." *Longman Scientific and Technical* (1990).
- [106] Chung, L. L., A. M. Reinhorn, and T. T. Soong. "Experiments on active control of seismic structures." *Journal of Engineering Mechanics* 114, no. 2 (1988): 241-256.
- [107] Ankireddi, Seshasayee, and Henry T. Y. Yang. "Simple ATMD control methodology for tall buildings subject to wind loads." *Journal of Structural Engineering* 122, no. 1 (1996): 83-91.
- [108] Etienne, J. O. L. Y. "Les nouvelles technologies du bâtiment au Japon." *Ambassade de France au Japon* (2005).
- [109] Lynch, Jerome Peter. "Active structural control research at Kajima Corporation." *The National Science Foundation's Summer Institute in Japan Program, Research Project* 17, no. 11 (1998).
- [110] Lametrie, Christine W. "A Literary Review of Structural Control: Earthquake Forces." *Parksons Brinckerhoff Automotive Division, Warren, Michigan* (2001).
- [111] Soong, T. T., and B. F. Spencer Jr. "Supplemental energy dissipation: state-of-the-art and state-of-the-practice." *Engineering structures* 24, no. 3 (2002): 243-259.
- [112] Ghaedi, Khaled, Zainah Ibrahim, Hojjat Adeli, and Ahad Javanmardi. "Invited Review: Recent developments in vibration control of building and bridge structures." *Journal of Vibroengineering* 19, no. 5 (2017): 3564-3580.
- [113] Spencer, B. F., and Michael K. Sain. "Controlling buildings: a new frontier in feedback." *IEEE Control Systems Magazine* 17, no. 6 (1997): 19-35.
- [114] Fujita, Takafumi. "Application of hybrid mass damper with convertible active and passive modes using hydraulic actuator to high-rise building." In *Proceedings of 1994 American Control Conference-ACC'94*, vol. 1, pp. 1067-1072. IEEE, 1994.
- [115] Sakamoto, M., Kobori, T., Yamada, T. and Takahashi, M., 1994, August. Practical applications of active and hybrid response control systems and their verifications by earthquake and strong wind observations. In *Proc. 1st World Conf. on Struct. Control* (pp. 90-99).
- [116] Kandasamy, Ramkumar, Fangsen Cui, Nicholas Townsend, Choon Chiang Foo, Junyan Guo, Ajit Sheno, and Yeping Xiong. "A review of vibration control methods for marine offshore structures." *Ocean Engineering* 127 (2016): 279-297.
- [117] Guo, Shuqi, Shaopu Yang, and Cunzhi Pan. "Dynamic modeling of magnetorheological damper behaviors." *Journal of Intelligent material systems and structures* 17, no. 1 (2006): 3-14.
- [118] Cho, Sang-Won, Hyung-Jo Jung, and In-Won Lee. "Smart passive system based on magnetorheological damper." *Smart Materials and Structures* 14, no. 4 (2005): 707.
- [119] Gavin, H. P., R. D. Hanson, and F. E. Filisko. "Electrorheological dampers, part I: analysis and design." (1996): 669-675.

- [120] Yang, Guangqiang, Billie F. Spencer Jr, Hyung-Jo Jung, and J. David Carlson. "Dynamic modeling of large-scale magnetorheological damper systems for civil engineering applications." *Journal of Engineering Mechanics* 130, no. 9 (2004): 1107-1114.
- [121] Rana, Rahul, and T. T. Soong. "Parametric study and simplified design of tuned mass dampers." *Engineering structures* 20, no. 3 (1998): 193-204.
- [122] Yucel, Melda, Gebrail Bekdaş, Sinan Melih Nigdeli, and Selcuk Sevgen. "Estimation of optimum tuned mass damper parameters via machine learning." *Journal of Building Engineering* 26 (2019): 100847.
- [123] Soto, Mariantonieta Gutierrez, and Hojjat Adeli. "Optimum tuning parameters of tuned mass dampers for vibration control of irregular highrise building structures." *Journal of Civil Engineering and Management* 20, no. 5 (2014): 609-620.
- [124] Elias, Said, and Vasant Matsagar. "Research developments in vibration control of structures using passive tuned mass dampers." *Annual Reviews in Control* 44 (2017): 129-156.
- [125] Providakis, C. P. "Effect of LRB isolators and supplemental viscous dampers on seismic isolated buildings under near-fault excitations." *Engineering structures* 30, no. 5 (2008): 1187-1198.
- [126] Zohair, KAAB Mohamed. "INFLUENCE DE L'AMORTISSEMENT SUR LA REPOSE DYNAMIQUE DES STRUCTURES AVEC SYSTEMES D'ISOLATION PARASISMIQUE." PhD diss., Université Mohamed Khider de Biskra, Département de Génie C, 2010.
- [127] Sivák, Peter, and Darina Hroncová. "State-Space model of a mechanical system in MATLAB/Simulink." *Procedia engineering* 48 (2012): 629-635.
- [128] Casciati, Fabio, Jose Rodellar, and Umut Yildirim. "Active and semi-active control of structures—theory and applications: A review of recent advances." *Journal of Intelligent Material Systems and Structures* 23, no. 11 (2012): 1181-1195.
- [129] Stefani, Raymond T., Bahram Shahian, Clement J. Savant, and Gene H. Hostetter. *Design of feedback control systems*. Oxford: Oxford University Press, 2002.
- [130] Heidari, Amir Hossein, Sadegh Etedali, and Mohamad Reza Javaheri-Tafti. "A hybrid LQR-PID control design for seismic control of buildings equipped with ATMD." *Frontiers of Structural and Civil Engineering* 12, no. 1 (2018): 44-57.
- [131] Alavinasab, Ali, Hamid Moharrami, and Amir Khajepour. "Active control of structures using energy-based LQR method." *Computer-Aided Civil and Infrastructure Engineering* 21, no. 8 (2006): 605-611.
- [132] Zhang, Jingjun, Lili He, Ercheng Wang, and Ruizhen Gao. "A LQR controller design for active vibration control of flexible structures." In *2008 IEEE Pacific-Asia Workshop on Computational Intelligence and Industrial Application*, vol. 1, pp. 127-132. IEEE, 2008.
- [133] Takács, Gergely, and Boris Rohal'-Ilkiv. *Model predictive vibration control: efficient constrained MPC vibration control for lightly damped mechanical structures*. Springer Science & Business Media, 2012.

- [134] Ulusoy, Serdar, Sinan Melih Nigdeli, and Gebrail Bekdaş. "Novel metaheuristic-based tuning of PID controllers for seismic structures and verification of robustness." *Journal of Building Engineering* 33 (2021): 101647.
- [135] Ezzraimi, Madjid, Rachid Tiberkak, Abdelkader Melbous, and Said Rechak. "LQR and PID algorithms for vibration control of piezoelectric composite plates." *Mechanics* 24, no. 5 (2018): 734-740.
- [136] Cao, Jun-Yi, Jin Liang, and Bing-Gang Cao. "Optimization of fractional order PID controllers based on genetic algorithms." In *2005 international conference on machine learning and cybernetics*, vol. 9, pp. 5686-5689. IEEE, 2005.
- [137] Zhao, Weiguo, Liying Wang, and Seyedali Mirjalili. "Artificial hummingbird algorithm: A new bio-inspired optimizer with its engineering applications." *Computer Methods in Applied Mechanics and Engineering* 388 (2022): 114194.
- [138] Zhao, Weiguo, Liying Wang, and Seyedali Mirjalili. "Artificial hummingbird algorithm: A new bio-inspired optimizer with its engineering applications." *Computer Methods in Applied Mechanics and Engineering* 388 (2022): 114194.
- [139] Altshuler, Douglas L., and Robert Dudley. "The ecological and evolutionary interface of hummingbird flight physiology." *Journal of Experimental Biology* 205, no. 16 (2002): 2325-2336.
- [140] Ward, Brian J., Lainy B. Day, Steven R. Wilkening, Douglas R. Wylie, Deborah M. Saucier, and Andrew N. Iwaniuk. "Hummingbirds have a greatly enlarged hippocampal formation." *Biology Letters* 8, no. 4 (2012): 657-659.
- [141] Mirjalili, Seyedali. "Genetic algorithm." In *Evolutionary algorithms and neural networks*, pp. 43-55. Springer, Cham, 2019.
- [142] Kumar, Manoj, Dr Husain, Naveen Upreti, and Deepti Gupta. "Genetic algorithm: Review and application." *Available at SSRN 3529843* (2010).
- [143] Mirjalili, Seyedali, Seyed Mohammad Mirjalili, and Andrew Lewis. "Grey wolf optimizer." *Advances in engineering software* 69 (2014): 46-61.
- [144] Etedali, Sadegh, Morteza Akbari, and Mohammad Seifi. "MOCS-based optimum design of TMD and FTMD for tall buildings under near-field earthquakes including SSI effects." *Soil Dynamics and Earthquake Engineering* 119 (2019): 36-50.
- [145] Liu, Ming-Yi, Wei-Ling Chiang, Jin-Hung Hwang, and Chia-Ren Chu. "Wind-induced vibration of high-rise building with tuned mass damper including soil-structure interaction." *Journal of Wind Engineering and Industrial Aerodynamics* 96, no. 6-7 (2008): 1092-1102.
- [146] Mirjalili, Seyedali, Seyed Mohammad Mirjalili, and Andrew Lewis. "Grey wolf optimizer." *Advances in engineering software* 69 (2014): 46-61.

SVCS Software

To easily simulate the vibration control of a building structure, a graphical user interface (GUI) is developed in MATLAB, we called this application SVCS (Structural Vibration Control Simulator) as shown in Fig. A.1 (Splash screen). Fig. A.2 represents the main window of the application.

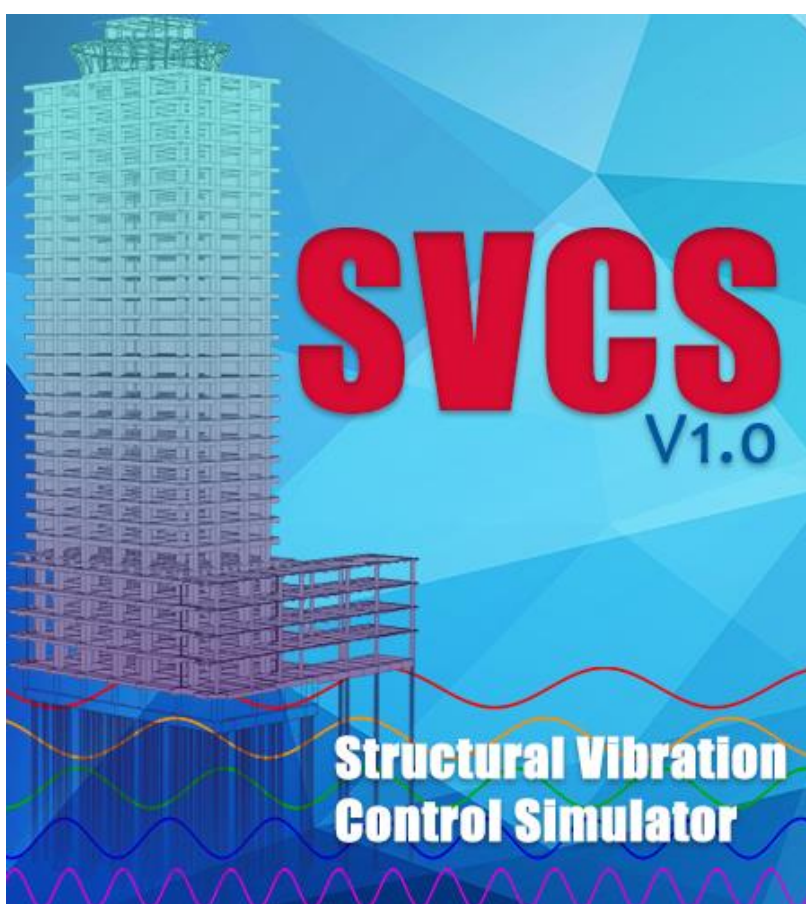


Figure A.1 : Splash screen.

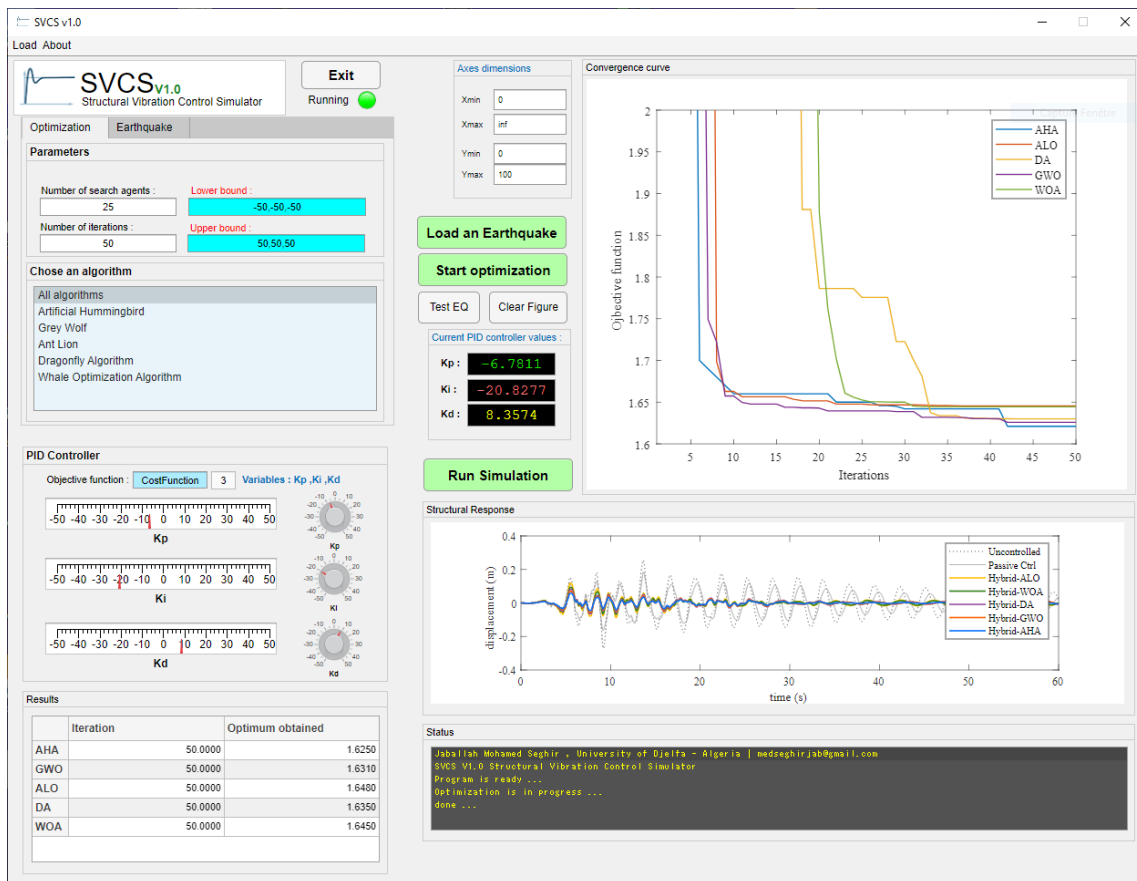


Figure A.2 : SVCS main window.

This application provides many features such as:

Earthquake input

This application includes a database base that contains the 22 most historically known earthquakes (El Centro, Northridge, Kobe, Chichi, ...). So, the user can directly select the desired earthquake excitation to be used for simulation. If not, this application allows you also to choose a custom earthquake from an external file (.txt format). This file should contain two-column data (time and ground acceleration), as shown in Fig. A.3.

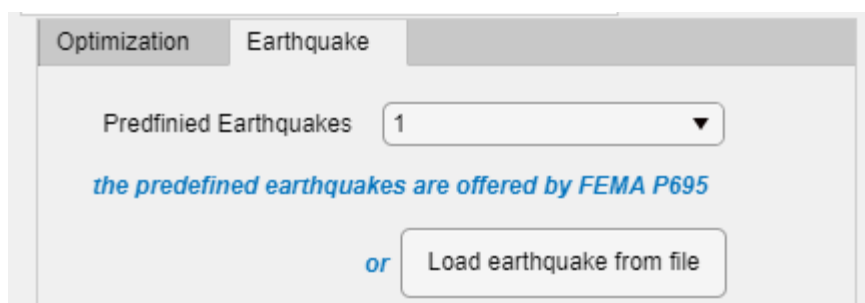


Figure A.3 : Earthquake input tab.

PID tuning

In this application, the user can tune the PID controller manually by typing K_p , K_i , K_d (Fig. 27) values or choose one (or many) optimization algorithms to tune automatically the PID controller.

The available tuning algorithms available in this version of the application are Artificial Hummingbird algorithm (AHA), Grey Wolf Optimization algorithm (GWO), Dragonfly Algorithm (DA), Whale Optimization Algorithm (WOA), and Ant Lion Optimization algorithm (ALO).

A user can define the following parameters for any algorithm: upper and lower bounds, number of iterations, number of search agents, as shown in Fig. A.4.

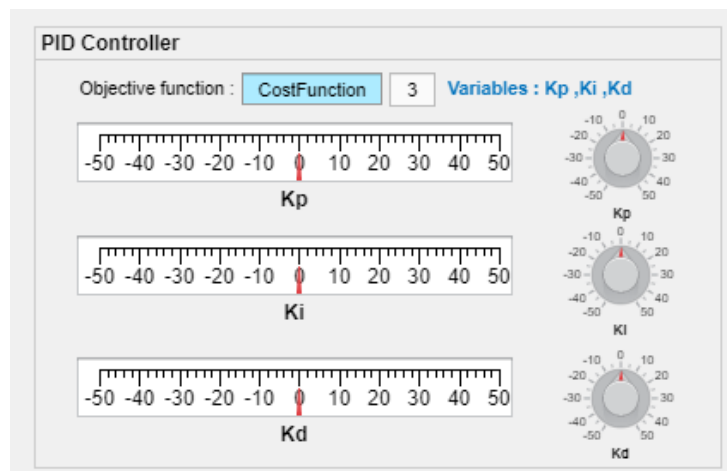


Figure A.4 : PID controller tab.

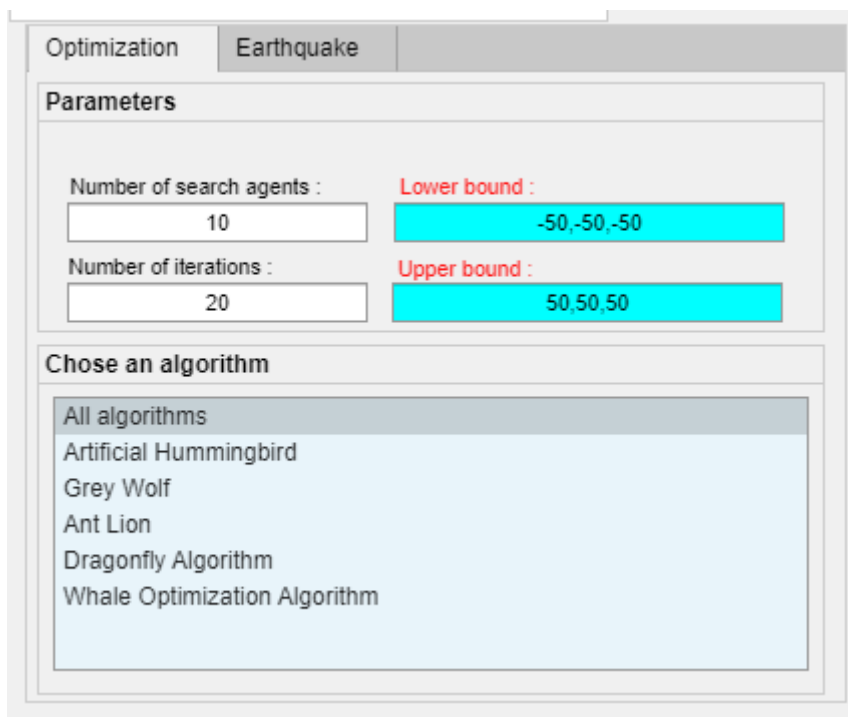


Figure A.5 : Optimizations tab.

Data preview and export

In this application, the user can preview the earthquake ground motion (Fig. A.6), the objective function convergence curve, and the table of optimum values obtained (Fig. A.6 and Fig. A.7). The results data can be exported as a Microsoft EXCEL file. And the plot data can be exported as (svg, png, tiff,) file format.

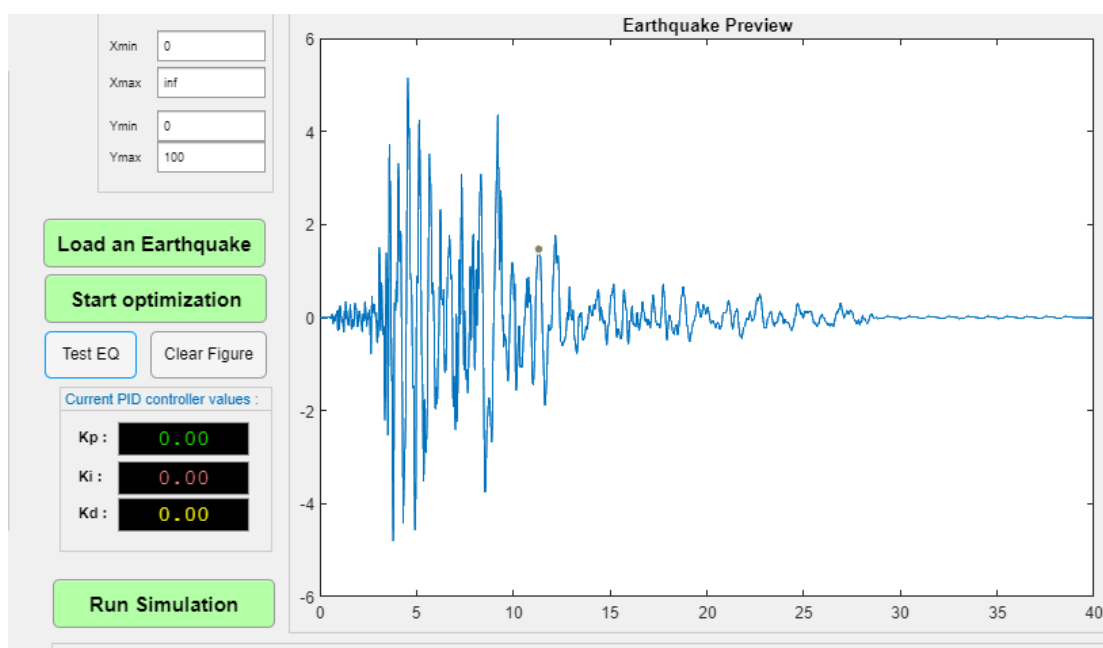


Figure A.6 : Earthquake preview window.

Results			
	Iteration		Optimum obtained
AHA		50.0000	1.6250
GWO		50.0000	1.6310
ALO		50.0000	1.6480
DA		50.0000	1.6350
WOA		50.0000	1.6450

Figure A.7 : Objective functions results table.

